Host recognition of Hepatitis B virus (HBV) and related pathogen-/danger associated molecular patterns (P/DAMPs) through pattern recognition receptors (PRRs)

Inaugural-Dissertation

zur

Erlangung des Doktorgrades

Dr. rer. nat.

der Fakultät für

Biologie

an der

Universität Duisburg-Essen

vorgelegt von

Mazen Atia

Geboren in Kairo

Essen, June 2019

Die der vorliegenden Arbeit zugrunde liegenden Experimente wurden am Institut für Fakultät für Medizinische Mikrobiologie der Universität Duisburg-Essen durchgeführt.

1. Gutachter: Professor Dr. Carsten Kirschning
2. Gutachter: Professor Dr. Sven Brandau
3. Gutachter:

Vorsitzender des Prüfungsausschusses: Professor Dr. Ralph Küppers

Tag der mündlichen Prüfung: 28.10.2019

_____

DOI: 10.17185/duepublico/70769
URN: urn:nbn:de:hbz:465-20220905-101046-4

Table of Contents

1. Introduction

1.1 The immune system: Innate and adaptive immunity

Our bodies are continuously exposed to pathogens through inhalation, ingestion or colonization onto the skin and mucous membranes. The ability of these pathogens to establish an infection depends primarily on the pathogens' virulence factors and the efficiency of the host immune system to prevent the invasion. The host immune system comprises several biological structures and processes, which form a network of cells, tissues, and organs that cooperate to not only protect the body against disease-causing microorganisms, but also to maintain integrity or trigger regeneration. Leukocytes, comprising merely 1% of circulating blood volume, are the cells of the immune system [1].

The immune system is divided into two arms, namely innate and adaptive immunity. Innate immunity is operative in all prokaryotes and eukaryotes including invertebrates, vertebrates and plants. Physical and chemical barriers such as skin, tears, mucous, saliva or gastric fluids form a first innate barrier besides the serum borne complement system. Neutrophils, macrophages, dendritic cells (DC), basophils, eosinophils, mast cells and NK cells form its cellular branch. The innate immune system mediates early ''nonspecific'' responses toward pathogens, whereas the adaptive immune response is slower, yet more pathogen-specific. The adaptive immune system is further subdivided into humoral and cell mediated immunity [2]. Contrasting to the old age of innate immunity, the adaptive immune system arose less than 500 million years ago with the advent of agnatha [3] .

1.1.2 The adaptive immune system

The adaptive immune system comprises lymphocytic cells, which represent 30% of the leukocytes of the healthy human body, namely B and T cells. The hallmark of adaptive immunity is the immunological memory, which provides to the host a propensity to rapidly respond against pathogen challenge upon secondary encounter. Like all leukocytes, B and T lymphocytes are derived from hematopoietic stem cells. Based on their co-surface receptors, T lymphocytes are subdivided into $CD4^+$ or $CD8^+$ T cells [4]. Activation of $CD4^+$ or $CD8^+$ T cells depends on priming by T cells receptor binding to antigen-presenting cells (APC) presenting antigens on their surface through either major histocompatibility complex (MHC) I or II for $CD8^+$ or $CD4^+$ T cells, respectively [5]. Priming signals such as co-stimulatory receptor for example CD80 and CD86 ligands expressed by APC to prime T cells beside the cytokine milieu are critical parameters towards T cell activation and, hence, effector function.

Naïve $CD4^+$ helper T cells polarize towards T helper Th1-, Th2-, Th9-, Tfh-, TBD-, Tr1-, Th17- polarized immune responses involving counteregulatory T cells (Tregs). The T cell polarization depends on the cytokine milieu and the identity of the encountered pathogen. For numerous viral infections, effector cytotoxic $CD8^+$ T cells are decisive for clearing the infection by lysis through release of perforins and killing by granzymes injection to program viral infected cell towards cell apoptosis. As down-regulators of immune activity, $CD4^+$ Tregs expressing the transcription factor forkhead box P3 (FOXP3), suppress autoimmunity and promote immune tolerance. On the other hand, B lymphocytes, which are activated upon encounter, either by T cell dependent or independent B cell activation (TD, TI, respectively) differentiate into plasma cells to secrete cell-clone-specific antibodies or memory B cells to long lastingly maintained adaptive immunity [6].

1.1.3 Innate immune system

An innate immunity concept was first brought up by Elie Metchnikoff (1845–1916) [7]. The innate immune system is a first line of defense which mediates an immediate immune response and is microbial clade rather than species specific. Physical anatomical barricades including skin, fluids such as saliva, gastric fluids, mucosal endo and exothelia and mucus serve to trap and entangle microorganisms [8] such as bacteria, viruses, fungi and parasites. If pathogens breach these primary barriers, they get exposed to the humoral and cellular lines of defense involving the complement system, macrophages, scavenger neutrophil granulocytes, natural killer cells (NK) and dendritic cells (DCs) in tissues and blood which sense pathogen presence. APC link the innate to the adaptive immune system, by exposing antigen onto MHC to specific T and B cell receptor evolved upon somatic gene recombination.

Recognition of conserved and constitutive microbial molecules termed pathogen-associated molecular patterns (PAMPs) depends upon pattern-recognition receptor (PRRs) expression. Also sterile inflammation engages PRRs activation, yet upon cellular release of host cell derived danger-associated molecular patterns (DAMPs). Sterile inflammation arises upon cell necrosis such as in trauma and triggers for instance release of ATP, a cognate DAMP.

Cellular innate immunity derives from myeloblasts out of myeloid progenitors which include monocytes and granulocytes. Granulocytes comprise neutrophils, eosinophils, basophils and mast cells. **Neutrophils** are the most abundant healthy host blood cell population, representing 70% of total leukocytes, while monocytes, basophils, and eosinophils represent 6%, 1% and 4%, respectively. Neutrophils are the immune cells that first migrate to the site of an infection and activated neutrophils degranulate to release for example antimicrobial

peptides, myeloperoxidases, histaminases, and alkaline phosphatases. Neutrophils also release extracellular traps, a web-like structure genomic DNA towards extracellular microbes that cannot be phagocytosed such as by helminths or *Salmonella typhimurium* [9]. Neutrophil phagocytosis counteracts small and intracellular microbes. Intracellularly, phagosomes fuse with cell lysosomes to form phagolysosomes, in which pathogens get degraded upon respiratory bursts involving reactive oxygen radical release. Circulating monocytes differentiate into tissue-resident **macrophages** or **DC**, depending on factors such as the cytokine milieu. Specifically, monocyte-derived DC differentiation depends upon the chemokine granulocytes monocytes colony stimulating factor (GM-CSF) and the cytokine interleukin 4 (IL-4), whereas monocyte-derived macrophages differentiation requires colony stimulating factor 1 (CSF-1) [10]. Macrophages and DC comprise three major functions, namely, phagocytosis, antigen presentation, cytokine and effector molecule release. The **complement system** consists of 20 blood borne glycoproteins (C1-C9) and activation of the complement system results in a cascade of ordered protease recruitments towards pore formation and death by osmotic lysis of invading pathogen. Moreover, soluble anaphylatoxins such as C3a and C5a cause inflammation and elevate the vascular permeability, promoting anti-microbial peptide penetration and antibody-microbia binding [11]. Pathogen opsonisation is binding of the complement complexes onto the microbe to enhance recognition and eventual phagocytosis. Parasitic infection such as nematodes is counteracted by **Eosinophils**. Parasite-IgE antibody immune complexes activate eosinophils through binding to the low-affinity Fc receptor (FcεRII). Consequently, eosinophils degranulate to release cationic antimicrobial proteins, peroxidases, and neurotoxins [12]. **Mast cells** are tissue resident cells [13] whereas **basophils** reside in the blood stream [13]. Similar to eosinophils and basophils, mast cells are activated by complexed IgE binding to their high-affinity Fc receptor (FcεRI) [14]. Mast cell degranulation releases trypsin and chymotrypsin, whereas basophils release vasoactive amines, histamine, and serotonin. The only lymphocytic cells of the innate immune system are the **NK** cells [15]. In contrast to T and B cells, NK cells lack an antigen-specific receptor on their surfaces. Their function is the elimination of infected cells. NK cells, via their Fc receptor (FcR), bind and neutralize antibody-coated cells. Moreover, NK cells recognize infected cells that lack constitutive MHC-I expression. Physical direct cell-cell contact leads to NK cells release of perforins and granzymes onto the infected cell surface. The former leads to formation of cell pores and the latter leads to cell apoptosis [16].

1.1.4 Pattern recognition receptors (PRR)

In contrast to somatic recombination based maturation of pathogen-specific T and B lymphocyte receptors, PRR are germ-line encoded. PRR activation mediates immune responses to defend the host such as by cytokine release and effectors such as antimicrobial peptide production and promotes antigen presentation. PRR activation also induces cell maturation such as DC towards their migration and antigen presentation accompanied by costimulation through expression of B7.1, B7.2 (CD80 and CD86), towards maximal T cell activation [17].

Subcellular PRRs reside cytoplasmically, endosomally or on the cell surface (Fig. 1). The family of cytoplasmic **nucleotide-binding oligomerization domain-like receptors (NLR)**, comprises 22 family members in mouse and 36 in human. They carry a C-terminal domain, an N-terminal domain, and a central domain [18]. The central domain is a nucleotide binding domain (NBD), the C terminus is a leucine reach repeats (LRR) and the N terminus is a variable six-helix bundle death domain, namely the caspase recruitment domain (CARD) or pyrine domain (PYD) [19]. NLRs often are involved in inflammasome assembles. Inflammasomes are stimulus-dependently formed multiprotein complexes. For example, synthetic or virus-derived double stranded ribonucleic acid (dsRNA) triggers NLRP3 inflammasome assembly [20], whereas asbestos toxin triggers NALP3 [21]. Furthermore, absent-in-melanoma 2 (AIM2) inflammasomes bind cytoplasmic deoxyribonucleic acid (DNA) [22]. Inflammasomes containing caspase-1 often bind to adaptor protein apoptosis-associated speck-like protein containing CARD (ASC) [23]. Consequently, caspases are proteases with an autolytic activity (12 family members expressed in human and 10 in mouse). Besides Caspase-1, Caspase-4 and Caspase-5 in humans, Caspase-11 in mice mediate cell pyroptosis and cleavage of pro-IL-1β, IL-18 and IL-33 towards their cellular release [24]. Canonical activation of inflammasomes involves a first signal such as a toll like receptor (TLR) ligand challenge to induce cytokine expression. A second signal is an inflammasome activator such as viral dsRNA, imidazoquinolines, bacterial RNA and toxins like nigericin or listeriolysin O [25][26][27]. Another class of cytoplasmic RNA sensors are **RIG-like helicases (RLH)** such as retinoic acid-inducible gene I (RIG-I), melanoma differentiation-associated protein 5 (MDA5) and laboratory of genetics and physiology 2 (LGP2). While LPG2 lacks a CARD domain, both RIG-I and MDA5 carry an N terminal CARD domain, a central RNA helicase DEA(D/H)-box domain, and a regulatory C terminal domain (CTD). Specifically suited self and xenobiotic single or double stranded RNA molecules activate RLH. Activation of RLH involves recruitment of mitochondrial antiviral-

signaling protein (MAVS) [28], to elicit antiviral responses upon consequent nuclear translocation of interferon regulatory factor (IRF) 3 or 7 [29] and interferon (IFN) type I gene activation [30]. Cytosolic cyclic GMP-AMP Synthase (**cGAS)** binds DNA [31]. Upon DNA ligation, cGAS homodimerizes and catalyzes 2′3′-cGAMP formation. Active cGAMP recruits stimulator of interferon genes (STING) which mediates phosphorylation of IRF3 by tyrosine B kinase 1 (TBK1) [32]. **DDX41** is an alternative DNA/RNA sensor such as in DCs and mediates signaling also through STING [33]. Depletion of the *DDX41* gene exacerbates IFN-β production in herpes simplex virus (HSV)- or influenza A virus infected cells [34]. **IFI16** is another DNA sensor that in a STING-TBK1 dependent manner mediates IFN-β induction. IFI16 binds vaccinia virus DNA [35]. **Scavenger receptors** such as SR-A I, SR-A II and MARCO, are fungal and bacterial carbohydrate-binding receptors which function in a $Ca2^{+}$ signaling-dependent or independent manner, and are solely expressed on the surface of myeloid-derived cells. Scavenger receptors phagocytose pathogens and apoptotic cells [36]. Often, they are not considered as PRRs due to lacking signaling property. Scavenger receptors dysfunction is associated with autoimmune diseases such as atherosclerosis [37] and Alzheimer's disease [38]. **C-type lectins** (CTLs) are also cell surficial located and carry C-type lectin-like domains (CLLD). CTL family includes Dectin-1/2, minncle, DC-SIGN, mannose receptor (MR) and mannose binding lectin (MBL). CLRs recognize fungal cell wall and thereby play a critical role in tailoring immune responses against fungal infections [39].

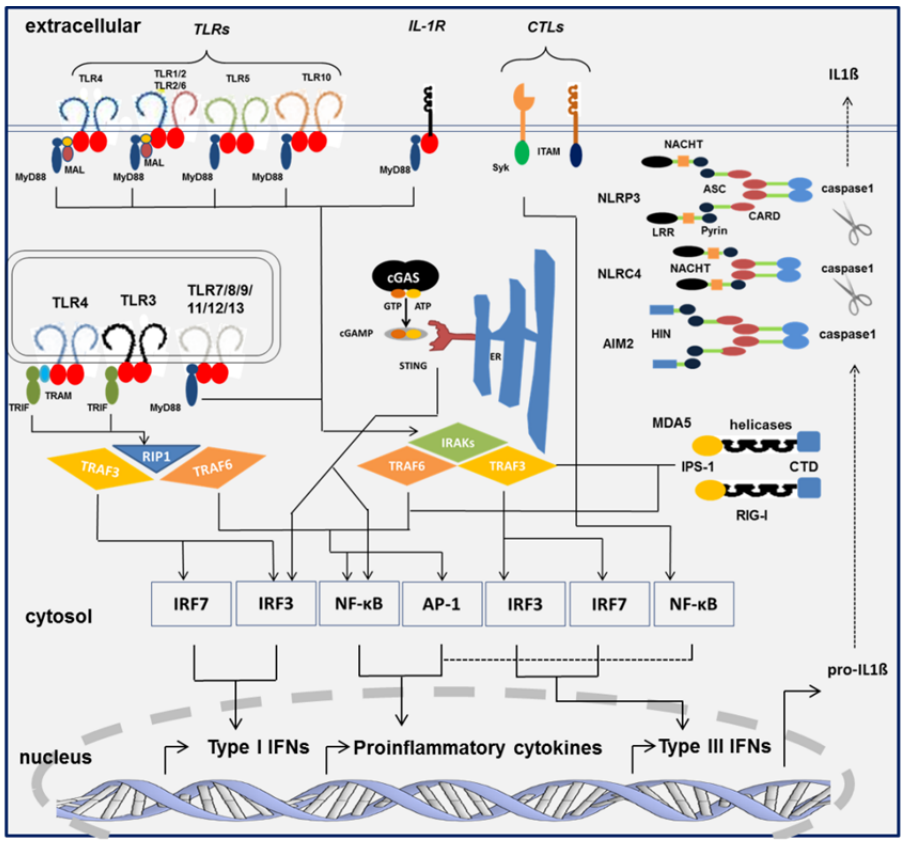

Figure 1. Pattern recognition receptor families. PRRs are expressed either cytoplasmically, endosomally or onto the cell surface. Cytosolic receptors include the inflammasome forming receptors NLRs, the RNA helicases and DNA sensors cGAS receptor. On the cell surface, IL-1R, CTL, or TLR are present. TLR nucleic acid sensors are endosomally localized. Following antigen ligations, downstream signaling is initiated towards proinflammatory cytokines / chemokine or type I/III IFN expression depending on the adaptor molecules and the transcription factors. All TLRs as well as IL-1R recruit MyD88, whereas TLR2 and TLR4 additionally deploy the adaptors MAL and TRAM. Uniquely, TLR3 in addition to TLR4 utilize TRIF molecule for their downstream signaling. (Modified from PhD thesis; Krüger 2016)

1.1.4.1 Toll like receptors (TLR)

TLR, as the first discovered signal transducing PRRs, are the most well studied classes of PRRs and mediate cell activation by P/DAMP. A wide variety of bacterial, viral, fungal, and parasitic or even host-derived products such as heat shock proteins (HSPs) trigger TLR activation. The Drosophila *Toll* gene product mediates embryogenesis such as towards dorsoventral polarization and mediates antifungal immunity in adult flies. Human toll like receptors implication as PRR [40][36] was surprising, because Toll is a cytokine receptor [41]. Two years later, PRR functions of TLR2 and TLR4 were consecutively identified, which marks the advent of signal transducing PRRs research [42][43]. Human expresses ten TLRs while mice lack TLR10, yet additionally express TLR 11, 12 and 13. TLR3, -7, -8, -9, -11, -12 and -13 reside in the endosome while TLR1, -2, -4, -5, -6 and -10 span the cell membrane

(Fig. 1). TLRs are expressed by vertebrate immune cells including monocytes, macrophages, NK cells, mast cells and DC and nonimmune cells such as intestinal epithelium, liver, kidney and neuron cells [44]. After ligand binding, TLRs undergo homodimerization, except for TLR2, which either homodimerizes or heterodimerizes with either TLR1 or TLR6 [45]. Upon phagocytosis, microorganisms undergo digestion in the endolysosomes, where high acidity and degrading enzymes are operational. Consequently, released nucleic acids are recognized by endosomal TLRs such as TLR3, -7, -8 and -9 [46].

TLR2 (CD282) is unique among TLR in terms of heterodimerization with TLR1 or TLR6. This explains the broadness of its ligands from bacterial, fungal, parasitic and viral origin [47] [48][49][50]. TLR1/2 heterodimers recognize triacylated bacterial lipoproteins. The synthetic triacylated lipo hexapeptide named tri-palmitoyl-Cysteine-Serine-tetra-Lysine (P_3CSK_4) is a widely used TLR1/2 ligand [51][52][48]. TLR2/6 heterodimers bind bacterial diacylated lipoproteins, while lipoteichoic acid (LTA) peptidoglycan (PGN), and yeast cell wall-derived zymosan are considered as TLR2 homodimers ligands [53][45][54][55]. Specific bacterial proteins are covalently N-terminally acylated in which the acyl chain numbers vary from one to three and the acyl lengths are variable in that they carry fourteen to nineteen carbon atoms. Out of three fatty acids one is amidically linked to the N-terminus of the N-terminal cysteine and the others esterified with the two free hydroxyl groups of a glycerol molecule esterified with the thiol group of the same cysteine. [56]. Since the abundance of sixteen-C containing (hexadecanoic or palmytic) acid was prominent, a synthetic hexapeptide with a polar aa sequence (CSK4) - not representing a known bacterial protein yet compensating for the lipophilicity of the acylations - was coupled with two or three palmitic acid molecules to yield P_3CSK_4 and P_2CSK_4, respectively [57]. They established themselves as ''the'' canonical TLR2 ligands since then. However, also shorter N-terminal triacylations of the polar $CSSK_4$ hexapeptide such as with lauric acid or myristic acid rendered it at least murine TLR2 and in the latter case even human and murine TLR4/MD2 stimulatory [58] [59] .

TLR3 recognizes endosomal dsRNA derived from viral replicates [60]. TLR3 consists of an N terminal and C terminal binding domains [61]. Activation of TLR3 by viral RNA or polyinosine-polycytidylic acid (polyI:C) triggers type-I and -III IFN expression via the adaptor molecule TRIF. This activation promotes DC maturation and subsequently enhance phagocytosis [62]. Importantly, hepatic non parenchymal cells (NPC) such as KC release antiviral cytokines, thereby inhibiting HBV replication upon TLR3 activation by polyI:C [63]. Bacteria - or virus derived single stranded RNA is endosomally recognized through **TLR7**

and -8. Vesicular stomatitis virus (VSV)- , influenza A virus, and endogenous retroviruses derived single stranded RNA (ssRNA) activated TLR7 [64][65], which is expressed primarily on DC and to a lesser extent on monocytes and macrophages. Like other endosomal TLRs, TLR7 mediates type-I IFNs induction upon activation [66]. TLR7 is activated by ssRNA or derivatives thereof imiquimod (R837), resiquimod (R848), CL075 (3M-001) [67] and loxoribine [68]. The oral TLR7 agonist GS-9620 has been evaluated in HBV infection animal models and elicited substantial antiviral immunity in both woodchucks and chimpanzees. Accordingly, sustained reduction of serum HBV DNA titters and seroconversion was observed. GS-9620 induced serum IFN-α production in a dose-dependent manner in chimpanzee liver and peripheral blood mononuclear cells [69]. While murine **TLR8** is inactive, human TLR8 mediates ssRNA and derivatives imidazoquinoline (R848) recognition [70]. TLR8 is expressed on myeloid DC, monocytes and macrophages, and it induces type-I IFN, TNF and IL-12 production [71]. **TLR9-**deficient mice are resistant to DNA Cytosine-phosphatidyl-Guanine (CpG-DNA) driven pathology [67]. *Babesia bovis-, Trypanosoma cruzi- and T. brucei*-derived DNA activate macrophages and DC TLR9 [72]. Oligo deoxynucleotides (ODN) of the ODN1585, 2216, and 2336 type encompass sequence of a palindromic phosphodiester-backbone as well as phosphorothioate stabilized 3'-poly-G end. The activation of TLR9 by these ligands induces type-I IFN and pDC maturation. A second group of ODNs such as ODN1668, 2006 and 2007 carries a phosphorothioate hexameric CpG motif and induces IL-6 production by human peripheral blood mononuclear cells (hPBMCs) and splenocytes.

1.1.4.2 Structure and Signaling of TLR

TLR contain 550-800 amino acids (aa) and are type I transmembrane proteins. TLR comprise an N-terminal extracellular/endosome-luminal ligand recognition domain (ECD), a single transmembrane domain, and an intracellular/ cytosolic C-terminal Toll-IL-1 receptor (TIR) domain. The ECD is a lineup of LRR (LXXLXXLXLXN, L: leucine, X: arbitrary aa, N: asparagine) motif and forms a horse-shoe-like solenoidal structure. Irregular loops protruding out of the LRR backbone are critical for ligand binding [73]. The intra- and extracellular domains of a TLR are connected by the 20 nonpolar aa spanning the cell transmembrane domain. The intracellular TIR domains are conserved to higher degree as compared to the ligand-specific ECDs [74]. The TIR domain comprises five alternating α-helices and β-sheets [44], and is made up of 150 aa forming three conserved regions named box 1, 2 and 3. Importantly, Box 2 harbors the BB-loop region, which mediates signal transduction through binding adaptor molecules [75]. Ligand binding results in receptor dimerization and an

allosteric conformational change of the receptor TIR domain [76] upon which the TIR domain recruits adaptor molecules. Six adaptor molecules are involved in TLR signaling. The Myeloid differentiation factor 88 (MyD88) is prominent while the Myd88-adaptor-like protein (MAL), the TIR domain-containing adaptor inducing IFN-β (TRIF/Ticam)-1, the TRIF related adaptor protein (TRAM/Ticam)-2, the sterile-α HEAT/armadillo motifs-containing protein (SARM) [75], and the B cell adaptor for phosphoinositid-3-kinase (PI3K)-BCAP) [77] play rather subordinated roles in signal transduction originated from TLR.

1.1.5 MyD88-IL-1 receptor-associated kinases (IRAK)

All TLRs, except for TLR3 and endosomal TLR4/MD2, employ MyD88 to mediate IRAK-1 and -4 phosphorylation, while TLR3 and TLR4/MD2 employ TRIF (Fig. 1) [78]. Following adaptor binding, IRAK-1/4-TNF receptor associated factor 6 (TRAF6) complex mediates phosphorylation of mitogen-activated kinases (MAPK) such as through the TAK-complex [79]. IKK-complex consists of IKK-α and β as well as the regulatory element NEMO/IKK–γ. Unphosphorylated IκB is bound to the transcription factor NF-κB subunits P65, p50 and p52, thereby blocking a translocation into the nucleus [80]. TLR activation results in phosphorylation of IκB and thus its proteasomal degradation towards translocation of liberated NF-κB complexes into the nucleus and specific proinflammatory gene activations such as proinflammatory cytokines.

1.1.6 TRIF

The TLR3, 4/MD2 specific pathway involves recruitment of the adaptor protein TRIF towards IRF1 or IRF7 driven type-I IFN production and IRF5 driven proinflammatory cytokines production [76]. TLR and MyD88 or TRIF interaction is bridged by downstream TIR domain containing adaptor (TIRAP) and TRAM molecules respectively (Fig. 1). The central role of TRIF is documented by the suffering of respective knock out (KO) mice upon viral and bacterial infection [81]. Endosomal TLR4/MD2 through TRAM-TRIF signaling is distinct from surficial TLR4/MD2 signaling through TIRAP-MyD88 signaling [82].

The polytypic endoplasmic reticulum-resident membrane **Unc93B1** protein shuttles endosomal TLR from the endoplasmic reticulum (ER) towards their subcellular destination in the endosomal membrane. Accordingly, endosomal localizations of TLR3, -7, -8,-9, -11, -12 and -13 rely on functional Unc93B1 expression [83].

1.2 Hepatits B virus (HBV)

Since identification by the Nobel laureate Baruch Blumberg in 1976, hepatitis B virus (HBV) remains the most prevalant cause of the severest form of viral hepatitides worldwide. According to the WHO 2017 report, the estimated global burden of chronic HBV patients is 257 millions of which annualy 887,000 cases are fatal due to virus-associated complications such as through cirrhosis or hepatocellular carcinoma (HCC). 50% of all HCC cases worldwide are estimated to be due to HBV infection [84].

HBV belongs to the family of *orthohepadnaviridae,* comprising two genera, namely *orthohepadna* virus, infecting human and other mammals, and avihepadna virus, infecting avians. The family *orthohepadna* is subclassified into nine genotypes (A-I) [85]. Collectively, 50% of all infecetd human cases worldwide are caused by genotypes A and D [86]. Genotypes A and D are mostly common in Asia and Europe whereas genotypes F and H are restricted to the Americas. Overall, the estimated global prevalance of the virus is 3,6%, with range from below 1% such as in Germany to 23% in South Sudan [87]. Hepadnaviridae viruses are hepatotropic with minor infectivity to the pancreas and kidney [88]. Importantly, human HBV infects human, chimpanzees and the treeshrew tupaia, which share the HBV entry receptor, namely sodium-taurocholate cotransporting polypeptide (NTCP) receptor [89]. HBV is transmitted either horizontally or vertically. Horizontal transmission occurs among individuals upon physical contact via blood, semen, or other bodily fluids, or sexually, whereas vertical transmission occurs by transmission of the virus from infected mothers to their babies perinatally (maternofetal) [90]. Two Hepatitis B surface antigen recombinant yeast-produced immunoglobulin vaccines, namely, Recombivax HB (Merck) and Engerix-B (GSK) are approved in more than 170 countries worldwide, yet fail to efficiently induce full virus clearance in infected young childern [91].

1.2.1 Virus morphology and genome

The spherical shape of HBV has been characterized by Dane Surrey and hence the virion carries his name (Dane particles) [92]. The HBV particles are covered by a double layer lipid membrane envelope under which the inner icosahedral nucleocapsid of a 22-42 nanometer (nm) in diameter size is located (Fig. 2A). The genome length is 3,2 kilo bases (kb). It is a partially complete dsDNA and also called relaxed circular (rc) DNA. The minus strand of the DNA is complete while the positive strand is incomplete [93]. Subviral particles (SVP) are HBV capsid enveloped particles devoid of nucleic acid (Fig. 2B). The genome encodes four overlapping open reading frames (ORFs). The first **S-ORF** encodes the viral surface envelope

proteins (HBsAg). The precore and core regions mRNA are transcribed from the second **C-ORF**, giving rise to the nucleocapsid protein (HBcAg) and the e-antigen (HBeAg) determined by distinct translation sites in the genes [94]. HBcAg mediates self-assembly of the capsid-like structure. Notably, the function of HBeAg remains undefined, yet it is being implicated as immune tolerogen and thus virus persistence promoting [95]. Clinically, HBeAg is considered as a marker for active viral replication and patient bearing elevated HBeAg amounts are highly infectious [96]. The polymerase protein is encoded by the third **P-ORF**, and its function is distributed into three domains. First, the terminal protein domain, which involves viral nucleic acid encapsidation, second, the reverse transcriptase domain initiates minus-strand synthesis from viral messenger RNA, and third the ribonuclease (H) domain, which degrades the pregenomic RNA simultaneously during the incomplete positive strand DNA synthesis [97]. The x-protein (HBx) is encoded by the fourth **X-ORF** and the function of its product is yet unclear**.** However, it was implicated in signal transduction and viral transcriptional activation in some studies [98]. Moreover, HBx has been considered as host DNA hijacking damage-binding protein 1 (DDB1) to degrade structural maintenance chromosome -5 and -6 (Smc5/6) as host restriction factor, to prevent host-derived viral DNA degradation [99].

1.2.2 HBV surface proteins (HBsAg)

HBV contains three closely related variants of the transmembrane HBsAg gene proteins that are collectively called ‘’the’’ surface protein (HBsAg). The HBsAg protein comprises a C terminus common to all the three HBsAg variants and is thus the main structural component of the viral surface proteins. The HBsAg coding sequence contains three in-frame translation start sites and a common termination codon [100]. As a result, the various HBV surface proteins are all related to each other by a shared region known as the S-domain (24 kDa) (Fig. 2C). The infectivity nonessential middle protein (M-HBsAg, 31 kDa) carries N-terminal PreS2 domain encompassing an additional 55 aa. The infectivity essential large protein (L-HBsAg, 43 kDa) encompasses an addional N-terminal extension of a 108 or 119 aa depending on genotype, named PreS1 [101]. The HBsAg on the mature HBV consists of 90% polypeptide S-HBsAg, 5-15% M-HBsAg and meerly 1-2% L-HBsAg [102]. The PreS1 domain contains at its N terminus a myristic acid moeity bound to it’s amino-terminal glycine and it is burried in the viral membrane where it positions preS1 to bind the NTCP entry receptor [103]. Collectively, the HBsAg macromolecular complex consists of ~75 % protein, 25 % lipid and N-linked carbohydrates [104]. In peripheral blood of chronic HBV patient

carrying a large amounts of circulating plasma HBsAg, TLR2-driven IL-12 production was impaired due to JNK-MAPK inhibition [105]

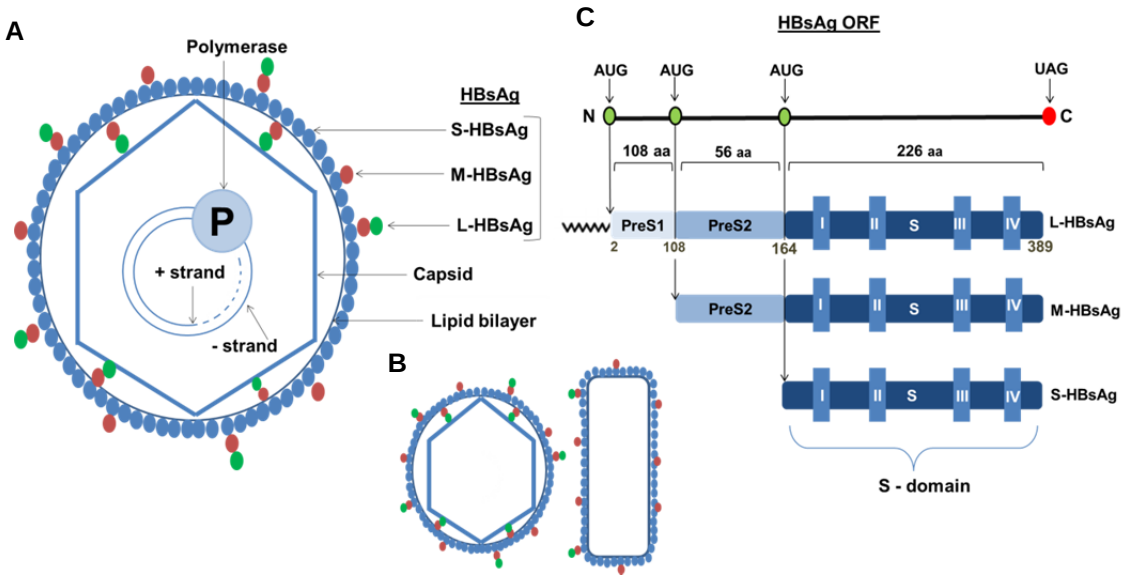

Figure 2. Morphology of HBV and surface protein open reading frames (ORFs). [**A**] The icosahedral capsid is surrounded by a lipid bilayer in which HBV surface proteins (L, M, S) are anchored as transmembrane domains. Mature HBV particles contain incomplete dsDNA to which viral polymerase is attached. [**B**] The small noninfectious enveloped capsid spherical or filamentous shape subviral particles (SVP) are devoid of viral nucleic acid [**C**] The HBsAg protein cds contains three in-frame translation initiation sites comprising a common C terminal and three different N terminal domains. N terminus is myristoylated (depicted in C as zigzag line) and the aa 9-18 epitope is the binding site for NTCP receptor. The aa 99-170 domain is a most immunogenic epitope to which α-L-HBsAg antibodies usually bind [106].

1.2.3 HBV replication

A prerequisite of the start of the HBV life cycle is the viral attachment to host cells by the PreS1 domain of L-HBsAg to the NTCP receptor [107]. Consequently, the virus translocates into the cytoplasm, where the nucleocapsid disassembles to release and translocate the viral genome into the nucleus. Upon viral genome delivery into the nucleus, the single-stranded gap region in the viral genome is repaired by the host enzymatic DNA repair enzyme upon which the viral DNA is circularized to form the covalently closed circular (ccc) DNA [108]. The HBV cccDNA serves as the template for transcription of genomic and sub-genomic RNAs and acts as stable reservoir for viral replication replenishment and confers resistance to antiviral therapy aimed at viral clearance. The genomic transcripts belong to two species, namely the pregenomic- and four subgenomic RNAs.

The 3.5-kb pregenomic RNA (pgRNA) acts as mRNA encoding both core and polymerase protein. It serves as template for reverse transcription by the viral polymerase. The

polymerase translation is initiated at the 5' end of the pol start codon of the pgRNA and at the same time the capsid protein is translated and simultaneously encapsidated. Within the viral capsid, the polymerase catalyzes the reverse transcription of the pgRNA into minus-strand DNA and subsequently positive-strand synthesis. The circular DNA is synthesized via several steps of strand transfer and primer translocation [109]. The cytoplasmic 2.4-kb subgenomic RNA encodes the L-HBsAg, whereas the 2.1-kb subgenomic RNA mediates both the M-HBsAg and S-HBsAg proteins translations. The subgenomic 0.7-kb RNA encodes the HBx protein. The nucleocapsid is formed by the envelope proteins within the ER which is secreted as mature virion upon nucleic acid and polymerase uptake towards the extracellular milieu (Fig. 3).

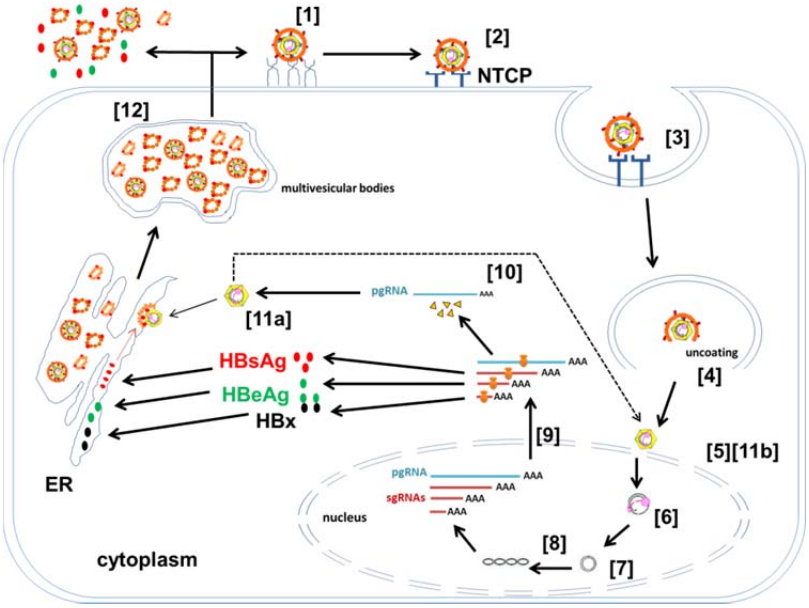

Figure 3. HBV replication cycle. The HBV attaches to hepatocytes via heparan sulfate proteoglycan receptor (*1*) and binds to NTCP receptor (*2*) upon which it is endocytosed (*3*). The uncoated virus envelope is uncoated (*4*) and the nucleocapsid translocates to the nucleus (*5*). Releases of viral dsDNA (*6*) and fill up of the incomplete dsDNA and cccDNA synthesis (*7*). Transcription of HBV genome to four mRNA transcripts (*8*) and transfer of mRNAs to the cytoplasm (*9*). Translation of pgRNA into capsid protein and mRNA reverse transcription by viral polymerase (*10*). Translation of other subgenomic sgRNAs and transport to the ER (*11a*). Retransport of the capsid back to the nucleus for viral DNA replenishment (*11b*) or translocation to the ER for capsid envelopment. Enveloped capsids or empty SVPs are released by infected cells (*12*) [110] .

1.2.4 Immune responsiveness to HBV

HBV infection is cleared by 95% of infected adults while merely 5% of them succumb to chronic HBV infection. On the contrary, newborns infected vertically by their HBV^+ mothers prior to or during birth and infected children below 12 years of age fail to clear infection in 90% of cases which consequently suffer chronic infection [111]

According to a common view, HBV is a ''stealth virus'', comprehensively escaping innate immune surveillance. Accordingly, HBV infected chimpanzee and prospectively acutely infected humans failed to induce IFN-related gene activation [112] and also in L-HBsAg positive patients an immune response was virtually non-detectable [113]. The adaptive immunity mainly executed through $CD8^+$ T cells is essential for HBV clearance. However, infected hepatocyte HBV clearance in naturally infected humans and chimpanzees was $CD4^+$ and $CD8^+$ T cells dependent [114][115][116]. Moreover, CD4-deficient mice failed to clear intrahepatic HBV, implicating a role of $CD4^+$ T cells in the HBV elimination [117]. Also, Fas and IFN-γ counteract HBV infection through modulation of the $CD8^+$ T cell response [117]. Importantly, $CD8^+$ T cell depletion from HBV-infected chimpanzees rendered them viral clearance incompetent [118]. Chronic HBV patient transplantation with naturally immune donor bone marrow conferred clearance of chronic HBV infection [119]. Antibodies against HBV proteins at high levels mediate anti-viral immunity [120]. Raising of antibodies towards the preS1-polypeptide of L-HBsAg enabled HBV carrier mice to clear experimental chronic infection [121]. Comprehensively, the importance of adaptive immunity towards successful viral clearance is obvious.

Since HBV infection is usually diagnosed weeks after the occurrence of infection, when the virus has already escaped the early innate immunity and viremia is peaked up [122], the contribution of innate immunity is therefore often overlooked. However, the innate immunity to HBV infection has been correlated with TRIF and MAVS expression since abrogation of them or overexpression interfered with viral carriage in the hepatocytes [123]. Furthermore, therapeutic vaccination of HBV transgenic mice with TLR ligands suppressed HBV replication in hepatocytes [124]. These studies implicate activation of innate immunity as means to control HBV infection.

1.2.5 Host recognition of HBV

Reports on innate host recognition of HBV are scarce and in some cases contradictory. The cytoplasmic RNA sensor MDA5 recognized a HBV-derived RNA motif transfected into immortalized hepatic huh7 cells [125]. Two years later, exclusively RIG-I mediated dependent HBV-derived RNA recognition [126]. Specifically, the εRNA region, forming the 5' terminus of HBV pregenomic RNA and a secondary loop structure to bind viral polymerase during initiation of reverse transcription is the RIG-I ligand. Here RIG-I mediated its effect in an IFN-III, namely IFN-λ dependent manner in hepatocytes towards antiviral effector activity. Moreover, recognition of nuclear HBV cccDNA was mediated by the DNA

sensor IFI16 upon binding of cccDNA to IFI16 and this complex translocates to the cytoplasm and undergoes degradation [127]. A collaborative study performed previously by colleagues in collaboration with us implicated $CD8^+$ T cell-mediated HBV clearance from hydrodynamically HBV expression plasmid injected mice [128]. Accordingly, MyD88, TRIF, and IRAK4 KO HBV-infected mice displayed significant increases of HBV-specific serum markers, namely HBsAg and HBeAg, as compared to their wild type (wt) controls 10 days post injection (Fig. 4). Importantly, secretion of cytokines such as TNF and IFNγ by $CD8^+$ T cells, as prerequisite cytokines for effector clearance of HBV, was significantly reduced in *Tlr2*$^{-/-}$ as compared to wt controls (Fig. 4B). These results imply a potential role of TLR2 as mediator of HBV clearance.

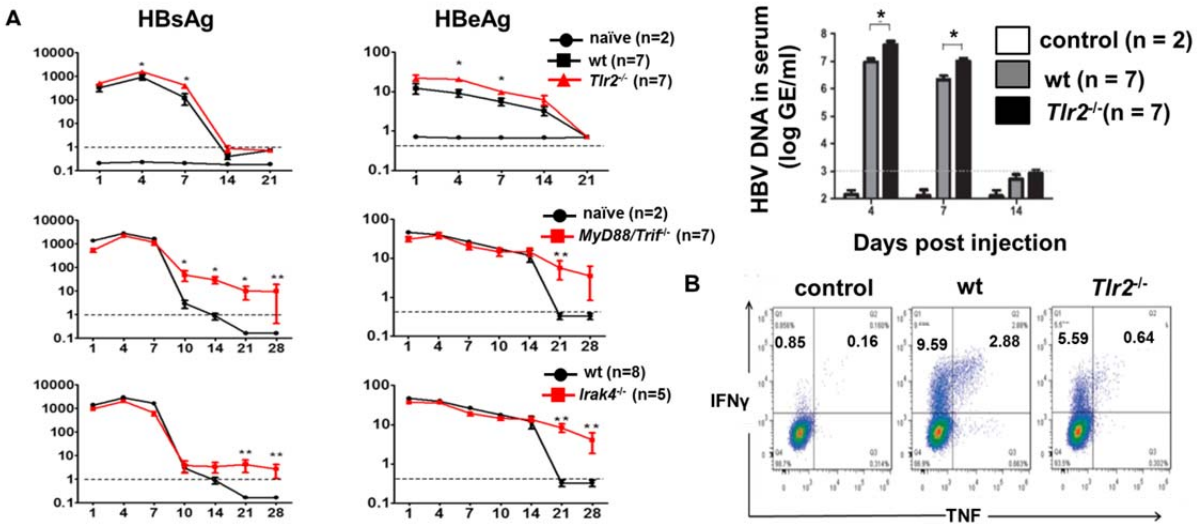

Figure 4. Enhanced HBV replication in *Tlr2*$^{-/-}$ and increased degree in *MyD88/Trif*$^{-/-}$ and *Irak4*$^{-/-}$ mice. [**A**] Intravenous hydrodynamic injection (HI) of plasmid encoding HBV (pSM2 plasmid) or PBS into wt and KO's mice upon which serum levels of HBsAg (left) or HBeAg (right) were analyzed by ELISA and HBV DNA quantification using real-time PCR at the indicated time points after HI. [**B**] HBV-specific blood $CD8^+$ T cells activation post HI was assessed by intracellular cytokine measurement upon 5 h stimulation *ex-vivo* with HBV envelope and capsid epitopes; Env190–197 or Cor93–100. Error bar represent the standard error of mean (SEM) [128] .

1.3 Types of post translational protein modification

Bacterial proteins are N-terminally mono-, di- and tri-acylated (section 1.1.4.1). These modifications alter biological activities of modified protein. For instance, protein folding, interaction, localization, and protein antigenicity are affected [129]. Phosphorylation, methylation, hydroxylation, ubiquitination, glycosylation, hydroxylation, disulfide bonding, and acylation (lipidation) are examples of protein modifications operative in eukaryotes and

prokaryotes [130]. For instance, up to 80% human cellular proteins are acylated [131]. Protein acylation is further sub classified into four major types, namely cholesteroylation, prenylation, glypiation and acylation. Cholesteroylation is an autocatalytic process which involves esterification of the C-terminus of a given protein with a cholesterol molecule [132]. Protein prenylation is a thioester bond formation between protein cysteine residues and either farnesyl or geranylgeranyl isoprenoids by prenyl transferase [133]. Glypiation is anchoring a glycosylphosphatidylinositol (GPI) to a protein's C-terminal cysteine residue by a transaminidase [134]. For instance, *Plasmodium* derived GPI is considered as a major driver of malaria pathology through TLR2 and TLR4 activation upon its release from ruptured infected red blood cells [135].

Protein acylation is the covalent attachment of fatty acids such as myristic acid (14 carbons) or palmitic acid (16 carbons) or other fatty acids to the N or C termini of or intra-molecularly to a protein. Like in prokaryotic bacteria (section 1.1.4.1), N terminal protein myristoylation occurs in eukaryotic cells and is operative also for viral proteins. Example are the myristoylation of the HBV surface protein (L-HBsAg), HIV NEF protein [136], and friend murine leukemia virus (FMuLV) gag protein [137]. Protein acylation is S, N, or O mediated. **S-acylation** is cysteine thioesterification. **N-acylation** is amide bond formation by a fatty acid with an N-terminal glycine in eukaryotic and cysteine or lysine in prokaryotic cells. Intramolecular serine or threonine tends to become **O-acylated** upon esterification [138]. N-myristoylation is the most common acylation in eukaryotic cells and operative even towards apoptosis during which caspases cleave specific proteins to expose their N terminal glycine residue to become acylated by N myristoyl transferase enzyme (NMT) [139].

1.3.1 Fatty acid synthesis

The fatty acid synthase cycle (FASC) takes place in the cellular cytoplasm and in eukaryotes employs fatty acid synthase (FAS) I which catalyzes all reactions in cyclical loops towards production of saturated fatty acid (Fig. 5) [140]. Acetyl-CoA and malonyl-CoA form the first condensate for chain extension involving CO_2 release. A ketone structure is then reduced by forming hydroxyl groups to subsequently become dehydrated upon which the C-C double bound is reduced. Successive repetition results in myristate and palmitate formation. For protein N-terminal acylation, myristoyl-CoA (myr-CoA) is activated by coupling of CoA to it in an ATP-demanding manner.

1.3.2 N terminal acylation in eukaryotes

Approximately 0.5-0.8% of total translated proteins in eukaryotes are myristoylated such as to facilitate cell membrane anchorage [141]. Myristoylation is strongly enhanced upon LPS challenge [142] and regulated by three enzymes in eukaryotic cells, namely methionyl-aminopeptidase, acyl-CoA synthetase and NMT. First the N terminal aa methionine (Met) is cleaved by methionyl-aminopeptidase to expose the position two aa glycine (Gly) at the N terminus. The coenzyme acyl-CoA synthetase activates the myristic acid CoA complex. The carbonyl group is positioned in the binding pocket, namely to the aa residues phenylalanine position 170 and leucine position 171 of NMT. The net positive charge on the carbonyl group allows nucleophilic attack of the glycine residue of the target protein. After amidic bond formation of the myristoyl moiety and the protein, CoA is released upon which NMT undergoes a conformational change to release the myristoylated polypeptide. Eukaryotic N terminal glycine monomyristoylated proteins are represented by a synthetic acyl-hexapeptide employed by us namely Myr_1GSK_4 (see next Fig.10A)

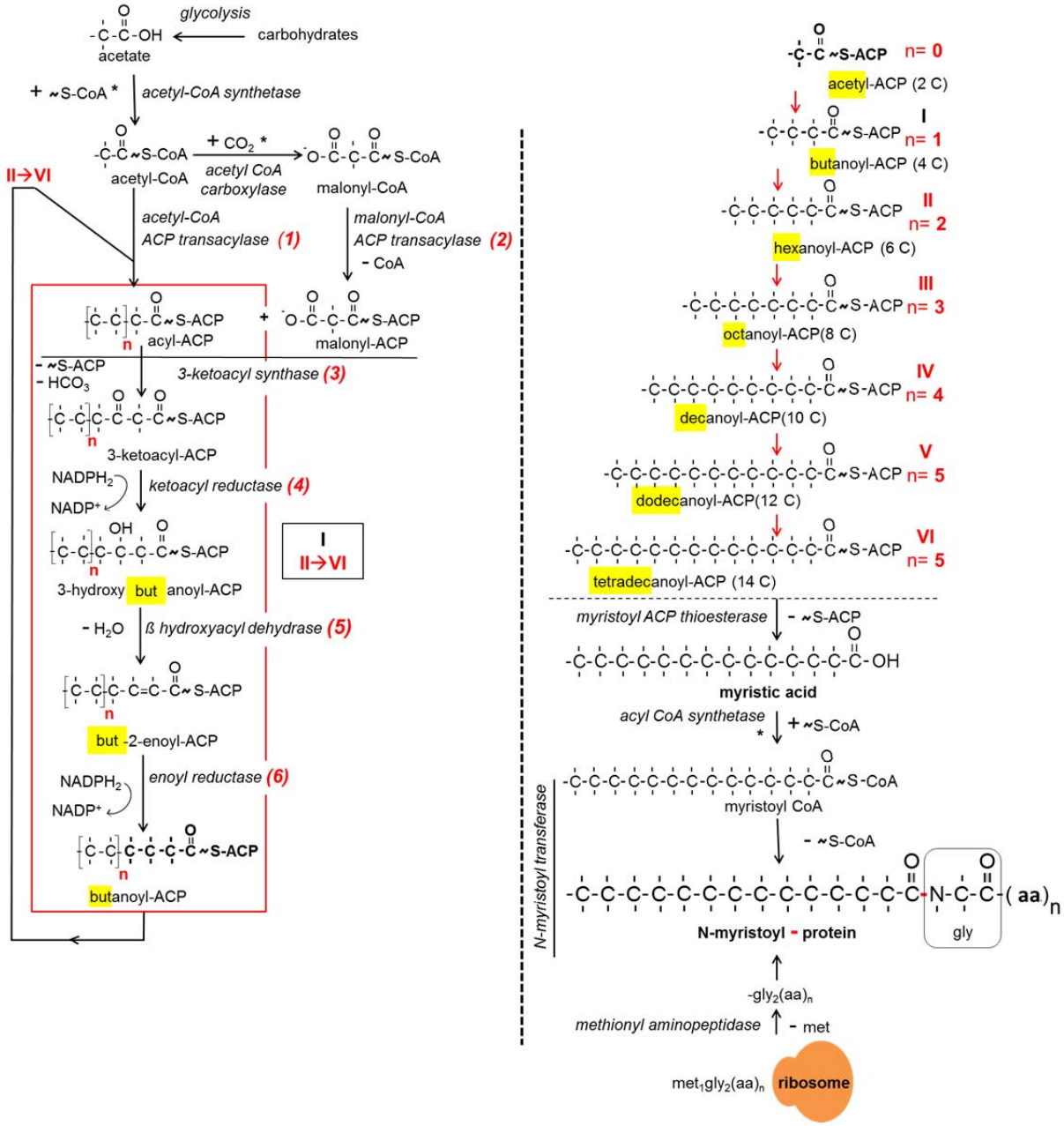

Figure 5. Fatty acid synthesis towards post translational N-terminal protein myristoylation. A post-glycolytic-pathway metabolite ''acetate'' is derivatized towards acetyl-CoA and malonyl-CoA. Both interact to extend the fatty acid backbone by 2 carbons through each reaction cycle repetition. *''I-VI''* represents numbers of reaction cycles (*left*) and resulting products (*right*). (*1-6*) illustrate each step of an individual reaction cycle (*left*). (*n*=) indicates the number of C-C carried upon step *6* in each cycle beyond the C-C carried by the initial acetyl-CoA already. N terminal coupling of myristoyl moiety to glycine is catalyzed by N myristoyl transferase. (Yellow box indicates successive extensions, ACP: acyl carrier protein, *: ATP → ADP + Pi, aa: amino acid, met: methionine, gly: glycine).

1.3.2.1 Myristoylated alanine-rich protein kinase C substrate (MARCKS) is and endogenous eukaryotic and stress inducible myristoylated proteins

MARCKS is the target substrate of protein kinase C (PKC), which shuttles between the plasma membrane and the cytoplasm [143]. MARCKS is highly expressed in the brain, spleen and lung and mediates biological functions such as cell adhesion and motility, inflammation, and phagocytosis [144]. Phosphorylation of MARCKS might be constitutive, yet its expression and myristoylation, beside phosphorylation is increased upon encounter of cell stress such as by being elicited by LPS challenge. [145][142]. Phosphorylation of MARCKS was induced by high mobility group box 1 (HMGB1) exacerbate Alzheimer pathology [146] which might be accompanied by increased myristoylation.

1.3.3 Protein fatty acid acylation in prokaryotes

Also in bacteria, protein acylation at the N terminus enables protein anchorage to the bacterial cell membrane phospholipid. Bacterial acylated proteins are critical for bacterial survival through mediating of nutrient uptake, signal transduction, adhesion and bacterial sporulation. They are also involved in bacterial antibiotic resistance [147]. Three enzymes are required for protein acylation in prokaryotes, namely diacylglyceryl transferase, lipoprotein signal peptidase and apolipoprotein N–acetyl transferase. In prokaryotes, the position two aa must be cysteine to qualify a protein as potentially acylatable with up to three fatty acid such as palmitic acid. Gram-positive bacteria derived lipoproteins often carry merely two lipid chains because they lack the amide-linked lipid chain [148].

1.4 Aim of the thesis

Previous data of us and others suggest a role of TLR2 not merely in therapy but also intrinsic anti HBV defense in mice *in vivo*. HBV clearance was largely abrogated in *Myd88/Trif*$^{-/-}$ and *Irak4*$^{-/-}$ mice and substantially delayed in *Tlr2*$^{-/-}$ mice (Fig. 4). Genetic loss of function by *Tlr2* mutation in human predisposes pathology for HBV similar to *Tlr2*$^{-/-}$ mice upon HBV hydrodynamic injection, in which these patients suffer from elevated serum alanine aminotransferase (ALT) levels and necroinflammation of the liver as compared to healthy individuals [149]. On the background of these evidences, the aim of my project was to identify an HBV recognition receptor(s) and the responsible HBV products.

The first part implicates TLR2 in HBV recognition, N-terminally myristoylated proteins, such as L-HBsAg, NEF-HIV, Gag-FMuLV, and endogenous MARCKS, as respective TLR2 activating P/DAMP. Furthermore, the assignment of a stimulatory P/DAMP function to N-

terminally myr-C moieties of lipoproteins is supported by analysis of impacts such through application of N-terminal protease, inhibition of myristoylation through N myristoyl transferase (NMT) inhibitor (Tris-DBA), or enhancement of protein myristoylation through NMT and myristoyl-CoA substrate application on murine and human immune cell activation. HBV immune properties of wt or mutant (L-HBsAg-G2A) were extensively studied – myristoylation-less mutant HBV lacked L-HBsAg driven immune stimulatory capacity. Characterizing the virus production, integrity and infectivity in hepatic cell line between both genotypes was performed.

The second part focuses on visualizing and quantifying protein N-terminal myristoylation *in situ*. Quantitative and qualitative detection of protein myristoylation through click chemistry and urea-tricine high percentage PAA gel electrophoresis was conducted.

The third part comprehends results performed to uncover the possible host nucleic acid PRR(s) involved in HBV DNA and RNA recognition. Here purified DNA and RNA isolated from HBV were studied.

Finally, the fourth part of the result verified the hypothesis that advocates an impairment of innate immunity as reason for failure to clear vertical HBV infection in newborns rather than toleration of the adaptive immunity. Umbilical cord blood obtained from healthy mother probands and healthy volunteer's adult blood were comparatively analyzed for HBV, TLR ligands and bacteria challenge responsiveness.

2. Materials and Methods

2.1 Materials

2.1.1 Equipment

Name	Supplier
Agarose gel cast stand	Bio Rad
Agarose gel electrophoresis chamber, Sub Cell	Bio Rad
Cell incubator, HERA cell	Thermo Scientific
Centrifuge, Heraeus Fresco 17	Thermo Scientific
Chemiluminescence imaging, Fusion Fx7	Vilber
EDTA K-tubes 2 ml	Sartedt
Electrophoresis chamber, Mighty Small SE250/260	Hoefer
Exhaust pump	Knf lab
Fastprep®-24 Instrument	MP Biomedical
JEM-1400 Plus Electron microscope	JEOL
Luminex® 200™ System	Luminex
Luminometer, Orion II	Berthold
Magnetic stirrer, SB 162	Stuart
Microplate-reader, Epoch	BioTek
Microplate-washer, 12-well	BioTek
Microscope, Axiovert 40C	Zeiss
Microwave MW 800	Continent
Mini centrifuge	Biozym
Multifuge X3R Haereus	Thermo Scientific
NH4- Heparin 9 ml tubes	Sartedt
pH-meter	Mettler
Pipettor	Hirschmann, Brandt
Pipetts	Eppendorf, Gilsen
Power supply	Bio Rad, Hoefer

Real-Time PCR-system 7500 Fast	Applied Biosystems
Refrigerator/freezer	Liebherr
Scale, Acculab	Sartorius group
Semi-dry Trans-Blot® TurboTM	Bio Rad
Shaker, Polymax 1020/1040	Heidolph
Shaking incubator, KS 400i	IKA
Sterile work bench, HERA safe	Thermo Scientific
Thermocycler	Eppendorf
Thermomixer	HCL Toledo
Tube roller, RM5	CAT
TC Flask T75,Standard	Sartedt
Ultrasonic bath Ultrasonic Clean	VWR
Ultrasonication bath	Clean VWR
UV-gel documentation system	Intas UV-System
Voltage supply	Bio Rad, Hoefer
Vortex mixer, VTX-3000L	LLG
Water bath	GFL
Water ultrapurification system, Easypure II	Werner

2.1.2 Kits

BCA Protein Assay Kit	Pierce
Click chemistry	Thermo Fisher
ELISA DuoSet	R&D Systems
NucleoBond Xtra Maxi Plus	Macherey-Nagel
OptEIA TMB Substrate Reagent Set	BD Biosciences
PCR purification kit	Stratec
peqGOLD Plasmid Miniprep Kit I	peqLab
Phusion HF polymerase	NEB
QIAamp DNA Blood Mini Kit	Qiagen
QIAquick Gel Extraction	Qiagen

Restriction enzymes (fast digest)	Thermo Fisher
Silver nitrate staining kit	Serva
Luminex assay kits	Luminex

2.1.3 Chemicals and solutions

Accutase	PAA
Acrylamide	Sigma-Aldrich
Adenosine-5`-Triphosphate	Sigma-Aldrich
Agarose	Roth
Alkyne-Biotin	Thermo Fisher
Ammoniumperoxide sulfate	Roth
Ampicillin	Sigma-Aldrich
Antibiotic / Antimycotic (AA)	PAA
Bafilomycin A1	Sigma-Aldrich
Beta-Mercaptoethanol	Sigma-Aldrich
Blasticidin	Invivogen
Bovine serum albumin (BSA)	Sigma-Aldrich
Calcium chloride	Roth
Chloroform	Roth
CL075 (3M002)	Invivogen
Click chemistry protein reaction buffer	Thermo Fisher
Competent cells DH5a	Invitrogen
Coomassie blue	Thermo Fisher
CpG-DNA (1668) / (2006)	MWG Eurofins
Deoxy ribonucleotide (dNTPs)	Thermo Fisher
Diethyl pyrocarbonate (DEPC)	Thermo
Dimethyl sulfide (DMSO)	Sigma-Aldrich
D-Luciferin	PJK
DMEM medium	Gibco
DNA Ladder 1kb	Thermo Scientific

DNA Loading buffer 5x	Thermo Scientific
DNaseI, RNase-free	Sigma-Aldrich
EDTA disodium salt dehydrate	Sigma-Aldrich
Ethanol 70% (EtOH)	Pharmacy, UK Essen
Ethanol, absolute 99,8% (v/v) (EtOH)	Lab Supply
Ethylendiamine tetra-acetate (EDTA)	Roth
Fetal Calf Serum (FCS)	Gibco
Ficoll® Paque Plus	Sigma-Aldrich
Flagelline	Invivogen
G418 Neomycin	PAA
Glucose	Sigma-Aldrich
Glutaraldehyde	Sigma-Aldrich
Glycerol	Roth
GM-CSF containing supernatant	own production
HEPES	PAA
Hydrochloric acid	Roth
Incidin	Ecolab
Interferon γ, recombinant murine/ human	Peprotech
Isopropanol	VWR
Kanamycin	Stratagene
Lipopolysaccharide, E. coli 0111:B4	Sigma-Aldrich
Loxoribine	Invivogen
Magnesium carbonate hydroxide	Sigma-Aldrich
Magnesium chloride	Roth
Magnesium sulfate	Roth
Methanol	Merck
Multicolor Low Range Protein Ladder	Thermo scientific
Myristic acid-azide	Thermo Fisher
MyristoylCoA lithium salt	Sigma-Aldrich
MyrGSK4 (Myristoyl Glycinyl-Seryl-etralysin)	Microcollections

N,N′-Methylenebis(acrylamide)	Sigma-Aldrich
Nonident P-40	Roth
Nonessential aminoacid (NEAA)	Gibco
Normal Goat Serum (NGS)	Invitrogen
Opti-MEM Glutamax	Invitrogen
PBS, Dulbecco, sterile	Gibco
PBS, Dullbecco, dry substance	Biochrome
Penicillin-Streptomycin (PS)	PAA
Phorbol-12-myristate-13-acetate (PMA)	Sigma-Aldrich
Phosphatase Inhibitor	Calbiochem
Phosphoric acid (H_3PO_4)	Sigma-Aldrich
Polyinosinic:Polycytidylic Acid (PolyI:C)	Sigma-Aldrich
Postassium Chloride	Roth
Potassium hydrogen Phosphate (K_2HPO_4)	Merck
Primers, PCR	MWG Eurofins
Reporter lysis buffer	Promega
Resiquimod (R848)	Invivogen
RiboRuler high range RNA Ladder	Thermo Fisher
RiboRuler low range RNA Ladder	Thermo Fisher
RNA gel Loading Dye (2X)	Thermo Fisher
RNA, 5'ppp-dsRNA	Invivogen
RNase away spray	VWR
Roti store cryo-tube	Roth
Roti-Aqua-Phenol	Roth
RPMI medium	Gibco
Sodium azide	Roth
Sodium chloride	Roth
Sodium dodecyl sulfate (SDS)	Roth
Sodium orthovanadate	Roth
Sodium phosphate (Na_2HPO_4)	Roth

ssRNA40/Lyovec	Invivogen
Streptavidin-HRP [ELISA]	R&D system
Sulfanilamide	Sigma-Aldrich
Sulfuric acid (H_2SO_4)	Roth
SybrSafe	Invitrogen
TLR2 antibody (clone T2.5)	Hycult
TMB ELISA substrate reagent set	BD Bioscience
Tri reagent (Trizol)	Sigma-Aldrich
Trichloroacetic acid (TCA)	Roth
Tricine	Roth
Tris	Roth
Tris/HCL	Sigma-Aldrich
Tris-Tricine/SDS Electrophoresis Buffer (10x)	Serva
Trypsin (1x in PBS)	PAA
Tween 20	Roth
Urea	Roth

2.1.4 Primers

Primers used for HBV protein sub-cloning (wt/G2A-L-HBsAg/-preS1)

FS_for_HBV	5-GCTCCACCGCGGTGGCGGCCGCGCCACCATGGGGCAGAATCTTTCCAC-3
FS_mut_HBV	5-GCTCCACCGCGGTGGCGGCCGCGCCACCATGGCGAGAATCTTTCCAC-3
Rev_Nter_S	5-AGTTTGGTGGAAGGTTGTGGAATTCCACTGCATGGCCT-3
F_Cter_S	5-CCTCAGGCCATGCAGTGGAATTCCACAACCTTCCACCAA-3
Rev_Cr_S	5-CATCCTTGTAATCCTCGAGGTCGACAATGTATACCCAAAGACAAAAG-3
Rev_pre	5-CATCCTTGTAATCCTCGAGGTCGACGGCCTGAGGATGAGTGTTT-3

Primers used for site directed mutagenesis

HBV_SDM_for	5-GCATGGCGCAGAATCTTTC-3
HBV_SDM_rev	5-TGTAGATCTTGTTCCCAAG-3
MARCKS_SDM_for	5-CATGGCTGCCCAGTTC-3
MARCKS_SDM_rev	5- GTGGC GGATCCGCCCGG -3

Primers used for HBV PCR / qPCR

HBV_forw1811	5_-GCTCAAGGAACCTCTATG-3
HBV_ rev1812	5_-TGTTGTACAGACTTGGCC-3
HBV1745fw	5′-GTTGCCCGTTTGTCCTCTAATTC-3
HBV1844rev	5′-GGAGGGATACATAGAGGTTCCTTGA-3

2.1.5 Oligonucleotides and peptides

myr/ non-myr 47pep-(+/- biotin)	EMC Microcollections
myr/ non-myr 6pep-(+/- biotin)	EMC Microcollections
$MyrGSK_4$	EMC Microcollections
myr/ non-myr NEF (LHP)	EMC Microcollections
myr/ non-myr MARCKS (LHP)	EMC Microcollections

2.1.6 Enzymes

Accutase	PAA
Trypsin	PAA
Polymyxin acylase	Sigma-Aldrich
α aminopeptidase	Sigma-Aldrich
DNase I	Sigma-Aldrich
RNase A	Sigma-Aldrich

2.1.7 Immunoprecipitation (IP)

Anti-FLAG® M2 Magnetic Beads	4% agarose beads recognizing FLAG sequence. Used for immunoprecipitation of flag-tagged overexpressed protein (Sigma Aldrich #M8823).

Pierce™ Protein A/G Magnetic Beads	Binding of protein A and G on one bead towards antibodies IgG domains. Used for immunoprecipitation of endogenous/overexpressed proteins – (Santa Cruz - #sc-2003)

2.1.8 Cell lines

HEK293	Adherent, Human embryonic kidney cells, fibroblast like cell line, ATCC: CRL-1573.
HepG2	Adherent, Human origin from hepatocellular liver carcinoma, ATCC: HB-8065.
HepG2.215	Adherent , HepG2 cells expressing HBV, [150]
Huh7-NTCP	Adherent, Huh7 cells expressing the NTCP receptor
THP-1	Suspension, human monocytoid cell line, originate from acute monocytic leukemia, ATCC: TIB-202

2.1.9 Bacterial strains and media

DH5alpha : (Hanahan 1985) (Invitrogen)

LB-medium	**LB plates**
10 g/l Bacto-Trypton, 5 g/l yeast extract, 10 g/l NaCl, pH 7,0 (NaOH), Autoclaved, Add corresponding antibiotics: 100 mg/l Ampicillin or 50 mg/l Kanamycin	10 g/l Bacto-Trypton, 5 g/l yeast extract, 10 g/l NaCl, 20 g/l Agar, pH 7,0 (NaOH) Autoclaved, Add corresponding antibiotics: 100 mg/l Ampicillin or 50 mg/l Kanamycin

2.1.10 ELISA

Murine ELISA kits	Human ELISA kits
TNF , IL-6 KC IL-10, IL-1α, IL-1β, IFN-λ	TNF, IL-6, IL-8,IL-10,IL-1α, IFN-λ, IL-1β

2.1.11 Luminex assay

Mouse cytokines/ chemokines

IL-6, CCL2, CXCL1, IL-33, TNF, MIP2, IL-1α, IL-1β, G-CSF

Human cytokines/chemokines

TNF, IL-6,IL-8, IL-10,MCP, IL-1α, IL-1β

2.1.12 Antibodies for western blot

Name	Species	Dilution factor	Producer
Anti-PreS1	Mouse monoclonal	1:500	Santa Cruz
Anti-L-HBsAg	Mouse monoclonal	1:500	Santa Cruz
Anti-Flag	Rabbit polyclonal	1:1000	Sigma Aldrich
Anti-MARCKS	Rabbit polyclonal	1:500	Abcam
Anti-MARCKS	Mouse monoclonal	1:500	Santa Cruz
Anti-gag P30	goat	1:5000	AG W.Bayer
Anti-envelope P70	goat	1:5000	AG W.Bayer
Anti-HBcAg	Mouse monoclonal	1:500	Santa Cruz
Anti-rabbit-HRP	Secondary antibody	1:5000	Thermo Fischer
Anti-mouse-HRP	Secondary antibody	1:5000	Thermo Fischer
Streptavidin-HRP	Secondary antibody	1:5000	Santa Cruz
Anti-goat-HRP	Secondary antibody	1:5000	Santa Cruz

2.1.13 Inhibitors

Name	Working concentration	Source
Chloroquine	5-10 µg/ml	Sigma Aldrich
Anti TLR2 (T2.5)	20 µg/ml	Hycult biotech
Anti TLR4 (3C3)	20 µg/ml	Hycult biotech
Polymyxin B	10 µg/ml	Sigma Aldrich
Tris-DBA	15 µM	Tocris

2.1.14 Vector constructs

Empty vectors

Name	Characters	Source
pRK5	P CMV, P SV40, P SP6, SV40 pA, pUC ori, ampR, lacZ, lacI, FLAG. Expression vector flag tagged 3' at of MCS.	U. Schindler

Cloned vectors

Name	Construct	Source
pFlag-CMV-1 mTLR2	Contains the complete cds of mTLR2. Cloned through NotI und BamHI restriction enzymes (RE).	C. Kirschning H. Wesche
pFlag-CMV-1 hTLR2	Contains the complete cds of hTLR2 (without leader sequence). Cloned through NotI und BamHI RE.	C. Kirschning H. Wesche
pFlag-CMV-1 mTLR3	Contains the complete cds of mTLR3. Cloned through NotI und SalI RE.	C. Kirschning H. Wesche
pcDNA3-mTLR9	Contains the complete cds of mTLR9. Cloned through NotI and SalI RE.	S. Bauer
mRIG-I	Contains the complete cds of mRIGI.	A. Krug
mMDA5	Contains the complete cds of mMDA5.	A. Krug
pFlag-CMV-1 hTLR8	Contains the complete cds of hTLR8.	C. Kirschning
6x NF-κB-TK-luc	Contains the reporter gene for luciferase upstream sequence of 6 NF-κB binding sites.	C. Kirschning
pIFNβ-luc	Contains the reporter gene for Luciferase upstream of the promotor sequence IFNβ.	A. Krug
pHBV1,3-wt	Contains 1,3 fold of the HBV genome. Cloned through Sac1 and HindIII RE.	M. Lu
pHBV1,3-G2A	Contains 1,3X fold of the HBV genome with G2A mutation.	Own work
pSM2-HBV	Contains dimers of HBV genome (ayw2) into pMac5-8 backbone vector the two genomes were cloned together through EcoRI RE.	[151]
pCMV-Tag4A hMARCKS	Contains the complete cds of human MARCKS through BamH1 and EcoR1RE.	K.Wurzenberger
pCMV-Tag4A hMARCKS-G2A	Contains the complete cds of human MARCKS with G2A mutation.	Own work
pCMV-Tag4A hNMT1- FL	Contains the complete cds. of hNMT.	K.Wurzenberger
pcDNAp65Gag	Contain FMuLV gag P30 protein full length. Virus clone FB29.	W. Bayer

pcDNAp65GagG2A	Contain FMuLV gag P30 protein full length with G2A. Virus clone FB29.	W. Bayer
pcDNAFMuLV_envelope	plasmids encoding the FMuLV proteins Env under control of the cytomegalovirus immediate early promoter	U. Dittmer W. Bayer

2.1.15 Mice

All mice inbred were maintained in a specific pathogen-free condition at the animal facilities of the University Clinic, Essen. The knockout strains were backcrossed at least 9 times at the background of C57Bl/6. Animal experiments were approved by the state office for nature, environment, and consumerism of North Rhine-Westphalia, Recklinghausen, Germany (G1230/11). For *in vivo* analysis, mice sensitization (shock model) was applied by intravenous injection of 1,25 µg/mouse IFNγ (Peprotech) and, 45 min later, 20 µg intraperitoneal α-D-galactosamine (0.8 g/kg) plus 10 µg Myristoylated 47 lipopeptides (M47pep) or 20 µg myristoylated 6 lipopeptides (M6pep).

2.1.16 Software & analysis tools

Blast	NCBI
Gene5	Bio-Tek
Illustrator, Photoshop, Acrobat	Adobe
Prism	GraphPad
Serial cloner	Serial Basics
Simplicity 4.2	Berthold
Windows office	Microsoft
Mendeley	Elsevier

2.2 Methods

2.2.1 Molecular biology

2.2.1a DNA isolation from eukaryotic cells

Genotyping of the mice was achieved by DNA isolation of a small piece the tail tip. The tail was digested by incubation with 500 µl tail buffer and (100 µg/ml) proteinase K and left overnight (o/n) at 55°C with shaking. A day later, maximum centrifugation for the digested suspension was done for 10 min and the supernatant containing DNA was transferred to a

new tube and an equal volume of 2-propanol was added to precipitate the DNA and this was pelleted by maximum centrifugation for 10 min. The DNA pellet was washed twice with 70% EtOH, air dried and resuspended in 400 µl water.

2.2.1b Plasmid isolation from bacteria

Plasmid DNA was isolated from bacteria (DH5α) on small or large scale using Mini- or Maxiprep kits. The choice depends on the purpose of DNA plasmid isolation. Instantly, for sequencing check after sub-cloning, Miniprep kit was initially used, and by confirming the desired sequence, Maxiprep kit was used. For DNA plasmid Miniprep isolation, a single bacterial colony was picked from the LB agar plate and transferred to 6 ml LB medium containing the corresponding antibiotic and was incubated at 37°C shaker at 200 rpm o/n. A day later, 3 ml of bacterial medium was applied to the DNA isolation using the provided column and the manufacture manual from peq GOLD Plasmid Miniprep KIT I (Peqlab). Maxiprep DNA isolation was done by incubating bacterial colony in 500 ml LB medium containing the corresponding antibiotic for bacterial selection. Similarly, the column-based DNA isolation was done according to the manufacture recommendation from (Macherey-Nagel).

2.2.1c Cell transfection

Different transfection reagents had been tested and used in this study to obtain the highest transfection efficacy with different applied samples.

Fugene (Promega)	**Calcium phosphate (Roth)**
(X) amount of DNA/RNA/virions, 1 ml optimem solution, 0,25% (v/v) Fugene reagent,	for 9 cm petri dish:
15 min incubation at RT	In 1,5ml eppi tube:
transfection volume : 1ml / reaction	(X) amount of DNA, 430 µl H2O, 73 µl CaCl2
	vortex and transferred by drop wise to another 1,5ml eppi containing 2X HBS solution (equal volume)
	15 min incubation at RT, transfect 1ml / reaction

2.2.1d DNA and RNA agarose gel electrophoresis

Viral DNA and RNA were run onto agarose gel for visualization and identified according to their size. For DNA, preparing the gel was achieved by mixing 1% agarose with 1x TAE

buffer and SYBR safe. Samples were mixed with 5X loading dye sample buffer electroporated at constant current of 100 voltages. As size reference, DNA marker was used. Before handling RNA, RNase away solution was used to clean up the working surface and the electrophoresis chamber and other equipment by immersing in 3% H_2O_2 solution for 30 min. RNA samples were mixed with (5x) RNA-gel loading dye. Casting the agarose gel was performed by 1X MOPS and suitable RNA marker covering the expected RNA bands was added into the gel. Samples were visualized using UV illumination (254 nm).

TAE buffer (10x) : 48 g Tris base, 11.4 ml Acetic acid, 20 ml 0.5 M EDTA, add. 1 l water, pH 8.5	**MOPS buffer (10x) :** 0.2 M MOPS, 50 mM NaOAc, 10 mM EDTA, ad 1 l DEPC water, pH 7 (NaOH)

2.2.2 Bacterial transformation

Chemical competent bacteria were used to transform DNA plasmid. *E. coli* strain DH5α was transformed into plasmid according to the manufacture recommendation. Briefly, DH5α was thawed on ice and transformed with 5 µl of DNA (10 ng-1 µg DNA) for 30 min., followed by heat-shock for 40 seconds (sec) at 42°C heat block then cooled down for 2 min again on ice and then supplemented with 900 µl LB liquid medium at RT. The bacteria was then put onto 37°C shaker for 1 h, centrifuged (5000 rpm, 5 min) and the bacterial pellet was resuspended in 100 µl LB medium and plated onto pre-warmed LB agar plate complemented with the desired antibiotic resistance encoded in the plasmid and placed in 37°C room o/n.

2.2.3 RNA, DNA and protein isolation from eukaryotic cells and HBV

For nucleic acid and protein isolations, the TRI-Reagent solution was used. TRI-Reagent contains a mixture of guanidinium thiocyanate and phenol in a monophasic layer, allowing isolation of DNA, RNA and proteins from cell lysate homogenate or viral particles. Applying chloroform after adding TRI-Reagent followed by centrifugation helps in formation of aqueous, organic and interphase layers [152]. Consequently, the upper aqueous layer contains RNA, whereas the DNA is in the interphase layer, and the protein resides in the organic phase. For RNA isolation, 1 ml of TRI-Reagent was added to cells or virus particles, vortex and then 200 µl of chloroform was added, vortex and incubated for 5 min at RT, centrifuged at 17000 g for 15 min at 4°C, resulting in phase separation. The aqueous layer was transferred to a new RNase-free tube and mixed with isopropanol by vortexing and then pelleted down by centrifugation at 17000 g, 20 min at 4°C. RNA pellet was then washed twice with 70% EtOH, air dried and then resuspended in 50-100 µl DEPC water. For DNA isolation, the DNA was

pelleted using 300 µl 100% EtOH, mixed up and incubated for 5 min, then centrifuged for 5 min at 2000 g at 4 °C. The supernatant containing protein was transferred to a new tube and the DNA precipitated as a pellet. The DNA pellet was washed twice with 1 M trisodium acetate-10% EtOH. The next step, DNA was pelleted with 2000 g for 5 min and resuspended in 75% EtOH, air dried and resuspended in 8 mM NaOH to dissolve the DNA. Finally, it was centrifuged at 12000 g for 10 min and any insoluble material in the pellet was discarded by transferring the DNA supernatant to a new tube. For protein isolation, 1.5 ml isopropanol was added to the organic phase and a sample was incubated for 10 min at RT then centrifuged at 12000 g for 10 min. The protein pellet was then washed 3 times with 2 ml of 0,3 M guanidine-HCL/ 95% EtOH and incubated each time for at least 20 min. Protein was pelleted down by 7500 g for 5 min at 4°C, air dried and resuspended in 200 µl 1% SDS-water, centrifuged at 10000 g for 10 min and any insoluble material was avoided by transferring the protein supernatant to a new tube.

2.2.4 Polymerase chain reaction

PCR reaction consists of three basic steps; denaturation, annealing and elongation. Designed complementary oligonucleotide primers in forward and reverse directions would anneal to the double stranded DNA after an initial denaturation step, then, the polymerase enzyme starts elongation by adding nucleoside triphosphate complementary to the original strand. This elongation step depends on the length of the original DNA template and the speed of the applied polymerase.

PCR reaction component	**PCR program of Thermocycler (exemplary)**	
Forward and reverse primers (0,5 µM)	1.Initial denaturation: 95°C for 2 min	
dNTP (200 µM)	2. Denaturation: 95°C for 30 sec.	25-30 cycles
DNA template (2-200 ng)	3. Annealing: 48-58°C for 45 sec.	
Polymerase (0,5 -1U)	4. Elongation: 72 for 1 min.	
PCR-buffer (1X)	5. Final elongation: 68-72°C 5 min.	
Water to a final volume of 25 µl	6. Hold at 4°C	

2.2.5 Quantitative PCR (qPCR)

The qPCR method was the standard method to quantify the HBV produced by stable or transient transfected cells. Therefore, the viral genomic DNA was isolated and served as template for specific primers targeting the viral surface protein (L-HBsAg). For quantification, a standard HBV-plasmid (pSM2) was used as reference to draw a standard curve and viral sample titer would be quantified in proportion to it. Serial dilution of the standard plasmid was calculated (10^{11}, 10^{9}, 10^{7}, 10^{5}, 10^{3}, 10 copy number/ml). The copy number calculation for the standard plasmid was achieved by calculating the plasmid mass (m) using the equation:

$$m = n \,.\, 1{,}096^{-21} \text{ (where } n = \text{plasmid size in base pair (bp))}$$

Consequently to the plasmid mass at the desired copy number/ml through the equation:

$$\text{copy number/ml} \,.\, \text{plasmid mass (m)}$$

Finally to obtain the desired copy number/ml at the desired volume, the following equation was used

$$\text{Copy number/ml} = \frac{\text{Plasmid mass at the desired copy number/ml}}{\text{Pipetting volume}}$$

Serial dilution stocks of the standard plasmid (pSM2) were prepared and stored at -80°C. DNA from HBV virion was isolated using QIAamp DNA Blood Mini Kit and according to manufacturer's instruction. Briefly, 1 ml of virions was incubated with 100 µl protease and 1 ml lysis buffer. Sample mixtures were heated at 56°C for 10 min. To dissolve the DNA, 1 ml of 100% EtOH was added to the mixtures and vortex. The mixture was then subjected to high affinity DNA column and subsequent washing steps for the column were performed and finally the DNA was eluted to clean1,5 ml eppi tube in 100 µl volume H_2O. For the qPCR reaction, master mix solution was prepared and calculated for 25 µl final reaction volume per well. At the end, the template DNA and the polymerase enzyme was added. After pipetting into the MicroAmp™ optical 96-Well reaction plate, plate was sealed with transparent plastic sheet and kept in dark and on ice till analysis.

Master mix	Thermocycler setting
- Primers (forward, reverse)	Stage Rep. Temp. (°C) Time (sec)

- Maxima SYBR Green/ ROX qPCR	1	1	95.0	00:10
- dd H2O to final volume of 25 µl	2	35	95.0	00:05
			60.0	00:30
			72.0	00:30
	3 (Dissociation)			
		1	95.0	00:15
			60.0	01:00
			95.0	00:15
			60.0	00:15

2.2.6 Sub-cloning of L-HBsAg full length and its PreS1 domain

The coding sequence of N-terminal wild type- (wt) or G2A-mutant whole L-HBsAg (WhS, 1170 aa), or the wt or G2A-mutant sequence of only the preS1 domain (324 aa) were sub-cloned into pRK5 vector, which carries a CMV promoter and encodes a flag sequence at it 3' end. Primers were designed in a way that they contain the wt DNA coding sequence of L-HBsAg a G2A mutantion by single nucleotide exchange (glycine; GGG to alanine; GCG) plus restriction site sequences Not1 (forward primers) and Sa1 (reverse primers). pSM2 plasmid encoding 2-fold-head-to-tail dimer HBV genome (genotype D) was served as template. PCR products were produced in thermocycler at the following program: initial denaturation at 95°C for 1 min, denaturation at 98°C for 20 sec', annealing at 65°C for 20 sec, and elongation at 72°C for 1,5 min (denaturation, annealing and elongation were repeated for 30 time repetitions), final elongation at 72°C for 2 min. Subsequently, PCR products were digested by respective restriction enzymes. Meanwhile, pRK5 plasmid was digested by the same restriction enzymes to form sticky ends followed by shrimp alkaline phosphates (SAP) treatment to prevent relegation of linearized vector, then loaded onto agarose gel and the empty vector was recovered from gel. PCR products and empty vector were ligated together using T4 fast ligase enzyme at 22°C for 10 min. Ligated products were transformed to DH5α. Miniprep DNA isolation was performed for DNA sequencing analysis and upon successful cloning larger bacterial transformation by Maxiprep plasmid was applied.

2.2.7 Site directed mutagenesis

For the purpose of introducing G2A mutation, in which the Glycine was substituted by Alanine aa, the Q5® Site-Directed Mutagenesis Kit was used according to the manufacture recommendation. Nucleotide substitution was achieved by introducing the nucleotide substitution in the center of the designed forward primer. The reverse primer was designed so that the 5´ ends of the two primers anneal back-to- back.

Sample	**25 µl reaction volume**	**Final Conc.**
- Q5 Hot Start High-Fidelity 2X	12.5 µl	1X
- 10 µM Forward Primer	1.25 µl	0.5 µM
- 10 µM Reverse Primer	1.25 µl	0.5 µM
- Template DNA (10 ng)	1µl	1-25 ng
- water	9 µl	

Cycling Conditions

Step	Temperature	Time
Initial Denaturation	98°C	30 sec
25 Cycles	98°C	10 sec
	50–72°C	10–30 sec
	72°C	20–30 sec/kb
Final Extension	72°C	2 min
Hold	4–10°C	

Immediately after finishing the synthesis through thermocycler, PCR products were subjected to kinase, ligase and DpnI enzymes (KLD). The kinase allows DNA phosphorylation, the ligase enable ligation/circularization while the DpnI remove original template by its recognition of methylated DNA, leaving only the new (mutant) encoding plasmid.

Sample	Volume	Final C.
PCR Product	1 µl	1X
2X KLD	5 µl	1X
10X KLD Enzyme Mix	1 µl	
Nuclease-free Water	3 µl	

2.2.8 Enzymatic protein demyristoylation

To deacylate the L-HBsAg protein or synthetic myristoylated lipopeptide analogs by removing the N terminus myristic acid, polymyxin acylase or α aminopeptidase enzymes were tested. **Polymyxin acylase** is produced in Gram negative *Pseudomonas* bacterium to deactivate the Polymyxin B antibiotic activity. Applied concentration ranged from 10-100 µg/ml. The lipopeptide and the enzyme were mixed together and incubated for 30 min at 37°C heat block.

α aminopeptidase (αAP) had been used as attempt to nonspecifically cleave N-terminal myristoylated-glycine at basic pH (pH 8) by lipopeptide treatment (1-10 µg/ml) at RT. α AP is isolated from *Aeromonas proteolytica*, a halophilic bacterium originally isolated from the intestine of a marine isopod [153]

2.2.9 Nitric oxide measurement (Griess assay)

The concentration of nitric oxide released in the supernatant of challenged murine BMDM (mBMDM) was measured by measuring nitrite ion on solution according to the Griess assay method [154]. Nitrite is one of two primary, stable and nonvolatile breakdown products of nitric oxide. 50 µl mixture of Griess assay solution A plus Griess assay solution B was added to 50 µl of supernatant from challenged cells for 10 min at RT in dark. The absorbance was measured by photometer (ELISA reader) at 540 nm and analyzed using Gen5 software. The amount of released nitrite in the supernatant was quantified according to the standard concentration of Sodium nitrite ($NaNO_2$)

Griess solution A: 0,4 g N-(1-Naphtyl) Ethylene diamide, dihydrochloride (0,2 %v/v), add till 200 ml water

Griess solution B: 4 g Sulphamilamide (2 % w/v), 10 g H_3PO_4 (5% v/v), add till 200 ml water

Stock of the two solutions was kept at 4°C and away from light.

2.2.10 Enzyme linked immuno sorbent assay (ELISA)

The amount of cytokines or chemokines released on the supernatant or in the serum or in cell lysate of challenged cells was measured through horse radish peroxidase (HRP)–linked immune sorbent-based assay through colorimetric detection. All proteins were measured through ELISA DuoSet Development System (R&D Systems) following the manufacture protocols. Briefly, ELISA plate was coated with 50 µl of capture antibody (diluted in PBS) and kept overnight on a shaker. A day later, the plate was washed with ELISA washer machine, in which 300 µl PBT solution was used three times/ well. To prevent unspecific protein binding, 200 µl of blocking buffer was applied per well for 1 h and the plate was maintained onto shaker. Next, the plate was washed again and either 50 µl sample (undiluted or 1:2 diluted with reagent diluent) or 50 µl of standard antibody of the respective cytokine/chemokine was applied (5; 2.5; 1.25; 0.63; 0.31; 0.16; 0.08 ng recombinant cytokine and water as blank) and the plate was kept in incubator at 37°C and 65 rpm shaking speed for 90 min. The plate was then washed as mentioned above and 50 µl of biotin labeled-detection antibody was added (diluted in reagent diluent) and the plate was kept in incubator at 37°C and 65 rpm shaking speed for 90 min. The plate was washed and labeled with 50 µl streptavidin-coupled HRP diluted 1:40 in reagent diluent for 20 min in incubator at 37°C and 65 rpm shaking in dark. After washing, freshly prepared substrate of Tetramethylbenzidine (TMB), by mixing reagent A with reagent B, is then added to the wells in 50 µl volume and kept in dark till blue color develop. Color development was stopped by applying 25 µl of stop solution (switching from blue to yellow) and sample and the standard plates were measured using ELISA reader at 450 nm and Gene5 software.

Blocking buffer: 50 g Sucrose, 10 g BSA, 500 mg NaN3, add till 1l PBS

Reagent diluent: 10 g bovine serum albumin (BSA), add till 1l PBS

Reagent diluent and blocking buffer are both filtered and stored at 4°C.

PBT solution: 0,05 % (v/v) Tween 20, add till 1l PBS

Stop solution: 2M (1M) H_2SO_4, add till 1l water

2.2.11 Luminex analysis

Similar to ELISA, Immunoassays based on Luminex (multi-analyte profiling) technology was applied to measure several mouse and human cytokines and chemokines at one single set. Briefly, 50 µL of standard or sample were applied per well. Subsequently, the provided diluted microparticle Cocktail were resuspended and 50 µL of the microparticle cocktail were given to each well of the microplate and incubate for 2 h at RT on a horizontal orbital shaker.

Washing steps were performed through using a magnetic device designed to accommodate a microplate through which the magnet face the bottom of the microplate and 100 µL wash buffer were added to each well. Subsequently, sample proteins biotinylation takes place by adding 50 µL of diluted biotin-antibody Cocktail to each well and incubated for 1 h at RT. Washing steps was repeated as mentioned before. 50 µL of diluted Streptavidin-PE were then added to each well and incubated 30 min on shaker at RT. Washing steps were followed then microplate wells were resuspended by 100 µL of wash buffer and incubated 2 min on shaker. Samples were then read by Luminex 200 reader.

2.2.12 Dual luciferase reporter assay

The luciferase reporter assay method is a method that measures the upregulation of gene upon stimulus challenge through measuring the activation of transcription factor or promoter activity by coupling to luciferase gene, which would correlate to the transcriptional activity and induce thereby ligand-receptor dependent gene signaling activation. To do so, the gene such as promoter was cloned into construct upstream of the luciferase gene from firefly (*Photinus pyralis*). Additionally, *Renilla reniformis* luciferase gene construct is also needed to serve as control for constitutive gene expression and normalization (independent receptor signaling). The quantified luciferase activity describes the promoter activity. 4 x 10^6 HEK293 cells were seeded onto 96-well plate with 10% FCS containing medium and incubated at 37°C for at least 5 h. Cells were then transfected with the promoter-luciferase construct, renilla construct and either receptor (mouse or human) or empty vector as negative control. The transfection was performed using calcium-phosphate reagent as follow:

In one tube : Water: 7,8 µl / well , $CaCl_2$ (2 M): 0,98 µl / well , promoter: NF-κB: 2 ng/ well or IFNβ: 15 ng/ well, renilla: 6,45 ng/ well, receptor : 3-15 ng/ well or empty vector (PRK5): 10 ng/ well. Contents are transferred drop wise and on pulse vortex to another tube containing equal volume of 2XHBS solution

2x HBS : 50 mM HEPES, pH 7.05 11.92 g, 10 mM KCl 745.60 mg, 12 mM Dextrose 2.16 g, 280 mM NaCl 16.36 g, 1.5 mM Na_2PO_4, dissolve in 1l water; pH adjusted at 7.05 and sterile filter.

The mixture was incubated for 15 min to allow calcium phosphate crystal formation and 15 µl of the mixture was given to the cells. A day later, cell medium was exchanged with fresh medium containing 2% FCS medium. Two h later, cells were challenged with the respective stimulus for 8-16 h by incubating at 37°C 5% CO_2 incubator. Subsequently, supernatant was

removed and 40 µl 1x Reporter Lysis Buffer (Promega) was added and placed on shaker (800 rpm – 1 h, RT) to lyse the cells. 20 µl of lysates were transferred to a white opaque microtiter plate. Luminometer Orion II (Berthold) supplied with D-luciferin and Coelenterazine (renilla substrate) were used to quantify both signals using software Simplicity 4.

Luciferase substrate: 470 µM D-Luciferin, , 270 µM coenzyme A, 33.3 mM DTT, 530 µM ATP, 1.07 mM (MgCO3)4Mg(OH)2, 2.67 mM MgSO4, 20 mM Tricine, 0.1 mM Na2 EDTA, pH 7,8

Renilla substrate: 1.43 µM coelenteracine, 1.1M NaCl, 2.2 M Na_2 EDTA, 220 mM $KHPO_4$, 1.3 M NaN_3, 440 µg/ml BSA, pH 5

2.2.13 Protein chemistry

2.2.13a Cell lysis

Cells that are expressing the protein of interest were lysed on ice either chemically using lysis buffer or physically using a bioruptor. The protein to be analyzed contained in total cell lysate or enriched by immunoprecipitation for either protein expression analysis by western blotting (functional assay), or metabolic labeling for acylation visualization by click chemistry or for challenge of immune cell challenge. For western blot, cell lysis was performed using lysis buffer containing detergent (NP40). Towards click chemistry based analysis and due to the interference of the detergent reagent in western lysis buffer with the metabolic labeling, different lysis buffer was applied in click chemistry procedures. Physical lysis of the cells expressing protein of interest was performed for primary cells immunostimulation assays. Here, cells were lysed by ultrasonication using bioruptor device (20 sec pulse 3x with interval 10 sec cooling down) or pulse ultrasonicator (two cycles of 20 sec pulse followed by 1 min incubating on ice).

Western lysis buffer : 50 mM HEPES pH 7.6, 50-150 mM NaCl, 1 mM DTT, 1 mM EDTA, 1 mM EGTA, 0.5-1.5% (v/v) nonident P-40 (NP40), 10% (v/v) Glycerol , 20 mM β-Glycerophosphate, 1 mM Na_3VO_4, 0.4 mM PMSF, 1 Tab/ml protease inhibitor cocktail Tablet

Click chemistry lysis buffer: 50 mM Tris/HCL (pH 8), 1% SDS, 1 Tab/ml protease inhibitor.

2.2.13b Western blot

Once the protein samples were separated onto the SDS-PAGE, the proteins were blotted into nitrocellulose membrane using wet blot protocol. To do so, the stacking gel is discarded and

the resolving gel was carefully used for blotting. Sandwich of SDS-gel and nitrocellulose membrane surrounded by two Whatman papers from the down and the top was applied with careful attention to remove air bubbles. The SDS-gel and nitrocellulose membrane sandwich was placed into the blotting chamber in position, in which the protein located in the cathode and would run towards the anode. Blotting was performed in cold blotting buffer using ice box during blotting and speed was adjusted at 95 V for 53 min. Once protein was blotted into the membrane, washed with PBT solution once, 20 ml Ponceau solution was poured to check the blotting efficacy by observing protein band(s). The membrane was then washed several times with PBT solution to remove the remaining Ponceau solution. Afterwards, the blocking buffer was applied to block protein unspecific binding for 1 h. By incubation of the membrane with primary antibody target (diluted in blocking buffer) the blotted protein was performed by O/N incubation at 4°C on turning wheel rotation. Consequently, the membrane was washed three times (5 min each) with PBT and the secondary antibody conjugated to horse radish peroxidase (HRP) target the host species in which the primary antibody raised in (diluted in blocking buffer) for 2 h. Finally, the membrane was washed three times with PBT (5 min each) and proteins were detected using Western Lightning Chemiluminescence substrate reagents. For further analysis, the membrane was stripped by washing 5 times with PBT, blocked for 1 h with blocking buffer and incubated with other primary antibody followed by secondary antibody as before.

Running buffer (10X)	**Blotting buffer (10X)**	**PBT solution**
288 g Glycine, 60,4 Tris base, 20 g SDS, 1,8 L ddH_2O.	58 g Tris, 29 g Gylcine, 200 ml Methanol, till 1000 ml ddH_2O.	1x PBS, 0.05% Tween 20.
Running buffer (1X)	**Blotting buffer (1X)**	**Blocking buffer**
100 ml 10X running buffer, Till 1 L ddH_2O.	100 ml 10X blotting buffer, 200 ml Methanol, till 1000 ml ddH_2O.	1X PBT, 3 ml normal goat serum (NGS), 50 g anhydrous milk powder.

2.2.13c Immunoprecipitation (IP)

Immunoprecipitation is a method for protein-protein interaction or protein-antibody interaction. Here, native or flag-tagged proteins are pulled down using protein specific antibodies-tagged beads. Unspecific bound proteins to the beads were removed by several

washing steps to the beads. The binding of the protein to the beads is eventually precipitated upon centrifugation, rendering enriched protein of interest, devoid of all other cell lysate proteins. For protein expression, transient transfection of plasmid encoding the protein sequence (4-10 µg) was transfected into HEK293 cells (10^7 cells/ 15 cm dish) using transfection reagent. 2 days post transfection, cells were lysed using western lysis buffer and the lysate was subjected to either flag-tagged M2 beads for flag tagged overexpressed protein. Consequently, washing steps for the beads were performed for 5 times by centrifugation (17000 g, 15 sec at 4°C) and suspending in 1 ml washing buffer. The washing buffer contains high salt concentration (150 mM NaCl), disrupting thereby unspecific and low affinity bead binding proteins. At the last washing step, protein bound beads were finally resuspended in 50 µl washing buffer and mixed with 5x loading sample buffer, boiled for 5 min at 95°C for dissociation of the protein from the beads, centrifuged to precipitate the beads and the protein in the supernatant was subjected to SDS gel electrophoresis and later immunoblotted to membrane as western procedure.

IP Washing buffer: 50 mM HEPES (pH 7,6), 150 mM NaCl, 1mM DTT, 1mM EDTA, 1% NP40, 10% Glycerol, 0,4 mM phenylmethylsulfonyl fluoride (PMSF), 1 mM EGTA.

2.2.13d Sodium dodecyl sulfate polyacrylamide gel electrophoresis

SDS-PAGE was performed using gel of 1.5 mm thick with resolving gel acrylamide percentage range between 10-14% or commercially available gradient gel (Bio-Rad). For manual gel casting, resolving gel was casted according to SDS-PAGE gel and covered with 400 µl isopropanol for better gel layer homogeneity. Once polymerized, the 4% was poured onto the resolving gel after removing the isopropanol and the comb was inserted. After polymerization, the casted gel was placed in electrophoresis chamber and immersed in Laemmli buffer. The protein sample, either from total lysate or IP, was mixed with the 5x sample loading buffer and boiled for 5 min at 95°C. 80-120 µg/ well of protein was loaded onto the SDS gel. Protein marker covering the expected protein size range was loaded with the sample (5 µl / comb). Electrophoresis of the gel was initiated at 80 volt (V) till the migration of the sample to the resolving gel then raised to 120 V till the end of the electrophoresis.

Gel	Resolving			Stacking	
Percentage (%)	10	12	14	4	
Acrylamide [ml]	3,3	4	4,6	0,66	
1,5 M Tris-HCL (pH 8,8) [ml]	2,5	2,5	2,5	2M Tris-HCL (pH 6,8):	0,3

10% SDS [µl]	100	100	100	200
ddH_2O [ml]	4	3,3	2,7	3,9
TEMED [µl]	5	5	5	5
10% APS [µl]*	50	50	50	25

5x sample loading buffer	**Laemmli buffer (1X)**
200 mM Tris-HCL (pH 6,8), 10% SDS, 16% Glycerol,	30.28g Tris, 208.2g Glycine, 50ml
400 mM DTT, 2 g/l bromphenol blue	10 % SDS, till 10 l ddH_2O

*** 10% SDS** : 10% SDS in ddH_2O, 10% APS : 10% ammonium persulfate in ddH_2O.

2.2.13e Lipo hexapeptide analogs of L-HBsAg, NEF and MARCKS

All synthetic peptide analogs of L-HBsAg (HBV), NEF (HIV) and MARCKS were ordered (EMC Microcollections) and received as lyophilized powder (purity ≥ 80 %). To ensure highest solubility, peptides were reconstituted according to published protocol [155]. Initially, peptide powder was dissolved in DMSO at final concentration of 0,1 µM then placed on shaker for 1 h at 50°C followed by sonication for 20 sec. then addition of tert-Butyl alcohol in dilution ratio to peptides 1:5000 v/v (%). Subsequently, sterile 50% bovine serum albumin (BSA) dissolved PBS was added to the peptides at final dilution ratio to peptide 1:100 v/v (%). Pierce assay was then performed to quantify the peptide final concentration and then aliquot from samples were done and stored at -20°C.

2.2.14 Click chemistry

Click chemistry was applied in this project to visualize and quantify the myristoylation of proteins, namely, overexpressed MARCKS. All the methods, concentration and incubation times were applied according to the manufacture recommendation. For instance, HEK293 cells (10^7 cells) were seeded into 15 cm Petri dish and transfected with protein-encoding construct. Two days later, the expressed protein was supplemented by myristic acid labeled-azide (10 µM working concentration) for 6 h. Consequently, the cells were lysed using click chemistry lysis buffer and either the total lysate or purified protein, through immunoprecipitation, was subjected to alkyne-biotin tagging (40 µM working concentration) in the presence of copper sulfate buffer in 1,5 ml eppi tube. A reaction tube was incubated for 20 min with continuous rotation end-over-end at RT. Labeled protein was then extracted using 400 µl methanol, 150µl Chloroform and washed out by methanol chloroform steps. Finally, the labeled protein was loaded onto a 12% SDS gel and blotted. Visualization of the labeled protein myristoylation was achieved by streptavidin coupled to HRP and the signal was measured by chemiluminescent

detection.

2.2.15 Urea-tricine high percentage SDS-PAGE

Applying tricine in the process of low sized-protein electrophoresis had been shown to be preferential compared to normal Laemmli SDS-PAGE [156]. Additionally, adding urea to the tricine-SDS further enhances the separation of very small proteins (< 1.5 kDa). Urea-tricine 16% SDS gel was used to visualize the difference between synthetic myristoylated and non-myristoylated peptide analogs from L-HBsAg (47pep/ M47pep), NEF (HIV) and MARCKS. Additionally, spacer gel layer between the stacking gel and resolving gel improves the protein denaturation. For this purpose, three types of gel, one over the other, were simultaneously prepared and allowed to polymerize together at the same time, namely, resolving, spacer and stacking gels.

Gel	Stacking	Spacer	Resolving
Percentage (%)	4	10	16
AB-6 [ml]	1	6	10
Gel buffer (3X) [ml]	3	10	10
Urea (6M) [g]	--	--	10,8
ddH2O [ml]	8	14	10
			filtered by vacuum for degassing and stirring for 10 min
10% APS [µl]	90	150	100
TMEMD [µl]	9	15	10

AB-6 (acrylamide:bisacrylamide) : 46,5 g acrylamide, 3 g bisacrylamide, ddH2O till 100 ml.

Gel buffer (3X): 3 M Tris, 1M HCL, 0,3 % (w/v) SDS, pH: 8,45.

After placing all the gels, one above the other, they were incubated to polymerize together at RT. Gels were then transferred to electrophoresis chamber. As a substitute to Laemmli buffer, basic anode and cathode buffers were used. (1x) Cathode buffer was poured between the gel and the chamber barrier, whereas anode buffer was poured at the bottom. The peptides were then mixed with sample loading buffer, boiled at 95°C for 3 min and loaded onto the cathode side. Since the urea forms secondary complex at temperature higher than 37°C forming cyanates, the entire electrophoresis time was performed at 30 V to avoid gel overheating.

Low-size protein marker was used to identify the protein size onto gel.

Sample buffer: 12% (w/v) SDS, 6% (v/v) mercaptoethanol, 30% (w/v) glycerol, 0,05% Coomassie blue G-250 (Serva), 150 mM Tris-HCL, pH7.

Electrophoresis buffer	Cathode buffer (10X)	Anode buffer (10X)
Tris (M)	1	1
Tricine (M	-	1
HCl (M)	0,225	-
SDS (%)	-	1
pH	8,9	~ 8.25

2.2.16 Polyacrylamide gel silver nitrate staining

Silver nitrate staining procedures were done according to the manufacture recommendation and on moderate speed shaker. Briefly, resolving gel was fixed with trichloroacetic acid solution for at least 1 h. Fixation solution was washed away by 2-time washing steps of the gel with 30% EtOH for 10 min. Gel was then pretreated with 30% Na-thiosulfate pentahydrate for exact 1 min. Gel was then washed thrice by ddH_2O for 10 sec each washing step. Gel staining was achieved by incubating with 10% Silver nitrate for 15 min. Gel was then washed twice by ddH_2O for 10 sec each washing step. Next, 20% sodium carbonate containing 0.001% formaldehyde was added to develop band color. Once visible, color development was stopped by washing once with ddH_2O for 10 sec and 10% glycine solution was poured into the gel for color fixation.

2.2.17 Cell culturing

2.2.17a Human embryonic kidney cell 293 (HEK293)

For protein functional assays or ectopic overexpression of receptors, the fibroblast-like cell HEK293 (ATCC-Nr. CRL-1573) was used. HEK293 are adherent cells that grow as monolayer. The cells were maintained by culturing at 37°C 5% CO_2 incubator and passaged routinely at confluence of 70%. To detach, cell supernatant was aspirated, washed with 5 ml warm PBS and trypsinized by 5 ml at 37°C for 5 min. Trypsin activity was stopped by adding an equal volume of bone marrow macrophage medium to the cells and then collected in 50 ml falcon tube, centrifuged at 1100 rpm for 5 min and 1/10 of the cell suspension was thoroughly transferred to a new cell petri dish with 20 ml medium.

HEK293 medium: 500 ml DMEM, 50 ml FCS, 5 ml Penicillin-Streptomycin solution, 5 ml Antibiotic-Antimycotic 100X solution.

2.2.17b THP-1 cells

The human monocytoid THP-1 cell line, isolated from the peripheral blood of a patient who suffered from acute myeloid leukemia, was used for immunostimulation assays. Cell suspension was grown in T175 cm^2 flask at 37°C, 5% CO_2 incubator. At 60-70%, confluence, 2 ml of cell suspension was transferred to a new flask. To differentiate the monocyte to macrophage, cells were stimulated with 200 nM 12-phorbol 13-myristate acetate (PMA) by seeding a cell count of $1x10^7$ cells/96 well plates with a medium containing PMA for 24 h, followed by a period of three consecutive days of PMA-medium free, or stimulated for three days with PMA-medium followed by a five-day period of PMA-medium free. Finally, cells were seeded on 2% FCS medium and stimulated for 16 h.

THP-1 medium: 500 ml RMPI1640, 50 ml FCS, 5 ml Penicillin-Streptomycin solution
5 ml Antibiotic-Antimycotic 100X solution.

2.2.17c Hepatic cell lines

HepG2 cells, derived from a 15-year old Caucasian male who suffered from well-differentiated hepatocellular carcinoma, was used for ectopic overexpression of HBV proteins or the nucleic acids isolated for comparative analysis as parental cells for other cell line expressing HBV (HepG2.215). Similarly, at 60-70% confluence, cells were trypsinized with 5 ml trypsin after washing with warm 5 ml PBS, cells were pelleted by centrifugation 400 g for 5 min and pellet was resuspended and 1/3 of the volume was transferred to new 75 cm flask**.**

HepG2 medium: 500 ml DMEM, 50 ml FCS, 5 ml Penicillin-Streptomycin solution, 5 ml Antibiotic-Antimycotic 100X solution.

Huh7-NTCP cells, expressing the virus entry receptor Sodium/bile acid cotransporter also known as the Na^+-taurocholate cotransporting polypeptide, was used to analyze the HBV infectivity or replication through measuring HBV related protein markers and for electron microscopic analysis of the whole virions. Cells were grown at 37°C 5% CO_2 incubator and at 60-70% confluence cells were passaged. Transfection of HBV was performed using inocula of 5.6 x 10^7 HBV copies/ml and 0.25% (v/v) Fugene transfection reagent in 1 ml Optimem solution and medium containing 6% PEG8000. A day later, the supernatant cells were aspirated and saved in -20°C, washed 3 times with warm PBS, and fresh medium containing 6% DMSO was applied for a further 5 days.

Huh7-NTCP medium: 500 ml DMEM, 50 ml FCS, 5 ml Penicillin-Streptomycin solution

0 µg/ml Blasticidin, 5 ml Non-essential aa (NEAA), 5 ml Antibiotic-Antimycotic 100X.

2.2.18 Preparation and culture of primary cells

2.2.18.1 Murine bone marrow-derived macrophage

For murine bone marrow-derived macrophage (mBMDM) generation, a mouse was sacrificed by cervical dislocation. The hind and fore limbs were dissected and bones were cleaned out. After cutting bone edges, bone marrow was flushed out of the femora, tibiae and humeri with a medium using a syringe and the flushed out marrow was collected in a clean 50 ml falcon tube. Bone marrow cells were centrifuged at 1100 rpm, 5 min at RT and the pellet was resuspended in 20 ml medium containing 15% L-cell supernatant-containing M-CSF and distributed in five 145 mm petri dishes per each mouse. After 3 days, a further 10 ml of fresh medium containing 15% L-cell supernatant was added to support cell differentiation. Within 5-6 days, bone marrow cells are terminally differentiated into macrophages. To harvest the macrophages, the supernatant cells were aspirated and washed with 5 ml warm PBS. 5 ml Accutase was added and cells were incubated for 5 min at 37°C for dissociation. Cells were then collected onto 50 ml falcon tube containing an equal volume of 10% FCS-medium for enzyme deactivation. The cell solution was centrifuged (1100 rpm, 5 min at RT) and the pellet was resuspended in a culturing medium. The cells were counted by Trypan blue and plated (10^7 cells per total 96-well plate in 200 µl medium/per well). In case they are not used, the cells were frozen at -80°C using 10% FCS-DMSO solution.

BMDM medium: 500 ml DMEM, 50 ml FCS, 5 ml Penicillin-Streptomycin solution, 5 ml Antibiotic-Antimycotic 100X solution, 50 µM β-mercaptoethanol.	**BMDM differentiation medium:** 500 ml DMEM, 50 ml FCS, 75 ml L- cell supernatant, 5 ml Antibiotic-Antimycotic 100X solution, 5 ml Penicillin-Streptomycin solution, 50 µM β-mercaptoethanol.

2.2.18.2 Isolation of splenocytes

Spleens from mice were isolated for immunostimulation assay. Mice were sacrificed by cervical dislocation and the body was disinfected with 70% ethanol. The spleen was carefully removed and placed whole in 10-cm petri dish containing 5 ml warm PBS. Using a syringe plunger and 70 µM cell strainer, the organ was mashed through the cell strainer. The PBS-spleen suspension was collected into a new 50-ml falcon tube filled with spleen medium and centrifuged (1100 rpm, 5 min at RT). The cell pellet was resuspended in the spleen medium and counted. 5 x 10^7 cells for whole 96 well plates were used for immunostimulation assay.

Spleen medium: 10% FCS in DMEM, 1% Antibiotic-Antimycotic, 1% Pen/strep.

2.2.18.3 Human peripheral blood mononuclear cell (hPBMCs) isolation

To isolate hPBMCs, heparinized buffy coat blood obtained from the blood bank of the University Clinic Essen, approved by ethic committee 14-5804-B0 was used fresh on the day of receipt. 13 ml blood was added slowly onto the top of 20 ml Ficol solution in 50-ml falcon tube and centrifuged at 400 g for 30 min at RT with 1x acceleration and zero deceleration speed. Centrifugation resulted in density gradient separation of the blood, in which the erythrocytes, owing to their high density, aggregate as pellet and the layer directly above it contains mainly granulocytes. The intermediate phase is the lymphocytes due to their lower density and the upper phase is the plasma. Carefully the plasma was collected in a new 50-ml falcon and heat inactivated (hi.) by 55°C for 30 min to inactivate the complement system and to be used later as autologous serum for cell culturing. The thin whitish intermediate layer was then taken to new 50-ml falcon tubes and washed to remove Ficol solution twice with warm 40 ml PBS by centrifugation 400 g 10 min with 9x acceleration and 9x deceleration speed. The cells were then filtered with 70 µm cell strainer, counted ($5x10^7$ / 96-well plate), and resuspended in 5% autologous serum-containing medium or frozen at -80°C (10% DMSO in autologous serum) till use.

PBMC medium: 500 ml RPMI1640, 5 ml autologous serum, 5 ml Penicillin-Streptomycin solution, 5ml Antibiotic-Antimycotic.

2.2.18.4 Human peripheral blood isolation

Both human peripheral blood and umbilical cord blood (UCB) isolation were conducted after ethical agreement from ethic committee commission from the faculty of Medicine of University Duisburg-Essen. As healthy donor control for total blood challenge assay, human peripheral blood was sampled. For full rounded shape 96 well plates, 27 ml peripheral blood was collected into ammonium-heparin (16 I.U Heparin/ml blood) tubes. The blood was distributed in the 96 well plates by 200 µl blood per well and immediately confronted with TLR agonists or HBV and incubated at 37°C, 5% CO_2 100%, water saturated atmosphere for 6 h. To obtain plasma free blood, the 96 well plates was then spun down at 4°C 400 g for 5 min. subsequently, 50 µl of blood plasma was retrieved and collected into new 96 well plate and applied to cytokine/chemokine analysis through luminex assay.

2.2.18.5 Human umbilical cord blood isolation

The isolation of umbilical cord blood from healthy mothers was conducted in accordance

with the declaration of Helsinki, with approval from the ethics committee of the affiliated University Hospital Essen. All newborns' mothers provided written informed consent. Umbilical cord blood was obtained by cesarean section after normal deliveries and were collected by 200 ml syringe and immediately transferred to ammonium-heparin tubes. 2 ml aliquot of the blood sample were collected in EDTA tube and subjected to differentiated blood count analysis by the Central blood laboratory of the University Clinic Essen. Meanwhile, 20 ml of the umbilical cord blood was seeded in 96 well plates and immediately challenged with TLR agonists or HBV and incubated and treated exactly as healthy adult peripheral blood for 6 h.

2.2.19 Generation of HBV virions

For HBV virion production, the hepatic cell lines HepG2.215 were used. HepG2.215 is derived from the human hepatoblastoma cell line HepG2 which is stably transfected with 2-fold HBV-DNA dimer expression plasmid [pDolTHBV-1] with neomycin resistance. HepG2.215 was cultured at 37°C 5% CO_2 incubator and seeded onto T-75 flask at their corresponding medium containing selection antibiotic (neomycin/G418 0.6%). At 70% confluence, cells were passaged by aspirating the supernatant, washing with warm 5 ml PBS, trypsinizing by 5 ml trypsin and then centrifuging at 1100 rpm for 5 min. The cell pellet was then split at a ratio of 1:3. To enforce virus production and release into the supernatant, the medium of HepG2.215 cell was exchanged by 2% FCS and 1% DMSO and incubated for 5 days. The supernatant was collected and centrifuged at 800 rpm for 10 min to precipitate cell debris. The supernatant was then transferred to a 50-ml falcon tube after being filtered with 45 nm filter and 6% w/v Polyethylene glycol 800 (PEG8000) was added, with vortex and incubated overnight at 4°C. A day later, the virus was pelleted by centrifugation at 16,000 g for 2 h at 4°C and the virus pellet was dissolved in 100-fold concentrate (proportional to the initial volume) in 10% FCS-PBS. The virus was kept in -80°C till use.

Culture HepG2.215 medium: 500 ml DMEM, 50 ml FCS, 5 ml Penicillin-Streptomycin solution, 5 ml Antibiotic-Antimycotic 100X solution, 5 ml HEPES 5 ml NEAA, 3,8 ml G418.	**Starving HepG2.215 medium:** 500 ml DMEM, 10 ml FCS, 5 ml Penicillin-Streptomycin solution, 5 ml Antibiotic-Antimycotic 100X solution, 5 ml HEPES, 5 ml NEAA, 5 ml DMSO.

2.2.20 HBV transfection and viral immune cells challenge

To study the immune stimulation potential of HBV and infectivity, the qPCR-quantified virions were subjected to immune cell confrontation. As a source for HBV virions, the

HepG2.215 cells were used. Another source was through transient transfection of huh7-NTCP with plasmids encoding HBV sequence (wt or mutant). Fugene transfection reagent was used to perform HBV construct transfection with small modification; specifically, 5,6 x 10^6 huh7-NTCP cells seeded in T75 flask were transfected with 10 µg DNA with 0.25% (v/v) Fugene solution dissolved in 1 ml Optimem solution. After 24 h, the medium was exchanged with huh7-NTCP medium containing 2% DMSO and incubated for 5 days at 37°C 5% CO_2. The supernatant containing the virus was collected and the virus was enriched by 6% (w/v) PEG8000 precipitation. The produced wt or mutant HBV virions were used to confront immune cells or other huh7-NTCP cells with or without transfection reagent to characterize their immune stimulation capacity or infectivity potential.

2.2.21 Friend murine Leukemia virus like particles production

Plasmid encodes FMuLV (virus clone FB29) gag P30 protein either in the wild type form (pcDNAp65Gag) or G2A mutant (pcDNAp65GagG2A) was co-transfected with plasmid encoding FMuLV envelope protein in HEK293T cells (5 x 10^7 cells/ 15 cm dish) . Cell transfection was performed using Polyethylenimine (PEI) at cell confluence of 80-90% as follow:

15 cm falcon tube-1: 75 µl PEI reagent [1mg/ml], Add till 900 µl DMEM solution.

15 cm falcon tube-2: 70 µg DNA gag plasmid (wt /G2A), 70 µg DNA envelope plasmid, + 825 µl DMEM solution.

Contents of tube-1 were then transferred to tube-2 and incubated for 20 min. Meanwhile, cells were carefully washed with warm PBS and the medium was exchanged with 1.5% serum. Next, cells were transfected, and 1 day post transfection the medium was exchanged with 10% serum and incubated for a further 2 days. The supernatant was then collected and cell debris was removed by spinning down the supernatant at 2000 rpm for 20 min at 4°C. In ultracentrifuge tube, 7 ml of 30% sucrose reagent was added and the supernatant was added slowly onto the top of sucrose reagent and ultracentrifugation was performed at 25000 rpm for 2.5 h at 4°C. After centrifugation, sucrose reagent was carefully removed by aspiration and VLPs pellet was dissolved by shaking with sterile PBS. Dissolved VLPs were aliquoted in PCR tubes and placed in -80°C or directly proceeded to protein quantification using pierce assay and western blot.

Transfection medium: 500 ml DMEM, 7,5 ml FCS, 5 ml Penicillin-Streptomycin solution, 5 ml Antibiotic-Antimycotic	**Enrichment medium:** 500 ml DMEM, 50 ml FCS, 5 ml Penicillin-Streptomycin solution, 5 ml Antibiotic-Antimycotic 100X solution.

2.2.22 Transmission electron microscopy (TEM)

Transmission electron microscopy was performed at the Imaging Center, Essen (IMCES) with technical support for sample fixation and analysis. To circumvent the small size of HBV pellet, I did fix the HBV virions with 4% gelatin. Briefly and as mentioned before, wild type or G2A mutant HBV collected from the supernatant of HepG2 or HepG2.215 cells (served as positive control) were precipitated with 6% PEG8000 overnight, filtered, spun down and resuspended in one tenth volume of the original total supernatant volume with cold 10% FCS-PBS. Consequently, warmed 4% gelatin was added and incubated to allow HBV to gelatinize. Further fixation was achieved by adding 1 ml of 2.5% glutaraldehyde and incubated for 1 h. For washing, 200 µl PBS was added three times and the sample was briefly centrifuged. The subsequent steps were done by the technician in IMCES; First, standard contrasting and Epon embedding achieved by post fixation by membrane and lipid staining with 1% osmium tetroxide in PBS onto ice for one h, followed by three times wash with millipore water and serial ethanol wash (30%, 50%). Block was contrasted with 70% ethanol and 1% Uranyl acetate for one h and incubated O/N in 70% ethanol. A day later, serial ethanol washing (80%, 96%, 100 %) was performed for 20 min, followed by 30 min wash by propylenoxide-ethanol 1:1 mixture then two times by absolute propylenoxide. The next steps were the infiltration of propylenoxide with Epon in 1:1 or 1:3 or 3:1 ratios and samples were polymerized by applying in oven at 60°C for 24 h without cover. Samples were then cut in ultra-thin layers and applied in copper-hexagonal nets. After applying samples on net grids, contrasting was achieved by 6 min incubation with 1% uranyl acetate in water, followed by 3 min incubation with 0.4% Pb-citrate in water. Analysis of the samples was achieved by the help of electron microscope expert. Positive staining analysis for FMuLV VLPs and HBV integrity had been conducted from protocol published before [157]. Briefly, sample in PBS was diluted 1:50 and premixed with methylcellulose and uranyl acetate. The mixture was then applied to the center of a support plastic-coated TEM grid as a 0.5 µl droplet containing 0.15% methylcellulose and 0.03% uranyl acetate.

2.2.23 Statistical analysis

Statistical analysis had been done on experiments repeated, unless indicated, at least three times and in biological triplicates (n=3). The significance level was calculated by one-way ANOVA using Turkey test for unconnected samples, with p-values indicated as "*" ($p \leq 0.05$), "**" ($p \leq 0.01$) or ‘’***’’ ($P \leq 0.001$).

3. Results

Adult individuals who are exposed to HBV virus are capable, in 95% of cases, to mount an efficient immune response against the virus and subsequently clear the infection. On the contrary, virus-exposed children and infants below the age of 6 years, in 90% of cases, fail to clear the virus and carry a lifelong chronic HBV infection [158][159]. The discrepancy in the HBV infection outcomes let us hypothesize that adults harbor an efficient immune response, which enables them to immunologically sense virus encounter and eliminate it, principally by innate immunity mediated recognition prior to subsequent adaptive immune response. Newborns might lack this HBV immune capacity. Therefore, the aim of this project was to comprehensively analyze a proposed innate pattern recognition which would mediate sensing, and HBV PRR/s and its/their ligand/s. My results encompass four paragraphs. The first part comprehends an immune stimulatory potential of integer HBV to activate cultured macrophages serving as experimental model of monocytes borne tissues, such as Kupffer cells in liver, which encounter and phagocytose circulating HBV systematically in the course of their immunosurveillance. First, the five HBV genome-encoded antigens were individually overexpressed and analyzed also for an immune activating propensity. Lysates of HEK293 cells overexpressing L-HBsAg - in contrast to counterparts containing each of other three HBV proteins – activated mBMDM to a substantial degree. Theoretical consideration led me to implication of the N-terminal modification of L-HBsAg, which is central in infectivity of HBV to human hepatocytes as TLR2 ligand candidate. Supporting it, synthetic analogs representing the L-HBsAg's N-terminus did activate mBMDM and transfected HEK293 cells through TLR2 to similar degree as HBV. Besides a PAMP nature of L-HBsAg which can be inferred from HBV affiliation, HBsAg also carries a – seemingly immune stimulatory – DAMP property due to its production by host's protein synthesis and modification machinery. Specifically, host protein such as MARCKS also undergoes N-terminal myristoylation such as towards inner cell membrane anchorage. This process is stress inducible or at least promoted such as by LPS challenge assigns a good candidacy as innate immune stimulatory DAMP to it. Indeed, not merely analogs of L-HBsAg but also these carrying the artificial ''CSK_4'' or the N-terminal MARCKS sequence and even smaller variants activated TLR2.

The second paragraph documents results on qualitative and quantitative analysis of N-terminal myristoylation of L-HBsAg and MARCKS as examples of numerous other viral and endogenous proteins known to be post-translationally in this manner which renders them TLR2 P/DAMPs. While murine sensing of HBV *in vitro* and *in vivo* depended upon TLR2

TLR2 P/DAMPs. While murine sensing of HBV *in vitro* and *in vivo* depended upon TLR2 expression exclusively, the human immune system surrogate whole blood, whole blood leukocytes, and PBMC employed an-/other sensor/s additionally as was deducible from inability of TLR2 blockade alone to prevent HBV driven cell activation. Accordingly, the third part of the results section illustrate the effort to narrow down TLR3,-7,-8,-9 or/and -13 specific HBV nucleic acid recognition upon observation of effective inhibition of HBV driven hPBMCs activation by TLR2 blockade if endosomal TLR2 activity was blocked in parallel. While HBV DNA isolates failed to activate murine TLR9 and HBV RNA isolates failed to activate murine TLR7 and -13, however, the latter activated both RIG-I and MDA5 which reconciles previous implications of others. In the final fourth paragraph of the results section, I outline my results of healthy probands and newborns, namely umbilical cord whole blood (UCB) to challenge with PRR ligands including HBV. Newborn blood characteristics were surprising.

3.1 HBV-, L-HBsAg-, and N-terminally myristoylated host protein- driven immune activation.

3.1.1 HBV production from stably transfected hepatic cell line HepG2.215.

HBV particles prepared from the supernatant of the stable transfected hepatic cell line HepG2.15. The HepG2.15 cells are genomically integrated with a plasmid which includes 2-fold-head-to-tail dimer HBV genome (genotype D). To establish virus production, HBV antigen (HBsAg and HBeAg) content analysis was performed. HBV release to the supernatant or within cell lysate was observed only upon DMSO application (Fig. 6A). Furthermore, analysis of total isolated RNA from parental cell (HepG2.N) and HBV-producing HepG2.215 cells documented total RNA and thus cell integrities (Fig. 6B). PCR analysis confirmed the presence of viral DNA in HepG2.215 and absence from control cells (Fig. 6C).

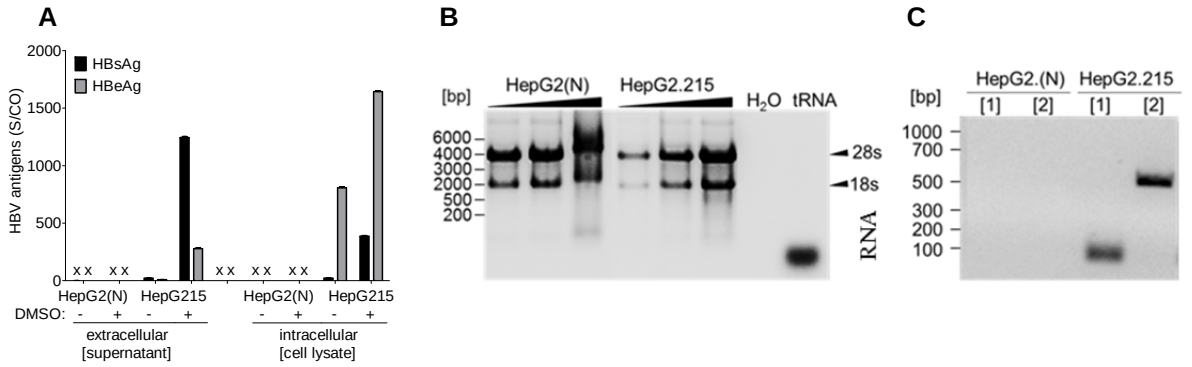

Figure 6. HBV expression and release from stable hepatic cell line HepG2.215. Induction of HBV produced by HepG2.215 cells ($5x10^6$ cells/ well) towards extracellular release of HBV antigens with 6% DMSO. [**A**] Quantification of extracellular (supernatant) and intracellular (cell lysate) HBeAg and HBsAg 5 days post induction of HepG2.215 and parental control HepG2(N) cells. [**B**] 1% Agarose gel electrophoresis of RNA from HepG2(N) and HepG2.215 cells at three different (0.5, 1 ,4 µg indicated by triangles) RNA concentrations to indicate cellular integrity. [**C**] PCR analysis of DNA isolated from HepG2(N) and HepG2.215 cells applying HBV gene specific primers (pairs (1): HBsAg gene region of 100 bp. (2): 580 bp length, adapted from Untergasser et al. 2006 [160] (x: not detectable, bp: base pairs; S/CO: signal to cutoff; obtained by measuring the signal strength of sample and the signal strength of an internal cutoff,(-) : untreated, (+) : treated).

3.1.2 HBV drives MyD88 and TLR2 dependent HBV-driven primary cell and immune cell line activation.

Macrophages represent the next line of innate immunity behind primary barriers such as skin and mucous. They phagocytose and kill host-invading pathogens and mobilize subordinated cells such as by chemokine and cytokine releases [161]. Thereof, I investigated whether primary immune cells such as mBMDM, hPBMCs and other monocytic cell lines including THP-1 and Raw264.7 cells recognize HBV particles by analyzing inflammatory and anti-inflammatory cytokine release upon confrontation with HBV.

To overcome experimental limitation in respect to attainability of immune sensory threshold, HBV was applied at very high titers towards immune cell confrontation. Accordingly, challenges at dose of 6-20 x 10^7 HBV virions /ml triggered detectable cellular responses in both murine macrophages and hPBMCs. This observation is consistent with a recent study on human macrophages confronted with high-titer HBV [162]. Accordingly, *Myd88*$^{-/-}$ and *Trif*$^{-/-}$ and *Tlr234579*$^{-/-}$ mBMDM failed to respond to HBV challenge, wt, *Tlr379*$^{-/-}$ and *Ilr1*$^{-/-}$ counterparts were activated by it to substantial degrees (Fig. 7A). Since TLR5 is not involved in viral recognition. HBV immune recognition could, so far, rely upon surface receptors, namely TLR2 or TLR4 receptor. To nail it down, which surface TLRs might be operative in HBV-immune recognition; single KO experiment performed either on *Tlr2*$^{-/-}$ or *Tlr4*$^{-/-}$

revealed failure of *Tlr2*$^{-/-}$ macrophage to respond to HBV challenge as compared to wt control or *Tlr4*$^{-/-}$ (Fig. 7B), implying a potential role of TLR2 as HBV PRR. Not only primary immune cells but also results of PMA-differentiated-THP-1 cell lines revealed non-responsiveness of HBV challenge in *Tlr2*$^{-/-}$ THP-1 cells but not in *Tlr4*$^{-/-}$ and *Tlr8*$^{-/-}$ THP-1 cells (Fig. 7C). *Unc93b1*$^{d/d}$ mutant THP-1 cells responded to HBV challenge as wt, implying the dispensability of the endosomal TLR in HBV-driven immune response. Reporter gene assay by ectopic overexpression of surface TLRs namely TLR2 or TLR4 with NF-$_K$B luciferase promoter in HEK293 cells displayed TLR2-dependent, TLR4-independent HBV-driven NF-$_K$B luciferase activity (Fig. 7D). Used as control, LPS driven luciferase activity was mediated by both TLR2 and TLR4 dependent manner, confirming that TLR2 sense not only acylated lipopeptide but also bacterial LPS [42][163].

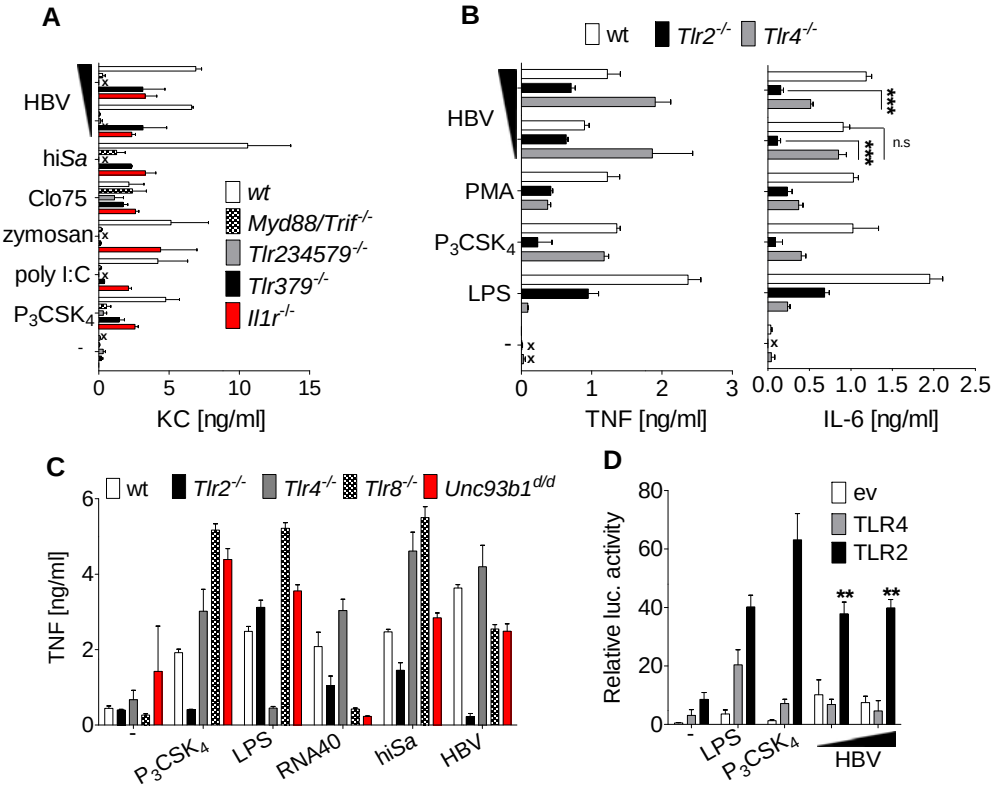

Figure 7. TLR2 dependence, endosomal TLR independence of HBV recognition in mBMDM and reporter gene assay. [**A**] mBMDM (10^7 cells/ 96 well plates) of different genotypes were challenged either with TLR ligands TLR2, TLR3, TLR7/8; (P_3CSK_4, 10 µg/ml; polyI:C, 10 µg/ml; Clo75, 5 µg/ml); zymosan, 15 µg/ml; or heat inactivated *S.aureus* (hi*Sa*) ($2x10^9$ CFU/ml) or HBV ($6/15x10^7$ virions/ml) for 16 h. [**B**] mBMDM of genotypes indicated were challenged for 16 h with TLR ligands (LPS, 0.1 µg/ml; P_3CSK_4,10 µg/ml), or PMA (phorbol myristate acetate), 10 µg/ml; or HBV ($6/15x10^7$ virions/ml). [**C**] PMA differentiated THP-1 cells were challenged for 16 h with P_3CSK_4 (10 µg/ml), LPS (0,1 µg/ml), RNA40 (5 µg/ml) or hi*Sa* ($2x10^9$ CFU/ml) or HBV ($6x10^7$ virion/ml). Cytokines content was measured by ELISA.

[**D**] Luciferase activity measurement for HEK293 cells ($4x10^6$ cell/ 96 well plates) transfected with NF-$_K$B-luciferase promoter (2 ng), renilla (6,45 ng) and murine TLR2 expression plasmid (6,25 ng) or TLR4 (10 ng) or empty vector (ev, 10 ng) for 16 h then challenged with LPS, P_3CSK_4 or HBV ($6/15x10^7$ virions/ml). Luciferase signaling normalized to renilla constitutive expression and unstimulated mock. Results shown are representative of two independent and error bards represent SEM. (x: not detectable, (-): untreated).

Aiming to enhance HBV-driven immune response, pre-heating of HBV virions at 50°C, possibly resulting in disrupting the virion integrity prior to cell stimulation enhanced the HBV-driven luciferase activity. On contrast, 100° C treatment for the same incubation time abrogated virions driven luciferase activity (Fig. 8). This observation suggests that the 50°C temperature pretreatment of HBV enhance its immunostimulation, possibly due to exposing certain PAMP(s) that is/are masked at normal temperature. Notably, HBV remains infectious upon with up to 60°C temperature treatment [164].

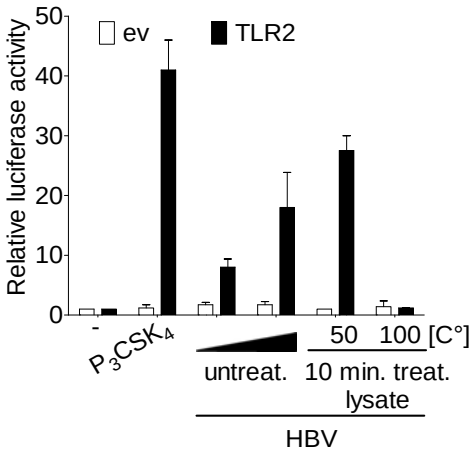

Figure 8. Resistance of TLR2 specific HBV activity to 50° C treatment. HBV untreated or 10 min incubated at 50° or 100°C were subjected to TLR2- (6,25 ng) or mock- (10 ng ev) transfected HEK293 cells ($4 x10^6$ cells/ 96 well plates) to analyze NF-$_K$B activity. Results shown are representative of three independent experiments and error bars represent SEM. (ev: empty vector, treat: treatment, (-) : untreated).

3.1.3 Analysis of single HBV protein properties to elicit mBMDM activity such as through TLR2.

Plasmids encoding five different HBV proteins, namely, large domain of surface protein (L-HBsAg), e–antigen (HBeAg), capsid protein (HBcAg) and x-protein (HBx) were transfected into HEK293 cells to analyze their individual immunogenicity in murine macrophage and hPBMCs activation. Lysates of HEK293 overexpressing each protein applied to mBMDM. Merely L-HBsAg elicited a substantial immune response of murine and human immune cells such as in respect to anti-inflammatory cytokine IL-10 production – the other overexpressed HBV proteins were largely non-immunostimulatory (Fig. 9).

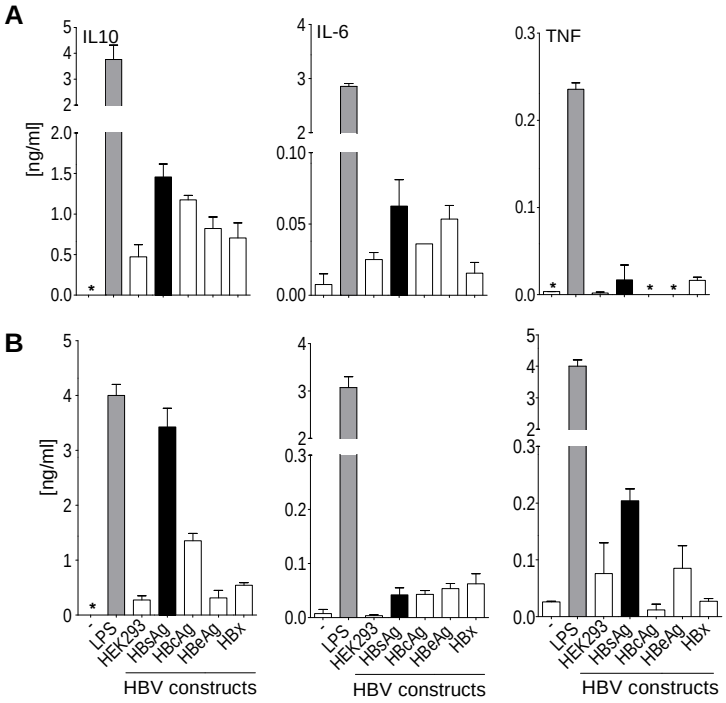

Figure 9. mBMDM stimulatory capacity of individual lysates of HBV protein overexpressing HEK293 cells. L-HBsAg, HBcAg, HBeAg or HBx overexpressing constructs were expressed in HEK293 cells (10 µg DNA per 4,5 x10^6 cells/ 9 cm dish). Two days post transfection, cells were lysed by ultrasonication (two times by 20 sec pulse and placed on ice) and protein concentration of the total cell lysate was measured (Bradford assay). Lysate (50 µg/ml protein) or LPS (0,1 µg/ml) was applied to either mBMDM (10^7 cells/ 96 well plates) [**A**] or hPBMCs (5x10^7 cells/ 96 well plates) [**B**] for 16 h. Results shown are representative of four independent experiments and error bars represent SEM. (*: not detectable, (-) : untreated).

3.1.4 HBV immunostimulation is attributed to TLR2-mediated recognition of myristoylated surface protein.

TLR2 recognizes the eukaryotic- (glycine monoacylated) and prokaryotic- lipoproteins (cysteine acylated) that are diacylated or triacylated by forming heterodimers with TLR6 or TLR1, respectively. Common protein-fatty acid acylation that triggers activation of TLR2 are protein-palmitoylation and -myristoylation. Generally, numerous proteins synthesized by bacteria or viruses have been observed to undergo myristoylation (myr). While some viruses carry multiple myr-proteins, monomyristoylation of L-HBsAg in HBV is the case, similar to eukaryotic proteins.

L-HBsAg consists of four transmembrane domains and myristoylated at its N-terminus. Myristoylation of L-HBsAg is prerequisite for the virus to interact with its hepatocyte entry receptor, namely sodium taurocholate cotransporting polypeptide (NTCP) [165]. However,

and to avoid the immunosurveillance, the myristoylation moiety is docked into the virion by insertion into the virus envelope phosphobilayer. Once the virus is in close proximity to the entry receptor, the myristoylation moiety undergoes conformational change and flips out for proper interaction. I asked whether this was a sufficient window for the host innate recognition during the early event of virus infection. Whether myr-L-HBsAg might be sensed by TLR2 similar to eukaryotic myristoylated peptide analog Myr_1GSK_4 (Fig. 10A), synthetic two L-HBsAg lipo peptides, namely, Myr-GTNLSV (M6P), representing the N-terminal aa 2-7 of L-HBsAg, and myr-GTNLSVPNPLGFFPDHQLDPAFGANSNNPDWDFNPNKDHWPEANKVGK (M47pep), representing 2-48 aa of L-HBsAg were synthetically ordered to dissect this question (Fig. 10B).

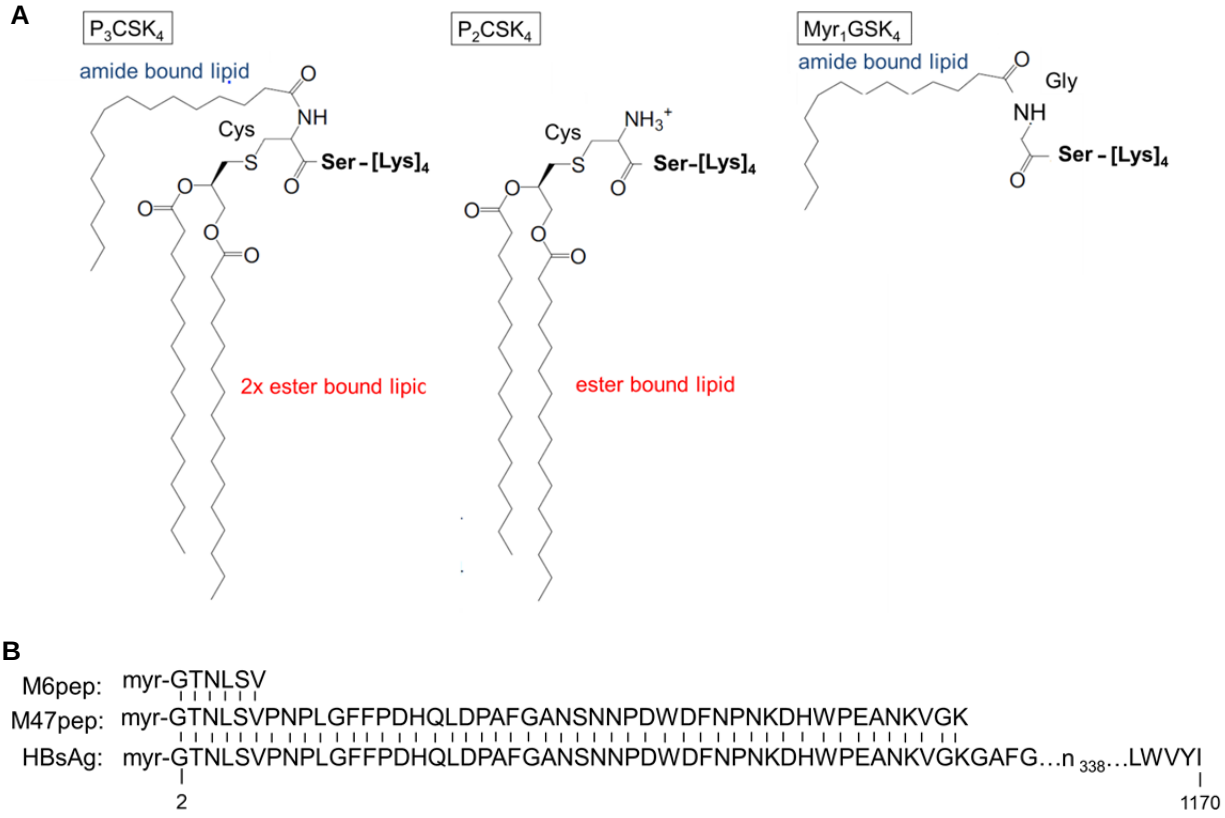

Figure 10. Prokaryotic and eukaryotic synthetic lipo hexapeptide structures and L-HBsAg synthetic analogs. **[A]** Schematic representation of synthetic lipo hexapeptides bacterial- ($P_{2/3}CSK_4$) and eukaryotic- ($Myr\text{-}GSK_4$) analogs as TLR2 ligands. Adapted from Kang et al. [55]. [**B**] Alignment of the L-HBsAg aa sequence with synthetic analogs M47pep and M6pep (letters in B are aa codes).

Subsequently, confrontation of mBMDM and hPBMCs with different length synthetic peptide M6pep or M47pep analogs of L-HBsAg triggered significantly immune response in a dose- and myristoylation-dependent manner but not their non myristoylated controls (Fig. 11A-B). *Tlr2*$^{-/-}$ mBMDM, but not *Tlr4*$^{-/-}$, were refractory to challenge by both myristoylated peptides

(Fig. 11C). In addition, myristoylated lipopeptides triggered nitric oxide release in IFNγ-primed macrophage (Fig. 11C). Similar to primary immune cells, luciferase reporter gene assays revealed myristoylation-dependent TLR2-mediated luciferase activity, but not TLR4, for challenge with synthetic monomyristoylated analogs of L-HBsAg (Fig. 11D).

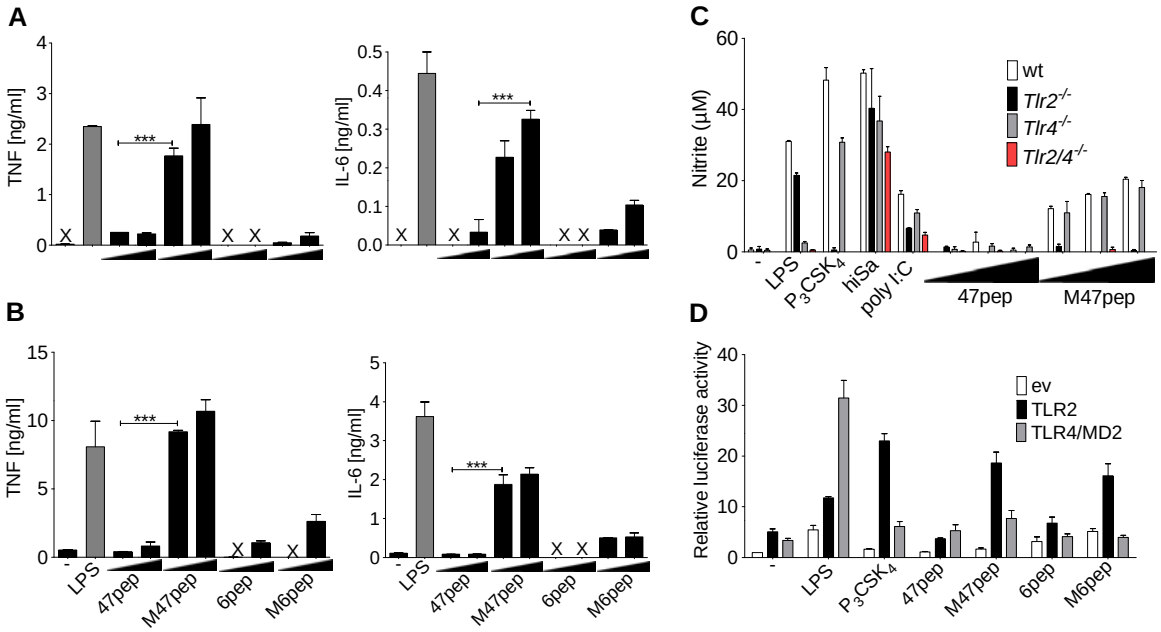

Figure 11. Myristoylated L-HBsAg derived lipopeptide analogs activate immune cell response in dose-dependent manner. hPBMCs [**A**] and mBMDM ($5x10^7$ cells/ 96 well plates) [**B,C**] were confronted for 16 h with 5 and 20 nM synthetic myristoylated (M) or non-myristoylated peptides (pep, first 6 or 47 aa of N terminus of L-HBsAg), or LPS (0,1 µg/ml), polyI:C (10 µg/ml), hiS*a* ($2x10^9$ CFU/ml), P_3CSK_4 (10 µg/ml). Cytokine and NO measurements were analyzed by ELISA and Griess assay, respectively. [**D**] HEK293 cells ($4x10^4$ cells/ well) were transfected with constructs encode NF-$_K$B luciferase (2 ng), renilla (6,45 ng) and either TLR2 or TLR4 or mock (ev) for 16 h then challenged with synthetic peptides, LPS, P_3CSK_4 for another 16 h. Luciferase activity normalized to renilla constitutive activity and related to unstimulated mock. Results are representative of three independent experiments and error bars represent SEM. (x: not detectable, (-): untreated).

In addition, myristoylated M6pep and M47pep elicited plasma release of numerous chemokines and cytokines upon their systemic application to IFNγ-primed and D galactosamine (D-Gal) sensitized wt mice, a phenotype that was not observed by *Tlr2*$^{-/-}$ mice (Fig. 12). Plasma obtained from sensitized wt mice two hour (h) post challenge with myristoylated lipopeptides significantly contained inflammatory cytokines in all measured cytokines/chemokines as compared to *Tlr2*$^{-/-}$ mice. For instance, CCL2 chemokine remained significantly higher only in wt mice 24 h post challenge. These results implicate the N-terminal mono-myristoyl-G moiety of L-HBsAg as a ligand for TLR2 *in vivo.*

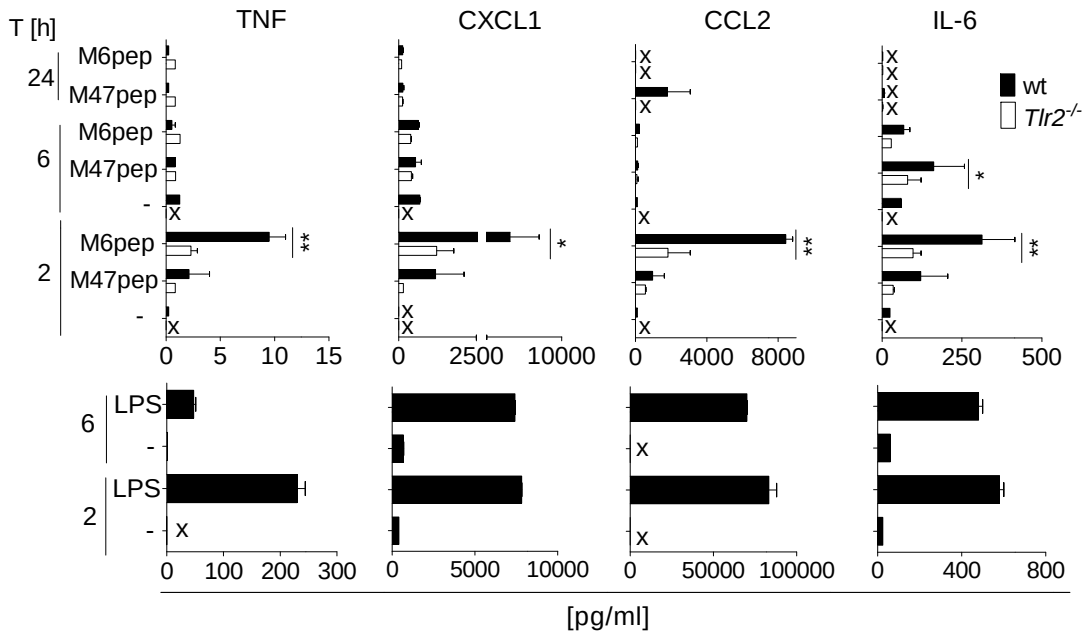

Figure 12. Synthetic myristoylated lipopeptides of L-HBsAg analogs trigger inflammatory cytokines and chemokines in wt but not in *Tlr2*$^{-/-}$ mice. wt or *Tlr2*$^{-/-}$ mice were hypersensitized by intravenous (i.v) IFNγ and 45 min later intraperitoneal (i.p) with D-Gal and peptides as indicated [upper panels]. LPS was applied to unsensitized wt mice [lower panels]. Blood was sampled after 2, 6 and 24 h by retrobulbar dotting and plasma was isolated. Results are from one experiment and measured in duplicates by luminex. Error bars represent SEM. (n=2 per group). (x: not detectable, T: time upon challenge, M: myristoylated, 6/47: number of aa, pep: peptide).

Further, monoclonal antibody (mAb) IgG1 mediated TLR2 blockade (clone: T2.5), that is cross-reactive to mice and human TLR2, significantly reduced TLR2 immune recognition of P_3CSK_4- and $MyrGSK_4$- as well as HBV-driven immune response in mBMDM and hPBMCs (Fig. 13).

3.1.5 Mutation of the L-HBsAg N-terminal myristoylation site in the HBV genomic context and innate immunological consequence.

Having established the link between N-terminal protein monomyristoylation of HBV as ligand for TLR2 and as mechanism for innate HBV recognition, and to further validate the role of myristoylation in HBV particles considering its role in virus integrity, production, and infectivity, a point mutation in the plasmid encoding genome sequence of HBV (1,3X fold) substituting the second aa in the coding gene region of L-HBsAg–glycine-to alanine was performed. Notably, protein myristoylation is known for anchoring of proteins to membranes. Thus, it has been shown that myristoylated proteins in cells regulate the cell integrity and signal transduction between membranes and cytoplasmic fractions. Therefore, whether the

myristoylation-deficient HBV would remain infectious for permissive hepatic cells and triggers innate recognition activation was a matter of investigation.

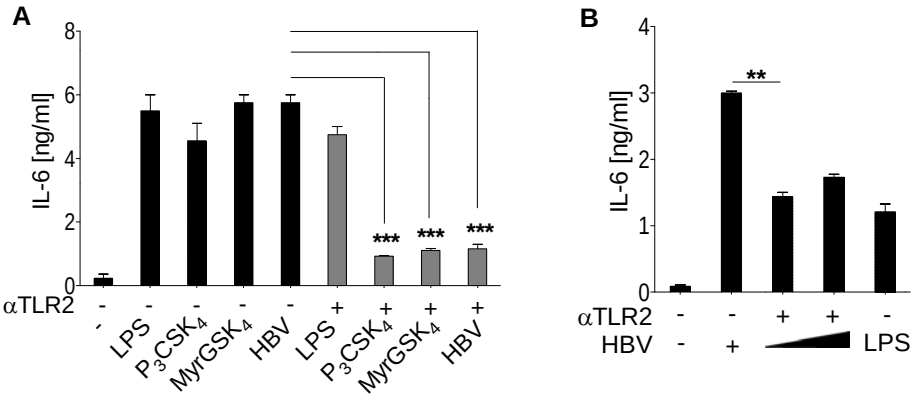

Figure 13. Blockade of TLR2 inhbits HBV-driven activation in mBMDM and hPBMCs significantly. hPBMCs ($5x10^7$ cells/ 96 well plates) [**A**] and mBMDM (10^7 cell/ 96 well plates) [**B**] were untreated or 30 min pretreated with αTLR2 mAb T2,5 (20 µg/ml) prior to challenge with either TLR ligands TLR4, LPS; TLR2 , P_3CSK_4 10 µg/ml, $MyrGSK_4$, 100 ng/ml; or HBV, $6x10^7$ virions/ml (A), or 6/12 $x10^7$ virions/ml (indicated by triangle in B). Results shown are representative of three independent experiments and error bars represent SEM.

3.1.6 Maintained viral morphology and infectivity yet impaired immunostimulation of G2A- L-HBsAg mutant HBV.

Transient transfection of constructs encoding wt- or G2A-HBV into the permissive hepatic cells huh7-NTCP was performed to characterize the viral production and replication. Indeed, comparable levels of viral antigen HBsAg and viral DNA titers as markers for virus replication were observed in wt and G2A 5 days post transfection. HBV produced from stable transfected HepG2.215 (2X HBV tandem genome fold) produced a markedly higher level of HBsAg as compared to transiently transfected cells (1,3x HBV genome fold) (Fig. 14A). The stable transfected cell line HepG2.215 produces very high titers of sub viral particles [166], which are composed of spherical HBsAg without DNA, and this possibly resemble the elevated levels of HBsAg in similar way to chronic HBV patient who suffer from elevated HBsAg titers in their circulating blood. On the other hand, quantitative PCR results showed that the virus replicates from transient transfection were significantly higher than stable transfected cells (Fig. 14B). Overall, wt and G2A HBV replications were in similar in hepatic huh7-NTCP cells.

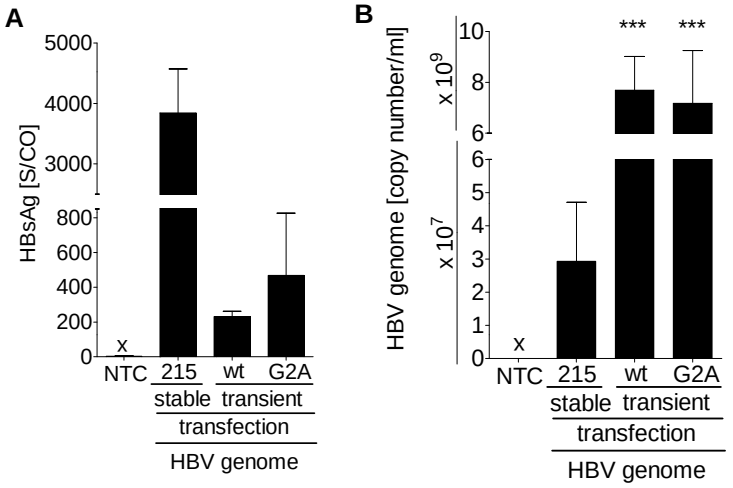

Figure 14. Comparable levels of wt and G2A-mutant HBV production in transiently HBV transfected hepatic cell line. HBV wt and G2A HBsAg ELISA [**A**] and genomic HBV-DNA qPCR [**B**] quantification in supernatant of transiently transfected (10 µg DNA constructs) huh7-NTCP cells 5 days post transfection from which supernatant was sampled and total DNA was isolated. Stable transfected HepG2.215 served as positive control. Results are representative of two independent experiments and error bars represent SEM. Data are statistically analyzed using One-Way-Anova and Turkey test. Significance levels were calculated in relation to stable transfection (215). (x: not detectable, S/CO: signal to cutoff, NTC: no template control, 215: HepG2.215).

To analyze virus integrity, transmission electron microscopic (TEM) analysis for either gelatin-fixed pellet of the cells that produced wt and G2A HBV virions (Fig. 15) or gelatin-fixed purified these virions (data not shown) was conducted. Analysis of the virus integrity of G2A HBV transfected to HepG2 cells did not display virus capsid degradation. Indeed, intact virions count and morphology of wt- and G2A- HBV were comparable. Therefore, the myristoylation of the L-HBsAg seems to be not critical in the capsid assembly (HBcAg) of HBV.

Furthermore, virus infectivity to hepatic cells was analyzed by confronting permissive cells huh7-NTCP for HBV by stable expression of the entry receptor NTCP, for 5 days with purified G2A- and wt- virions with or without transfection reagent (Fugene). In agreement with previous studies [101][167], G2A failed, unless transfected, to infect huh7-NTCP cells, indicating that myristoylation of L-HBsAg is indispensable for viral infectivity (Fig. 16A). huh7-NTCP transfected cells with wt and G2A express envelope and capsid proteins of both genotypes to similar degree 5 days post transfection (Fig. 16B).

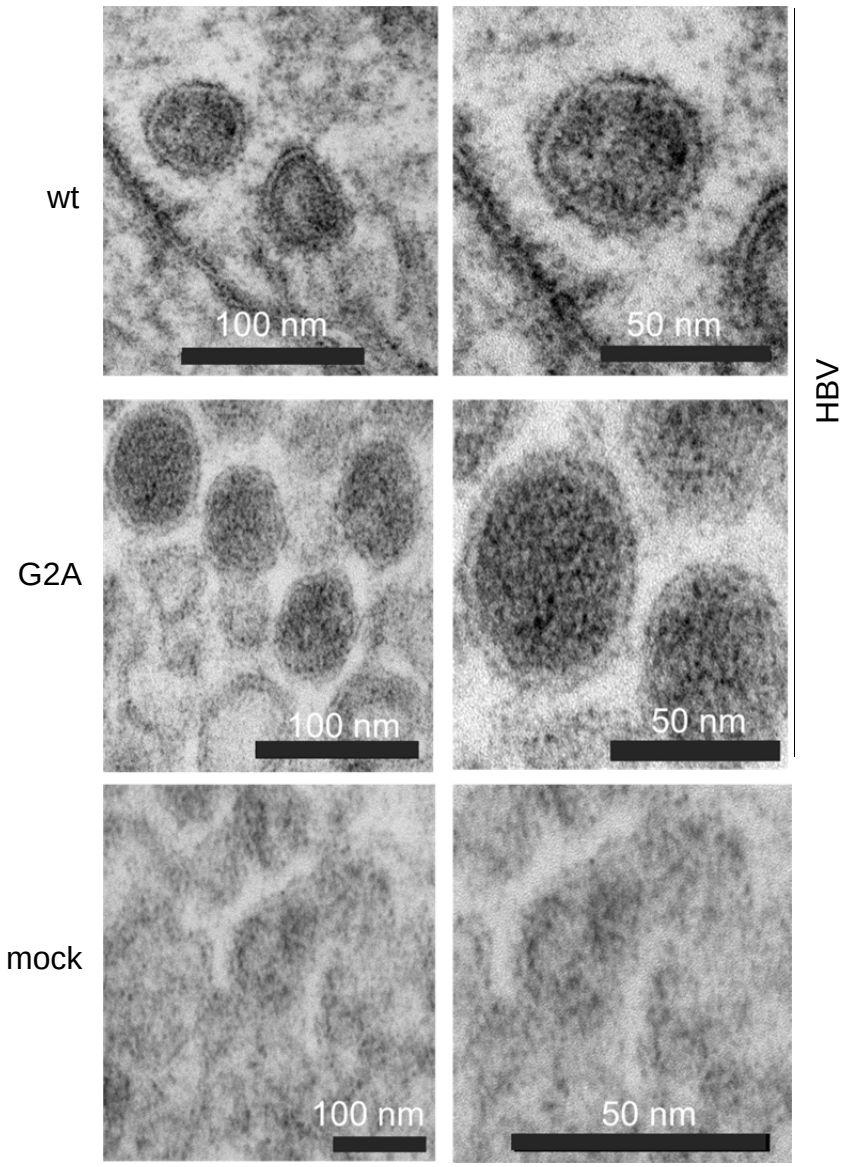

Figure 15. L-HBsAg G2A mutation does not affect the viral integrity of mutant HBV. HepG2 cells were either mock transfected or with 1,3 X constructs encoding wt- or G2A- mutant expression plasmids and incubated for 5 days . Pellets (transfected with wt or G2A HBV) were fixed with 4% gelatin for 30 min and incubated in 2.5% glutaraldhyde for 1 h followed by three times of washing with PBS. Samples were subjected to TEM analysis.

Subsequently, the immunogenic capacity of G2A- and wt HBV virions was assessed. Indeed, mBMDM and murine splenocytes as well as hPBMCs were confronted with both HBV genotypes. G2A-HBV failed to stimulate murine and human immune cells as compared to wt HBV (Fig. 17A-C), a phenotype mediated by wt HBV if subjected to *Tlr2*$^{-/-}$ immune cells (Fig. 17D). Taken together, these results prove that the functional G2A mutation exclusively affected the virus immunostimulatory properties and viral infectivity but not virus morphology or replication.

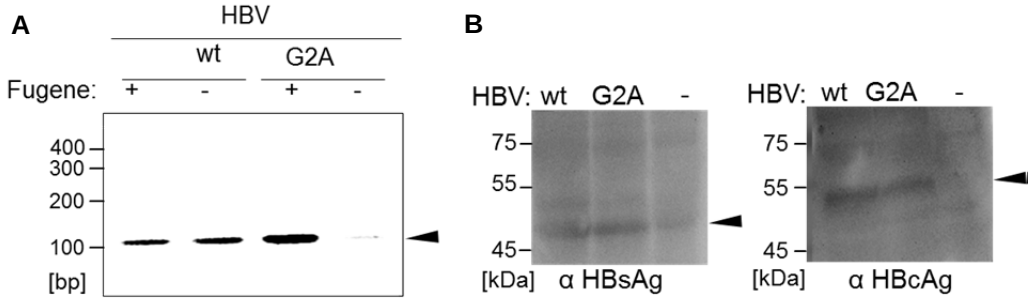

Figure 16. G2A mutated and thus myristoylation deficient L-HBsAg expressing HBV fails to infect hepatic cells unless it is transfected. [**A**] wt- or G2A-HBV purified virions ($6x10^7$ virions/ml) were subjected to huh7-NTCP cells ($6\ x10^5$ virions/ml) for 5 days with or without transfection reagent Fugene. Cells were then washed 3 times with PBS and total cell DNA was isolated for PCR analysis using HBV specific primers. While wt HBV was infectious with or without transfection reagent, specifically transfected G2A-HBV infected the cells. [**B**] Immunoblotting analysis of total lysates of huh7-NTCP cells that were transiently transfected with wt/G2A HBV expression plasmid for 5 days and their lysates analyzed with α L-HBsAg mAb (~ 47 kDa) and α capsid mAb (HBcAg) (~ 51 kDa). Results are representative of two independent experiments.

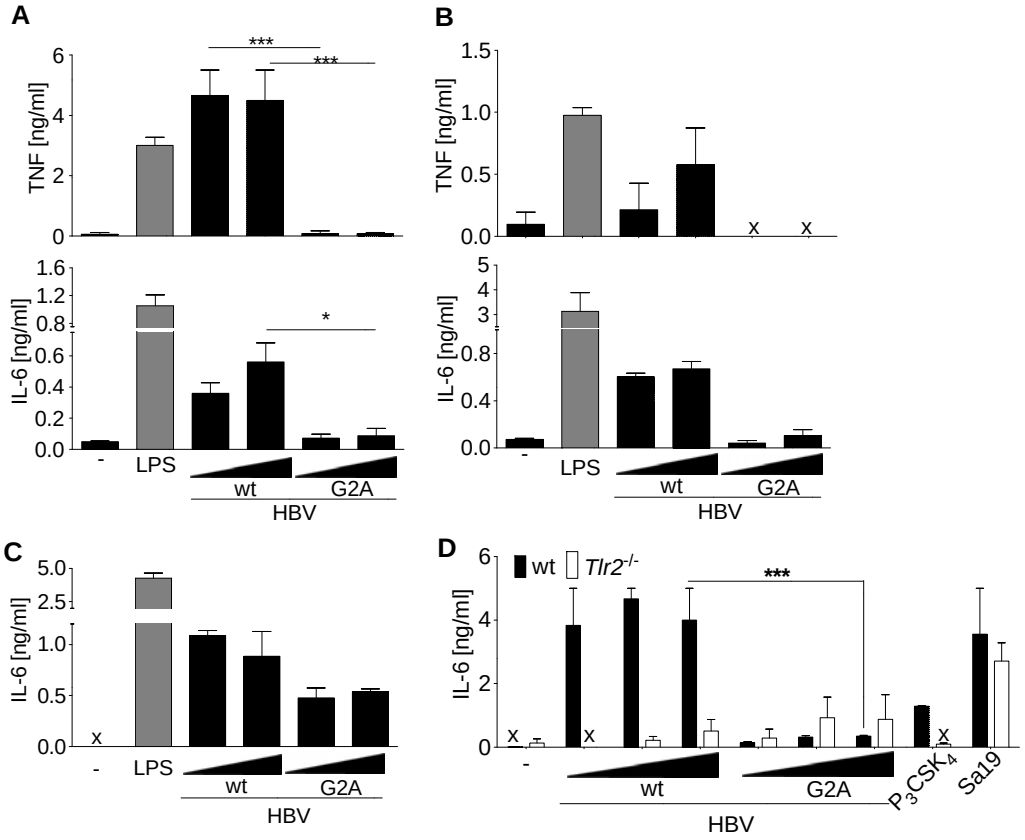

Figure 17. G2A L-HBsAg mutant HBV failed to activate immune cells. hPBMCs ($5\ x\ 10^7$ cells/ 96 well plates) [**A**] or mBMDM (10^7 cells/ 96 well plates) [**B,D**] or murine splenocytes ($7{,}5\ x\ 10^7$ cells/ 96 well plates) [**C**] were confronted with either wt- or G2A-mutant HBV (6, 20 $x10^7$ in A-C or 6, 15, 20 $x10^7$ in D

virions/ml) purified from transiently transfected hepatic huh7-NTCP cell line. 16 h post challenges, supernatant cytokines analysis from cells were measured by ELISA. Results shown are representative of three independent experiments (SEM, x: not detectable, (-): untreated, Sa19: TLR13 ligand). Data are statistically analyzed using One-Way-Anova and Turkey test.

3.1.7 Failure of HEK293 cells to overexpress wt L-HBsAg despite their ability to overexpress G2A- L-HBsAg and endogenous myristoylated protein.

For further analyze protein myristoylation and consequent TLR2 activation, sub cloning of four constructs of L-HBsAg was conducted. Specifically, the wt and G2A mutant coding sequences of L-HBsAg (Whs-wt, Whs-G2A) as well as the wt and G2A mutant preS1 epitope sequence of L-HBsAg (PreS1-wt, PreS1-G2A). Despite the successful sub cloning, confirmed by DNA sequencing (data not shown), both wt L-HBsAg and preS1 were not detectable by western blot, yet G2A- L-HBsAg was expressed (Fig. 18). Notably, L-HBsAg expression is weekly expressed in HEK293 and HepG2 cells but expressible in CHO cells [168]. The faint expression of wt L-HBsAg and not of G2A is speculated to be due to the myristoylation, through which the protein expression is hindered by anchoring to the subcellular compartment, since only G2A- L-HBsAg was detectable.

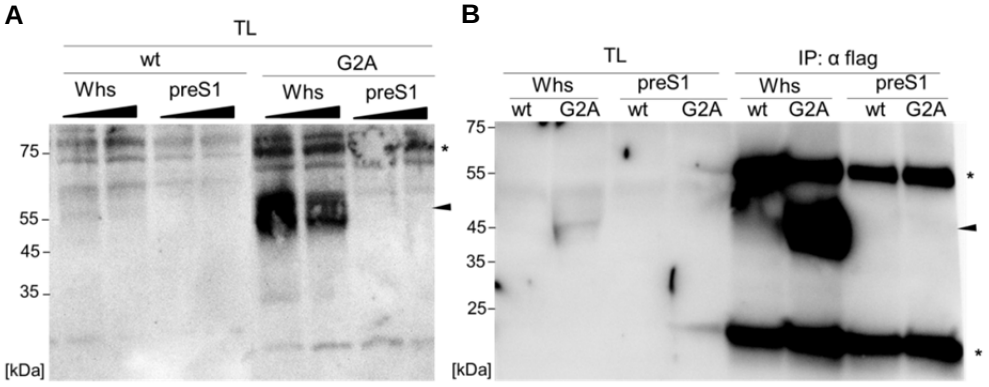

Figure 18. Detectable expression of subcloned G2A L-HBsAg but not its wildtype form. HEK293 cell lysate immunoblotting analysis directly [**A**] or upon immunoprecipitation (IP) [**B**] upon myristoylated L-HBsAg overexpression . Analysis of overexpressed flag taged- L-HBsAg; whole S (~ 47 kDa; Whs), wt, G2A and preS1 (~ 13 kDa) wt, G2A (see Fig. 2B for more detail) upon overexpression in HEK293 cells (10^7 cells/ 15 cm dish). IP was performed using flag beads. Detection was performed using anti-flag antibody. Specific and unspecific band are indicated by black triangle and asterics, repsectively.

To circumvent the week expression of L-HBsAg, the eukaryotic-derived myristoylated alanine-rich C- kinase substrate (**MARCKS**) protein was used as alternative. L-HBsAg and MARCKS are both N-terminally monomyristoylated. MARCKS is a transmembrane protein

that binds to plasma membrane via N terminus myristoylation and the phosphorylation site domain. This protein plays an important role in cell signaling, motility and cell cycling. In normal state, dephosphorylated MARCKS binds to plasma membrane and cross-links actin. Phosphorylation of MARCKS leads to its translocation from the plasma membrane to the cytosol where it functions in actin cytoskeletal remodeling, Ca^{2+} signaling through binding to calmodulin. Notably, MARCKS expression is enhanced by PAMP [169] [142]. Indeed, 16 h LPS, IFNγ or PMA/ionomycin stimulations of Raw264.7 cells and LPS for primary mBMDM clearly upregulated endogenous MARCKS in primary cells and to a substantial degree in RAW264.7 cells (Fig. 19).

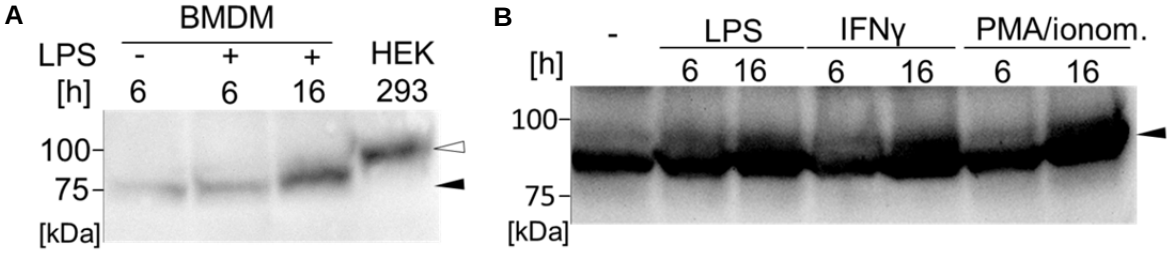

Figure 19. LPS induces MARCKS upregulation in mBMDM and Raw264.7 cells. Immunoblot analysis of total lysate (80 µg) of mBMDM [**A**] or Raw264.7 cells [**B**] either untreated (-) or challenged with 100 ng/ml LPS (only A) or with IFNγ [20 ng/ml] or PMA [0,1 µg/ml] + ionomycin [1 µg/ml] [**B**] for either 6 or 16 h. MARCKS protein band was visualized using mouse αMARCKS mAb. Specific and unspecific bands are indicated by black and white triangles, respectively (h: hour, ionom. : iononmycin).

G2A mutated MARCKS expression plasmid was engineered by site directed mutagenesis from wt form of MARCKS and equal expression of wt and G2A MARCK as total lysate (TL) or immunoprecipitated purified MARCKS (IP) was ensured for further comparative analysis between both constructs (Fig. 20).

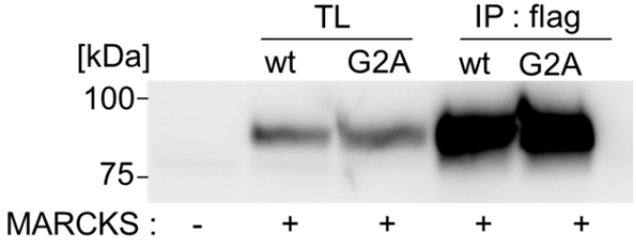

Figure 20. Immunoblotting of HEK293 cell lysate directly or immunoprecipitation of overexpressed MARCKS in transfected HEK293 cells. Transfection of flag tagged MARCKS expression plasmid (6 µg DNA) into HEK293 cells (10^7 cells/ 15 cm dish). Total cell lysate (TL) or M2-flag

beads-immunoprecipitated (IP) MARCKS were immunoblotted and detected using αMARCKS mAb. ((-) : untransfected, (+) : transfected).

3.1.8 Myristoylated synthetic lipopeptide analogs of HIV derived NEF protein or eukaryotic MARCKS activate immune cells through TLR2 engagement.

Similar to myristoylation of L-HBsAg in HBV, several other viruses are known to carry N-terminal myristoylated proteins. Indeed, retroviruses including HIV and Friend, Moloney, and Rauscher murine leukemia retroviruses, as well as Lassa viruses all utilize the host protein acylation machinery towards expression of their -NEF and -GAG, as well as Z proteins, respectively, in an N-terminally mono-myristoylated (myr) forms. To broaden my analysis of TLR2-dependent myristoylated lipopeptide recognition, synthetic myristoylated 6 aa length synthetic lipopeptides of NEF (HIV) and MARCKS were synthesized and non-myristoylated forms of them were served as controls. Additionally, myristic acid alone, and myr-G were also included in my analysis. Stimulation of mBMDM with these short lipopeptides at low conncentration (50 nM) did not trigger a detectable immune response (data not shown). However, at higher concentration, these lipopeptides triggered myristoylation-dependent immune response mirrored by secretion of various inflamatory cytokines. Myristoylated 6 aa lipopeptides were more detectable on silver stained urea gel as compared with their non-myristoylated control (see next chapter for urea tricine gel). Interestingly, the fatty acid myristic acid alone did not activate macrophages, while myristic acid coupled with glycine myr-G weekly stimulated macrophages. These results suggest that myristic acid alone is non immunostimulatory unless it is N-terminally glycine acylated towards peptide/protein (Fig. 21).

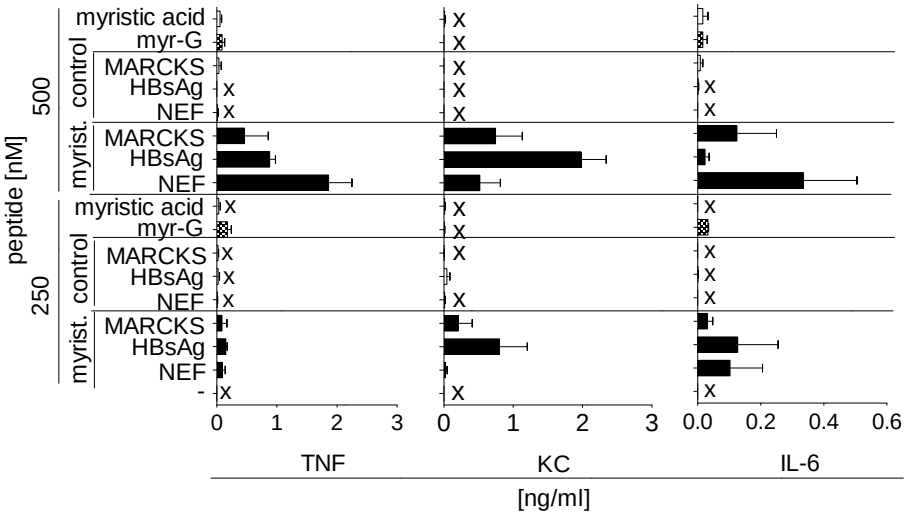

Figure 21. Myristoylated lipo-hexapeptide analogs representing MARCKS, L-HBsAg, and NEF activate mBMDM. Lipo hexapeptide analogs of L-HBsAg (HBV), NEF (HIV) or endogenous MARCKS N-termini activated mBMDM (10^7 cells/ 96 well plates) in 16 h challenge in a dose dependent manner was analyzed by ELISA. Results are representative of two independent experiments and error bars represent SEM. (x: not detectable).

3.1.9 Myristoylated lipopeptide-driven TLR2 activation is N-terminal G as well as peptide length dependent.

Having observed the differences of the immune response by different lengths of N terminus myristoylated lipopeptides, investigation for the possible minimum length of myristoylated lipopeptides that ligate to TLR2 and activate immune response was explored. As observed before, myr-G alone was weekly immune stimulatory in mBMDM. However, the immune response towards the lipopeptides was positively coinciding with the increasing length of the lipopeptide. Indeed, up to 47 myristoylated lipopeptide clearly triggered immune response higher than 15 length aa upon confrontation in mBMDM. Interestingly, only N terminal glycine myristoylated lipopeptides activated TLR2, yet, N-terminal lysine (K) failed to do so (Fig. 22). These data suggest that the short lipopeptides, despite binding to TLR2, might not be sufficient to fully activate the receptor downstream signaling pathways to initiate immune response unlike long N terminus glycine-myristoylated lipopeptides.

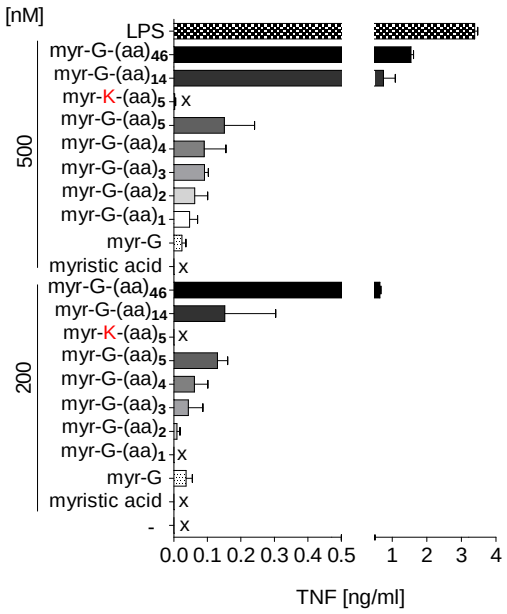

Figure 22. N-terminal G and length dependent TLR2 activation by myristoylated-lipopeptides. Differently sized synthetic lipopeptide analogs representing the L-HBsAg N terminus, namely, $(aa)_1$, (T); $(aa)_2$, (TN); $(aa)_3$, (TNL); $(aa)_4$, (TNLS), $(aa)_5$, (TNLSV); K-$(aa)_5$, (KTNLSV); $(aa)_{14}$, (TNLSVPNPLGFFPD); or $(aa)_{46}$ (47pep sequence as mentioned before in Fig. 10B) were applied in two doses indicated for 16 h to mBMDM (10^7 cells/ 96 well plates). Supernatant-contained cytokines were analyzed by ELISA. TNF is representative of 3 measured cytokines and similar results of two independent experiments and error bars represent SEM. (x: not detectable).

3.1.10 Attempts to enzymatically demyristoylate lipopeptides.

One of the bacterial evading strategy to presist infection is the production of certain enzyme to inactivate target-antibiotics [170]. Polymyxin acylase (PA) is among bacterial lipase virulence factor. PA is an enzyme produced by Gram negative *Pseudomonas sp*., targets the long chain fatty acyl group of polymyxin B (PmB) antibiotic, thus, deacylases the polymyxin group with consequent loss of antibiotic function. Accordingly, I tested whether PA would N-terminally deacylate myristoylated protein.

The antibiotic PmB attenuates the biological Gram negative-derived LPS-mediated TLR4 activation, through binding to lipid A (Fig. 23A). Indeed, incubating mBMDM for 1 h with PmB antibiotic prior to challenging with LPS significantly attenuated LPS-driven immunestimulation (Fig. 23B), while LPS incubation for 1 h with the enzyme at 37°C prior to challenging with PmB-treated cells recovered the LPS immune activity. Meantime, PA alone did not directly affect LPS immune response (Fig. 23B,C). Therefore, I tested whether PA act as N-myristoyl cleaving enzyme in HBV derived protein, thereby, abolish HBV immune activity. Interestingly, HBV-driven immune stimulation was dramatically reduced already 2 h

post incubation with PA at applied concentration of 5 µg/ml. Contrarily, the enzyme did not affect the immunostimulatory potential of bacterial tripalmitoylated lipopeptides (P_3CKS_4) or LPS (Fig. 23 C).

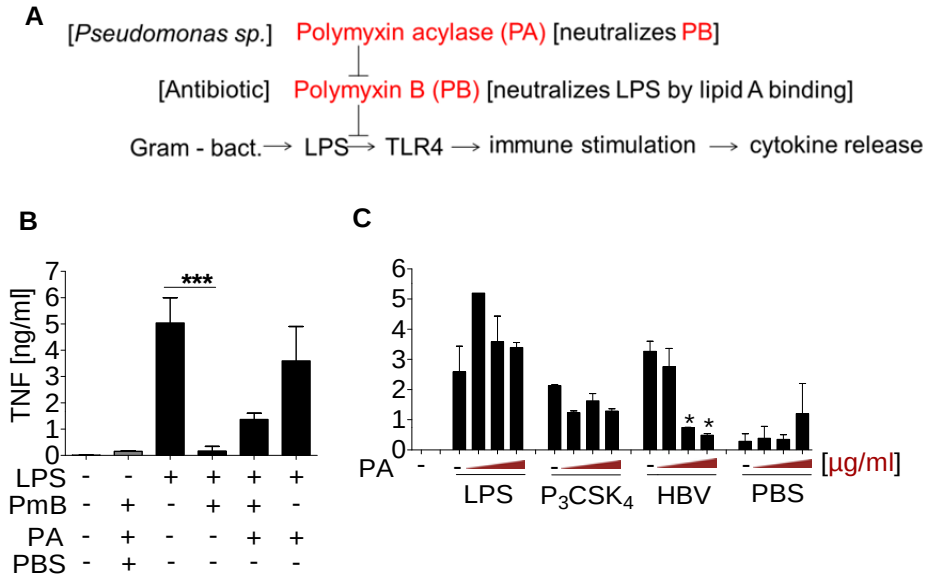

Figure 23. Abrogation of HBV-driven immunostimulation upon polymyxin acylase pretreatment. [**A**] Schematic representation of the polymyxin acylase (PA) mechanism of action. PA abrogates PmB-mediated LPS neutralization [**B**]. mBMDM (10^5 cells/ well) were subjected to 16 h challenge with 60 min untreated- or PA pretreated- [5 µg/ml] LPS [100 ng/ml] or PBS. [**C**] mBMDM (10^7 cells/ 96 well plates) were challenged for 16 h either with LPS [100 ng/ml], P_3CSK_4 [10 µg/ml], or HBV [10^9 virions/ml], which were either incubated at 37°C for 120 min (heat block) as untreated or pretreated with PA at final concentrations of 0.5 , 5 , or 50 µg/ml. supernatant TNF was analyzed by ELISA. Result is representative of two independent experiments and error bars represent SEM. Data are statistically analyzed using One-Way-Anova and Turkey test. Significance levels were calculated in relation to untreated control. (PBS: phosphate buffer saline, PA: polymyxin acylase, PmB: polymyxin B, (-): untreated, (+): pre-treated).

Having observed the attenuation of HBV-driven immune response in mBMDM upon incubating with PA, visualizing the underlying demyristoylation mechanism by PA was approached. To do so, N terminus myristoylated C terminus biotinylated lipopeptide analogs of L-HBsAg (M47pep) or their control (47pep) were ordered and incubated upon resuspension with different concentration of PA. The demyristoylation properties of the PA enzyme were not observed by applying the untreated versus PA-treated lipopeptides to urea-tricine gel (Fig. 24A). The fast migrating myristoylated lipopeptide (~ 10 kDa) on urea gel was not as slow as the non-myristoylated peptide controls (~ 17 kDa) if they were treated with PA enzyme at any applied dose of the enzyme. Therefore, the reason for the ambiguous effect

of PA on HBV immune response and the purified myristoylated lipopeptides (Fig. 24B) remained unanswered question.

α aminopeptidase (αAP) enzyme is produced by *Aeromonas proteolytica*, a halophilic bacterium originally isolated from the intestine of a marine isopod [153] and was used in my study as alternative to cleave N-terminal myristoylated-glycine by treating the lipopeptides for 20 min at RT with this enzyme. α AP has its N terminus peptidase activity at RT [171]. Testing α AP enzyme on biotin labeled myristoylated / non-myristoylated peptides demonstrated its enzymatic degrading property; peptide treatments with α AP at a higher concentration were completely digested (5 g/l) (Fig 26 B). Down titrating the concentration of the α AP demonstrated its degrading properties onto myristoylated lipopeptides and upshift them to band at similar level of non-myristoylated peptide controls (Fig. 24C), while longer incubation (90 min) renders the enzyme activity unspecific and causes degradation of the peptide regardless of its acylation pattern, suggesting that the enzyme has exonuclease activity (Fig. 24D). Incubation dose of 1 µg/ml of α AP with HBV or myristoylated synthetic lipopeptide, but not LPS, for 60-90 min was sufficient to degrade their immunostimulatory properties in murine macrophages (Fig. 24E).

3.1.11 TLR2 dependent HBV recognition in hPBMCs, yet additional contribution of endosomal TLRs.

Upregulation of TLR2 and TLR4 in hPBMCs is a common phenomenon in bacterial infection and liver cirrhosis leading to secretion of inflammatory cytokines such as TNF [172]. Furthermore, TLR2 and TLR4 expression levels are closely similar in hPBMCs in response to LPS challenge [173]. Experiments performed in this thesis on murine macrophage demonstrated the selective TLR2-dependent HBV immune response *in vitro* and the contribution of TLR2 in HBV clearance *in vivo*. Therefore, I asked whether these observations are also the case in hPBMCs.

Prior to confrontation, hPBMCs were 30 min incubated either untreated, chloroquine-treated, anti-TLR2 antibody treated, anti-TLR4 antibody treated, isotype control treated (IgG1) or in combinations. Chloroquine inhibits endosomal TLR activity by inhibiting endosomal acidification and raising the lysosomal pH [174]. As expected, P_3CSK_4 immunostimulatory properties were inhibited upon incubating hPBMCs with anti-TLR2 antibody alone or in combination with other inhibitors, while the same was observed by LPS upon incubating the cells with anti-TLR4 antibody alone or in combination with other inhibitors. On the other

hand, the immunostimulatory response of TLR7/8 ligand loxoribine was attenuated by chloroquine treatment.

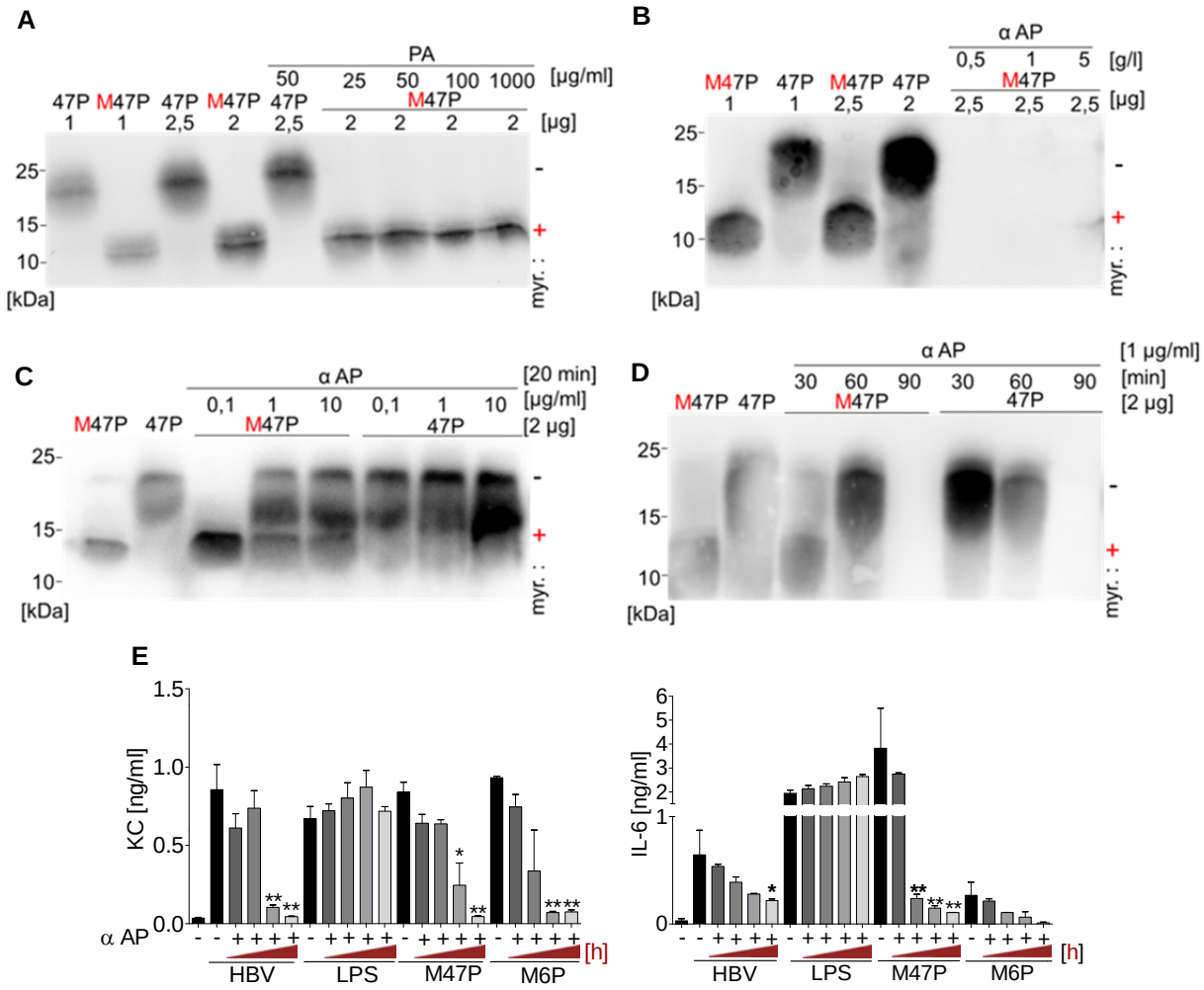

Figure 24. Lipopeptide enzymatic demyristoylation by αAP but not by PA pretreatment.

Urea-tricine 14% SDS-PAA gel loaded with C terminal biotin-labeled N-terminally myristoylated 47 lipopeptide (M47pep) or non-myristoylated control (47pep) as untreated or pretreated with polymyxin acylase [**A**] or α aminopeptidase (αAP) [**B-D**] for the indicated times and concentrations identified. Detection was achieved by streptavidin-HRP. [**E**] HBV (10^9 virions/ml), LPS [100 ng/ml], myristoylated 47P (M47pep) [10µg/ml] or myristoylated 6P (M67P) [10µg/ml] were incubated either alone or with α AP [1 µg/ml] for 0.5, 1.0, 1.5, and 2 h at RT and applied to mBMDM (10^7 cells/ 96 well plates) for 16 h. Released cytokines were measured by ELISA. (Myristoylated/demyristoylated peptides [A-D] are indicated by plus and minus signs where in all indications myristoylation in red). Immunostimulation result is representative of two independent experiments and error bars represent SEM. ((-): untreated, (+): pre-treated, h: hour).

Importantly, the response of HBV-driven immunostimulatory properties was genotype-dependent; wt triggered its immune response if TLR2 was not blocked, while G2A mutant if endosomal TLRs were not blocked (Fig. 25). Moreover, immunostimulatory properties of wt

HBV was at least 2 fold higher than G2A. This finding might shed light on possible HBV related nucleic acid recognition, which is masked if myristoylation of HBV particles is operative.

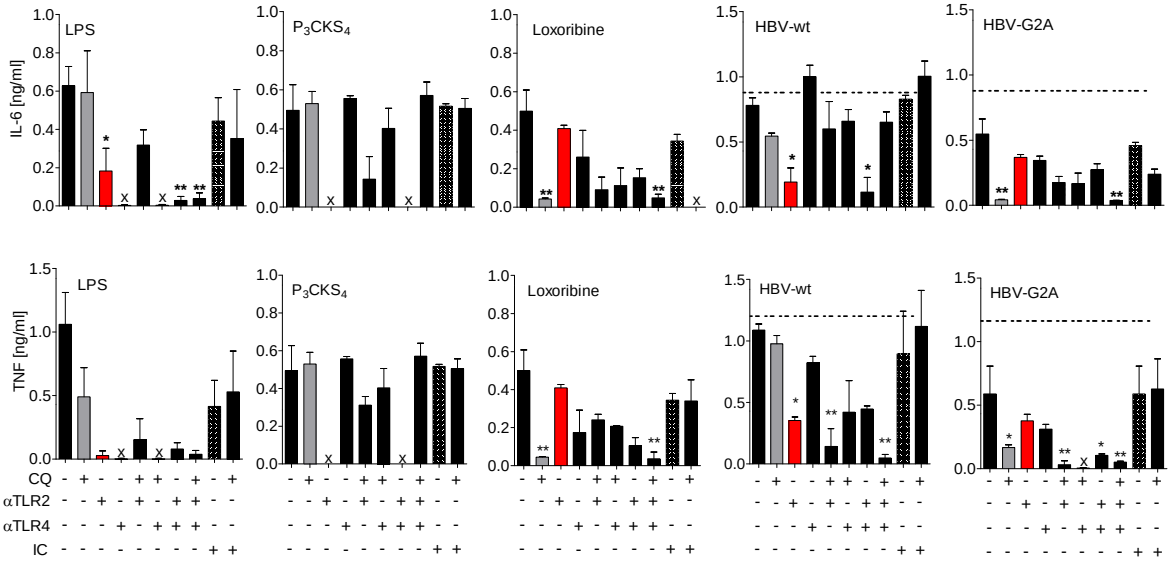

Figure 25. Largely TLR2-dependent recognition of wt HBV, yet endosomal TLR involvement in recognition of G2A-L-HBsAg HBV by hPBMCs. hPBMCs were seeded in 96 well plates (5 x10^7 cells) and incubated either untreated or pretreated with different TLR inhibitors; αTLR2 mAb (clone T2,5 : 20 µg/ml), αTLR4 mAb (clone 3C3: 10 µg/ml), endosomal TLR inhibitor (chloroquine: 10 µg/ml), isotype control (IC, IgG : 15 µg/ml) or in combinations of one or two or three of inhibitors as indicated for 30 min followed by cell stimulation with TLR ligands LPS, 0.1 µg/ml; P_3CSK_4, 10µg/ml ; Loxoribine, 1mM or wt and G2A-mutant HBV (15x10^7 virions/ml) for 16 h. Released cytokines in the supernatant were measured by ELISA. Results shown are representative of three independent experiments and error bars represent SEM. (x: not detectable, (-): untreated, (+): pre-treated).

3.1.12 Protein overexpression and promotion of myristoylation correlates with increased stimulatory potential of cell lysates.

Protein myristoylation in eukaryotic cells is launched by targeting translated protein with myristoyl group that is carried by carrier molecule CoA (myristoyl-CoA) through N-myristoyl transferase enzyme (NMT) after cleaving the first methionine aa catalyzed by methionine amino peptidase. Considering this as a prerequisite for protein myristoylation, I asked whether protein myristoylation is enhanced by feeding MARCKS-transfected cells with both myristoyl-CoA and NMT enzyme, and, consequently, more TLR2 immune activation would be expected. To test this hypothesis, NMT- and MARCKS transfected HEK293 were fed with 50 µM myristoyl-CoA two days after transfection and cell total lysates applied for mBMDM confrontation. Results indicated that MyrCoA feeding and NMT coexpression with MARCKS

potentiated the myristoylation-mediated MARCKS-driven immune stimulation as compared to single overexpressed MARCKS. Notably, MARCKS + NMT transfections without myr-CoA did slightly enhance the overall immunostimulatory properties of MARCKS (Fig. 26).

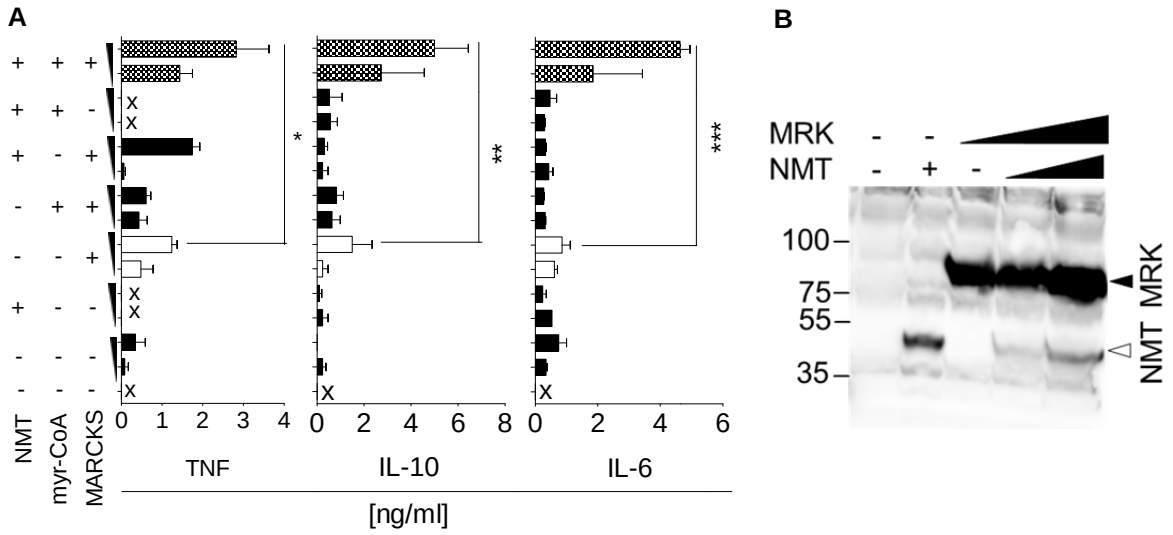

Figure 26. Enhanced immune response of hPBMCs confronted with lysates of differentially pretreated HEK293 cells to increase cellular protein myristoylation. [**A**] HEK293 cells (4,5 x10^6 cells/ 9 cm dish) were either single transfected with MARCKS constructs (6 µg DNA) or cotransfected with constructs encoding MARCKS and NMT (4 µg DNA) 48 h and 6 h before cell harvesting cells were fed with myristoyl-CoA (15 µM) to boost protein myristoylation. Cells were then lysed through ultrasonication using bioraptor (20 sec pulse, 3 times at 0°C). Protein concentration was measured by pierce assay and mBMDM (10^7 cells/ 96 well plates) was subjected to total lysate challenge (10/20 µg/ml). [**B**]. Western blot of HEK293 cells total lysate transfected with constructs encode MARCK (4, 8, 12 µg DNA) or NMT (2, 4 µg DNA) or in combination of both. Results are representative of two experiments and error bars represent SEM. (MRK: MARCK, NMT: N myristoyl transferase, x: not detectable, (-): untransfected/ untreated, (+): transfected).

3.1.13 Wildtype-, but not G2A-, Friend Murine Leukemia Virus like particles activate TLR2 mutant.

Gag protein of Friend murine leukemia virus (FMuLV) plays an important role in virus budding. It is processed by the viral protease during virion maturation and counteracts host restriction factor such as APOBEC3 [175][176]. Interestingly, myristoylated deficient FMuLV transfected cells do not shed out FMuLV particles and supernatant from these cells failed to infect T lymphoblastoid cells [177]. Whether the myristoylation of Gag protein of FMuLV triggers TLR2-dependent immunostimulation to a similar degree as that observed by L-HBsAg from HBV was a matter of investigation. Therefore, and to omit any possible

involvement of nucleic acid-derived immunostimulatory response, only virus like particles (VLPs) consist of two proteins, namely, Gag and envelope proteins, were overexpressed to assemble FMuLV VLPs. HEK293 cells were cotransfected with either myristoylated (wt) or non-myristoylated (G2A) Gag with envelope constructs. Western blot analysis and gel staining analysis confirmed the expression of both proteins forming VLPs (Fig. 27B). Further, TEM analysis revealed that the integrity of VLPs was not myristoylation dependent – by comparing G2A versus wt VLPs (Fig. 27A) - an observation that was previously observed in G2A HBV mutant.

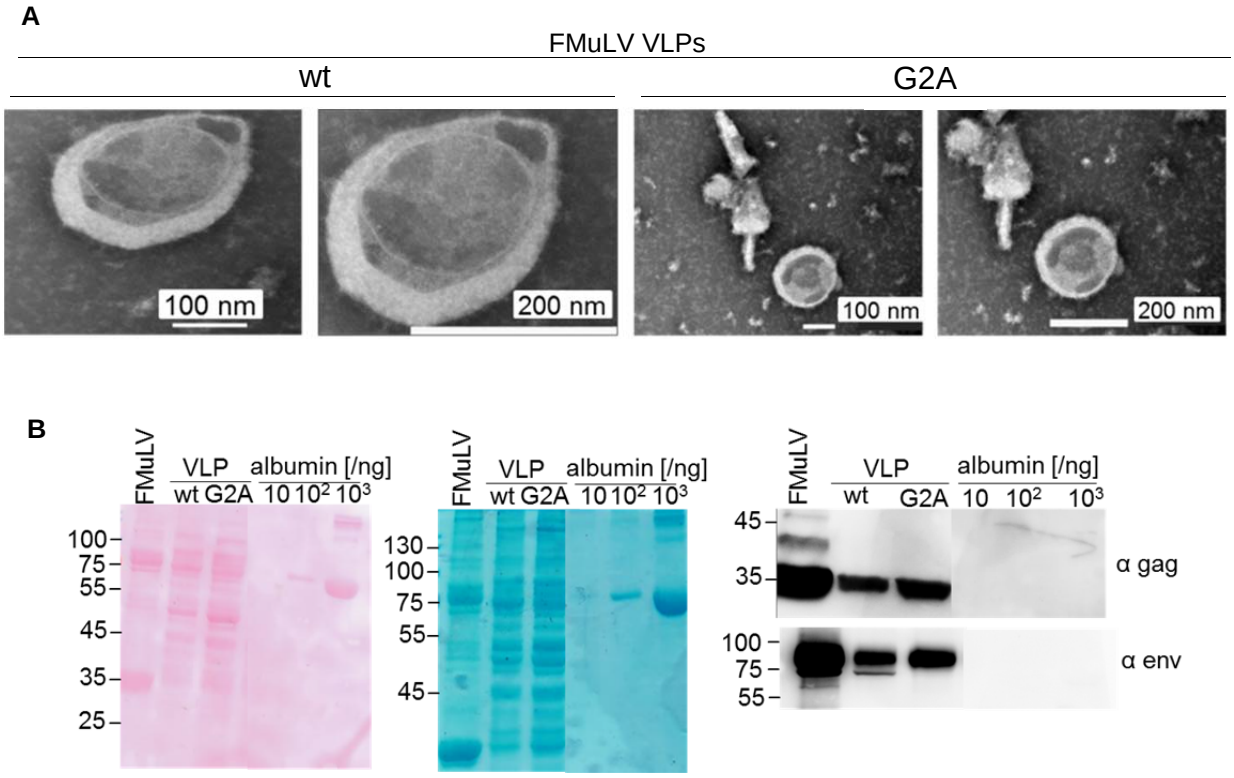

Figure 27. Unimpaired integrity of wt and G2A-GAG FMuLV derived VLPs. [**A**] TEM of VLPs integrity of G2A as compared to wt FMuLV derived VLPs produced by co-transfecting HEK293T cells (5 x 10^7 cells/ 15 cm dish) with expression plasmids encodes either wt or G2A-mutant gag (70 µg DNA) with plasmids mediating envelope expression (70 µg DNA). VLPs host transfected cells were fixed by 2,5 % glutaraldehyde followed by washing twice with PBS and negative staining analysis. Scale bar: 100 nm. [**B**] Stained for nitrocellulose membrane and upon blotting to 14% SDS gel (upper and lower panels, respectively) as well as specific VLPs immunoblot analysis western blot analysis by loading 4 µg protein concentration of VLPs on two 14%SDS gels. Once electrophoresed, the first gel was stained with Coomassie blue reagent, while the other gel was immunoblotted for western blot and subjected to Ponceau staining. Albumin (~ 67 kDa) was applied at different concentration as loading and specificity control.

On the other hand, wt Gag-derived VLPs triggered immune stimulation in murine and human immune cells to similar levels as whole virus (FMuLV) itself, while G2A VLPs were immune tolerant. Additionally, both wt and G2A constructs of VLPs failed to respond if TLR2 was

lacking in mBMDM (Fig. 28). These results broaden our knowledge that the protein myristoylation regularly activate TLR2 regardless of its origin.

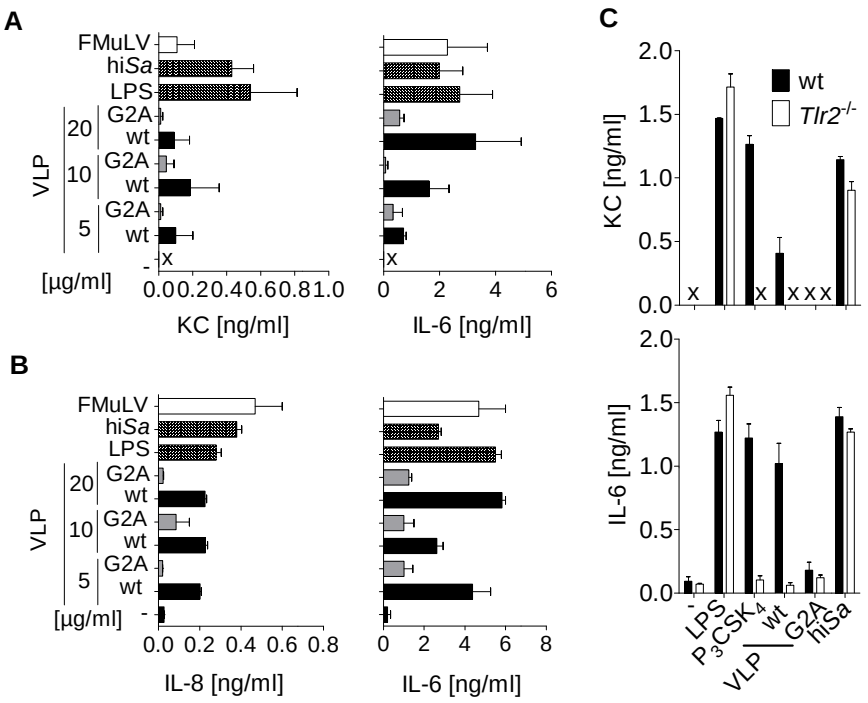

Figure 28. G2A-gag FMuLV derived VLPs failed to activate immune cells while wt counterparts activated immune cells in TLR2 dependent manner. mBMDM (10^7 cells/ 96 well plates) [**A,C**] and hPBMCs ($5x10^7$ cells/ 96 well plates) [**B**] were subjected to immune challenge by stimulation with either LPS (0,1 µg/ml), hi*Sa* ($2x10^9$ CFU/ml) or purified wt or G2A-GAG FMuLV derived VLs (20 µg/ml) (black and gray bars) or purified FMuLV virions (white bars) for 16 h. [**C**] Wt or *Tlr2*$^{-/-}$ mBMDM (10^5 cells/ well) were challenged with P_3CSK_4 (10 µg/ml) and LPS (0,1 µg/ml) ligands, hi*Sa* or purified wt or G2A- mutant formed VLPs (20 µg/ml) for 16 h. Cytokine supernatants were measured by ELISA. Results are representative of two independent experiments and error bars represent SEM. (x: not detectable).

3.2 Visualization of protein myristoylation.

Previous method to visualize protein acylation was based on using radioactive-labeled substrates, such as 9,10-^{3}H. The disadvantage of this method is the biological hazard by using low energy beta emitter. Recent advances in chemical biology techniques utilize click chemistry to study protein acylation. Additionally, mobility difference of myristoylated versus non-myristoylated peptides is visualized by loading them in urea-tricine high percentage SDS gel.

3.2.1 Visualization of MARCKS myristoylation via click chemistry mediated biotinylation of activated myristic acid derivative fed to cells towards N-terminal protein coupling.

Click chemistry was first introduced by Sharpless et al. in 2001 that describes metabolic visualization of protein by covalent linking of chemical groups such as myristoyl group at certain sites of a target protein with high site-selectivity [178]. In the presence of copper, addition of (fluorescent- or biotin labelled)-alkyne group favored cycloaddition between myristoyl-azide (myr-N_3) and alkyne forming triazole complex (Fig. 29A). The complex is visualized by detecting the fluorescent dye or, as used here, through streptavidin-HRP towards biotin on SDS membrane. Click chemistry is described as ''biorthogonal'' reaction since it does not interfere with the natural protein acylation pathway.

Surrogate to eukaryotic cell derived protein; MARCKS was used to visualize its N-terminal monomyristoylation. Immunoprecipitated MARCKS subjected to click chemistry displayed a myristoylation band, detected by streptavidin. Moreover, click chemistry results indicated that overexpressing cells do not require external NMT to myristoylate MARCKS and endogenous NMT was sufficient to carry on MARCKS myristoylation, since NMT coexpression was dispensable for myristoylation detection (Fig. 29B). However, lacking myr-N_3 or alkyne biotin hampered myristoylation detection.

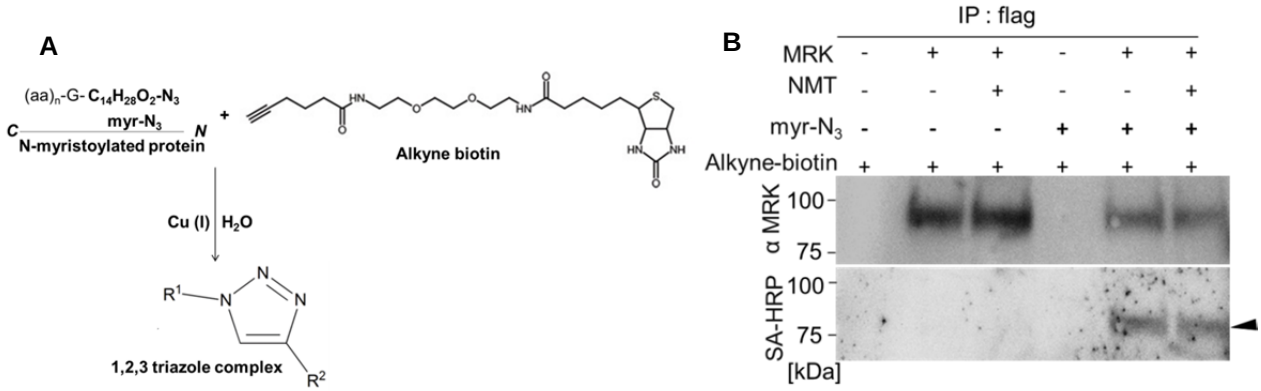

Figure 29. *In-situ* detection of MARCKS myristoylation through click chemistry. myr-N3 was fed to flag MARCKS overexpressing cells for 6 h prior upon which cell lysis followed by flag- IP and biotinylated-alkyne labeling. Consequently, a 1,2,3 triazole complex was formed in the presence of Copper ion. HEK293 cells (10^7 cells/ 15 cm dish) were transfected either with flag tagged human MARCKS (12 µg) alone or in combination with NMT expressing plasmids (4 µg). 16 h later, medium was changed and cells were fed with myr-N_3 (20 µM) prior to cell lysis. MARCKS in cell lysate was immunoprecipitated (IP) using flag beads. Purified MARCKS was labeled with alkyne biotin and subjected to immunoblotting. MARCKS myristoylation was detected first using streptavidin-HRP (lower panel) and day after MARCKS expression was detected by

mAb anti-MARCKS (uppper panel). Black triangle indicates specific band. (MRK: MARCKS, SA-HRP: streptavidin-HRP, *N,C* : protein N, C terminus, n: aa given number, kDa: kilo Dalton).

Since MARCKS is N terminally myristoylated and their G2A-mutant form cannot be myristoylated, click chemistry analysis was preformed to validate and confirm this hypothesis. While the expression levels of wt and G2A MARCKS in HEK293 cells were similar (Fig. 30B), both G2A MARCKS, and also L-HBsAg, failed to undergo myristoylation upon *in situ* labeling, but not wt MARCKS (Fig. 30A). This result qualifies click chemistry as quantitative method for ''myr-G'' acylation detection.

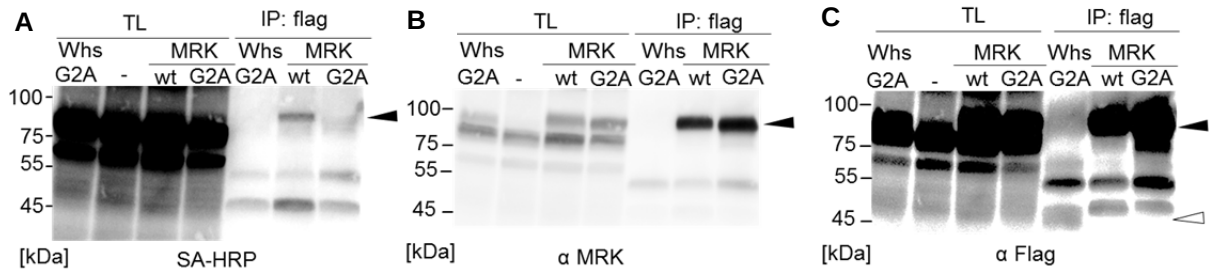

Figure 30. wt MARCKS, but not its G2A or L-HBsAg mutants, is myristoylated upon overexpression in HEK293 cells. Click chemical analysis of HEK293 cell lysate (10^7 cells/ 15 cm dish) transfected with flag tagged wt and or G2A L-HBsAg (Whs) (12 µg) expression plasmids. Cells were fed (incubated) with myr-N_3 for 6 h prior to cell lysis. Flag IP was performed and incubated with alkyne biotin. Total lysate (TL) and protein IP were immunoblotted and incubated with streptavidin – HRP **[A]**, anti-MARCKS mAb on day 2 **[B],** and rabbit anti-flag on day 3**[C]**. Click chemistry specific band on **[A]** at 80 kDa. MARCK wt and G2A ~80 kDa in **[B]**, flag L-HBsAg specific band ~ 47 kDa (unfilled triangle) **[C].** Results are representative of two individual experiments. The same membrane was used in A, B, and C. Black triangle represents MARCKS myristoylation [A] or expression [B, C]. (MRK: MARCKS, SA-HRP: streptavidin-HRP, kDa: kilo Dalton, (-) : untransfected).

Given that protein myristoylation demands the activity of NMT enzyme, NMT-inhibitor (Tris-DBA) was applied to attenuate MARCKS myristoylation prior protein post modification, or post modification by treating myristoylated MARCKS with PA or α AP enzymes as mentioned before. While immunoprecipitated myr-N_3 labeled- MARCKS expression itself was slightly reduced by enzymatic treatment with PA, yet it was not affected by NMT inhibition (Fig. 31A). However, click chemistry demonstrated the abrogation of myristoylation by three determent options as compared to untreated MARCKS (Fig. 31B).

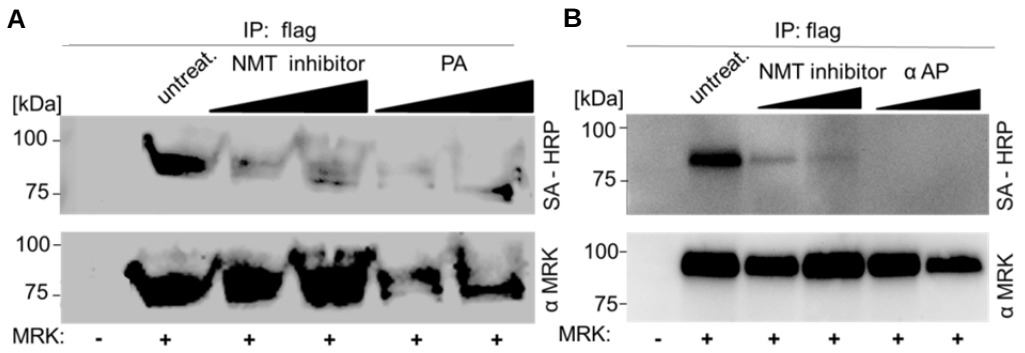

Figure 31. Enzymatic demyristoylation and inhibiting myristoylation through NMT inhibitor application. HEK293 cells (10^7 cells/ 15 cm dish) were either mock- or MARCKS- transfected (12 µg) using $Ca_3(PO_4)_2$ transfection reagent. A day later, cells were labeled with myr-N_3 (20 µM) and 30 min later either untreated or NMT inhibited by Tris-DBA (20/60 µM). 6 h later, MARCKS was subjected to IP using flag beads and was either untreated or placed in PBS containing 10/20 µg/ml PA for 1 h at 37°C **[A]** or with α AP 10/100 µg/ml for 20 min at RT **[B]**. Subsequently, MARKCS was alkyne-biotin labeled, washed and run on 12% SDS gel towards immunoblotting. Protein expression was detected by αMARCKS mAb (two lower panels), while MARCKS myristoylation was analyzed by streptavidin-HRP application (two upper panels). (MRK: MARCKS, SA-HRP: Streptavidin-HRP; kDa: kilo Dalton, (-): untransfected).

3.2.2 Visualization of lipopeptides on high percentage urea tricine gel.

For optimal separation of very small proteins (< 30 kDa), the use of Tricine–SDS-PAGE is more recommended than the conventional glycine–SDS-PAGE [179][156]. The difference between glycine and tricine separation relies strongly on the different pK values of the functional group of both molecules. This difference leads to different electrophoretic mobility shifts of the proteins [180]. Moreover, urea addition to the gel enhances the resolution of small proteins. Indeed, urea enhances protein denaturation and potentiates the hydrophobic protein movement onto SDS gel. Therefore, addition of urea enhances the overall separation of protein on SDS gel depending on their molecular size and charge of the basic media (pH 8.9). Interestingly, myristoylated lipopeptides run more freely onto urea-tricine gel and the difference between myristoylated and non-myristoylated 47-peptides was observed, yet small non-myristoylated 6 peptide (6pep) was invisible in contrast to myristoylated 6 lipopeptide (M6pep) (Fig. 32). Therefore, urea gel application method enables qualitative visualization of myristoylation peptides that at least longer as 47 aa.

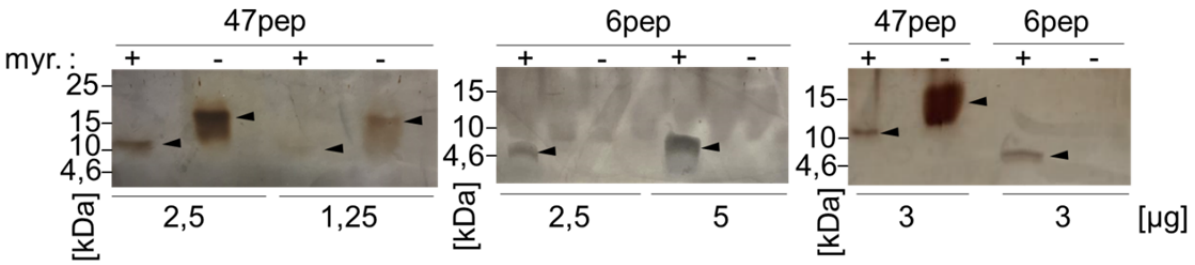

Figure 32. Silver staining of myristoylated and non-myristoylated peptides on urea gel. 6pep (myrist. 1,267 kDa, non-myristoylat. 1,057 kDa) and 47pep (myrist.: 5,867 kDa, non-myrist.: 5,657 kDa) were resuspended in loading buffer, incubated at 95°C for 5 min, and loaded onto specific PAA gels ; (8 M urea tricince-16% SDS resolving gel, 10% SDS spacer gel, 4% SDS stacking gel). Consequently, gel was washed and fixed in 10% glutaraldehyde for 30 min, then washed, and subjected to silver staining. Difference in (lipo)-peptide molecular weight is visualized by using low-range protein marker. Concentrations peptides are indicated in the figures. Note that the small non-myristoylated 6pep was not observed even at the highest applied concentration (5 µg), and that myristoylated peptides ran faster as compared to controls.

3.3 Characterizing HBV's nucleic acids for their property to activate immune cells.

HBV-derived nucleic acid is a poor inducer of innate immune activation due to the virus intrinsic characteristics of its life cycle. For instance, the viral relaxed circular DNA (rcDNA) is recognized as damaged, non-methylated, and non-self DNAs. Being synthesized within nucleocapsid, rcDNA is protected from potential recognition by DNA sensors. Therefore, it remains skeptical the assumption that the HBV RNA is PAMP for innate immune recognition. On the other hand, HBV-derived DNA, namely cccDNA, have been reported to be recognized through the nuclear DNA sensor IFI16 leading to cccDNA translocation to the cytosol and subsequent degradation. Due to scarcity and discrepancy of studies performed on HBV nucleic acids, screening for possible PRRs that might play a role in HBV nucleic acid recognition was studied.

3.3.1 Isolation of HBV RNA and DNA.

Isolation and purification of viral-derived DNA and RNA from intact virions were performed and visualized by running into agarose gel. Interestingly, enrichment of viral purified RNA was higher than viral DNA (Fig. 33A). The excessive amount of HBV RNA over DNA could possibly be due to accidental RNA delivery during virus encapsidation. Enzymatic digestion of viral DNA and RNA with DNaseI and RNaseA, respectively, confirmed their purity (Fig. 33B).

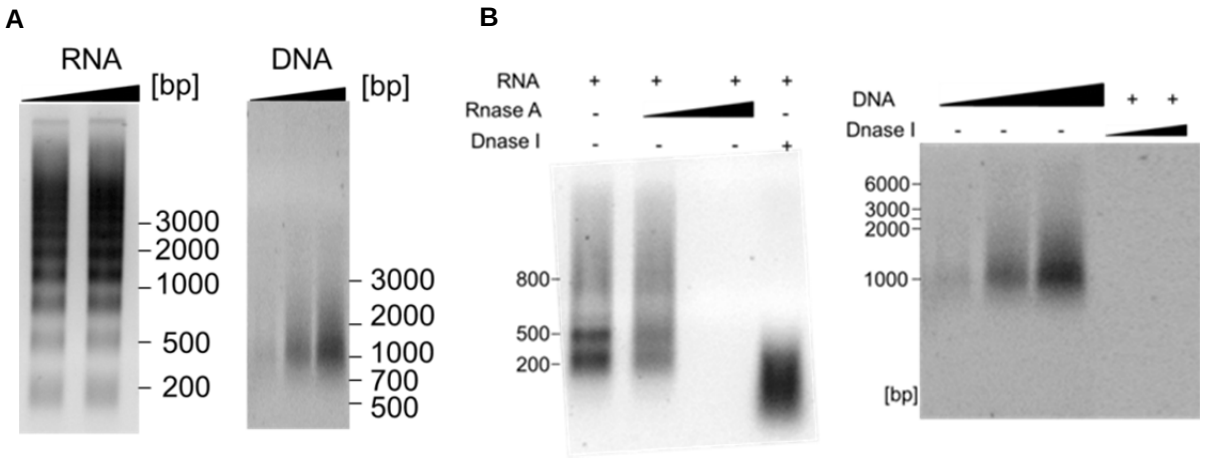

Figure 33. Purified HBV particles nucleic acid isolation and degradation. HBV purified from HepG2.215 cell supernatant was subjected to RNA (1.0, 2 µg) and DNA (0.5, 1.0, 2 µg) extraction through phenol chloroform solutions [**A**] or treated with RNaseA (10, 100 µg/ml) or DNaseI (0.5, 1 U/mg DNA) for RNA (2 µg) and DNA (0.5, 1.0 , 2 µg), respectively [**B**].

Reporter gene assays for nucleic acid receptors revealed that cells overexpressing RIG-I, MDA5, or TLR3 displayed luciferase signaling upon confrontation with HBV RNA, while human TLR8 or murine TLR13 displayed luciferase signaling only for their respective ligands and not HBV RNA (Fig. 34).

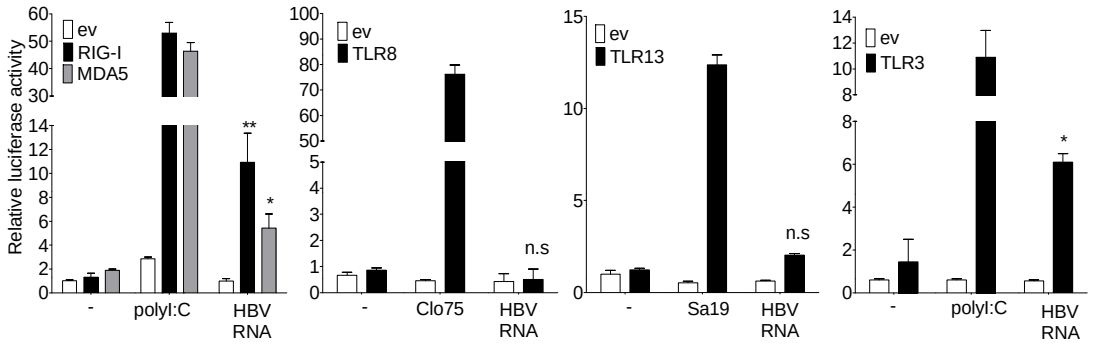

Figure 34. Purified HBV RNA induces IFN-β luciferase activity through TLR3, RIGI and MDA5. HEK293 cells (4 x10^6 cells/ 96 well plates) were transfected with IFN-β luciferase (10 ng), renilla (6,45 ng) and either empty vector (ev) or PRR (mTLR3,10 ng; mTLR13, 5 ng; hTLR8, 15 ng; mRIG/MDA5: 10 ng) expression plasmids. 16 h later, cells were challenged for 16 h with either ligand-specific receptors or (fugene) transfected HBV-RNA (10 µg/ml). Results are representative of three independent experiments. Data statistically analyzed through One-Way-Anova, Turkey test and significance levels was calculated in relation to unstimulated ev and error bars represent SEM. (n.s: not significant, (-) : untreated).

TLR9 was presented to play a protective role in tackling HBV entry into hepatocytes by direct binding to HBV virions and neutralizing its binding potential to the entry receptor NTCP Gain of function assay by overexpressing TLR9 revealed substantial TLR9 mediated NF-$_K$B driven

luciferase activity upon HBV DNA confrontation (Fig. 35). Notably, DNaseI treated HBV-DNA failed to drive luciferase signaling through TLR9 (data not shown). Collectively, these results comprehend that HBV-derived nucleic acids may not be strong activator of PRRs and the protein acylation of HBV envelope is rather the decisive PAMP in HBV specific innate activation.

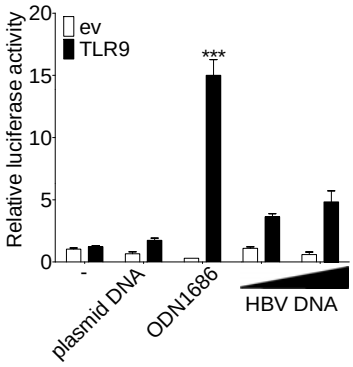

Figure 35. Purified HBV activates NF-$_K$B through mTLR9. HEK293 cells (4 x10^6 cells/ 96 well plates) were transfected with NF-$_K$B luciferase reporter plasmid (2 ng) as well as renilla (6,45 ng) and either empty vector (pRK5 plasmid) or murine TLR9 (10 ng) expression plasmid. 16 h later, cells were challenged for 16 h with either ligand-specific ODN1668 (non-transfected), or fugene transfected HBV-DNA (5/10 µg/ml). (ev: empty vector). Results are representative of three independent experiments and error bars represent SEM. (-): untreated).

3.4 Comparative analysis of adult probands healthy-mother's newborn umbilical cord full blood responsiveness to PRR activating stimuli.

Some studies suggest that in-utero infection may be the main cause of immune failure towards HBV. However, there is lack of evidence regarding the most likely period of occurrence of perinatal transmission. Furthermore, it remains unknown whether the viral chronicity state of the newborn is due to adaptive immune tolerance transmitted prenatally to the newborn from the mother immune reaction to the virus, or due to lack of effector immune recognition, i.e. response, as a result of immature immune system.

On account of this hypothesis, comprehensive characterization of the immune response of umbilical cord blood (UCB) from newborns of healthy mothers against healthy adult derived peripheral blood was done. Total blood cell count analysis showed that the UCB possesses significantly higher levels of lymphocytes and significantly less neutrophils than adult peripheral blood. Levels of all other non-immune cells tested were comparatively similar between the two groups (Fig. 36).

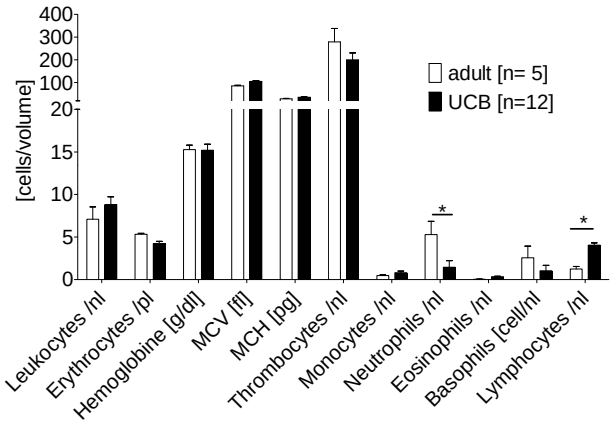

Figure 36. Newborn umbilical cord blood contains significantly more lymphocytes, yet less neutrophils compared to adult peripheral blood. Comparative analysis of differentiated newborns UCB and adult EDTA-blood counts. Mean corpuscular volume (MCV) and mean corpuscular hemoglobin (MCH) are markers of erythrocytes. Statistical analysis was performed with One-Way-Anova, Turkey test and error bars represent (SEM). (dl, deciliter; pl, picoliter; fl, femtoliter).

Unexpectedly, challenge of adult total peripheral blood and UCB revealed the enduring superior response of UCB to HBV challenge in dose response as compared to adult peripheral blood cells. Accordingly, myristoylation of HBV was a prerequisite for UCB responsiveness to HBV challenge since G2A weekly activates UCB or adult peripheral blood cells as compared to wt HBV virions (Fig. 37), a phenotype that were previously observed by hPBMCs confronted with HBV wt and G2A.

Additionally, the immunostimulatory capacity of ligands activating TRL2, TLR3, TLR4, TLR5, TLR7/8, TLR9 were comparable in adult- and newborn-derived immune cells (Fig. 38). For instance, inflammasome activity, measured by IL1β levels, was remarkably higher in newborn blood compared to adult upon challenge with its canonical ligands (TLR ligand + nigericin/ATP). In contrast, TLR9 responsiveness was rather week in both groups.

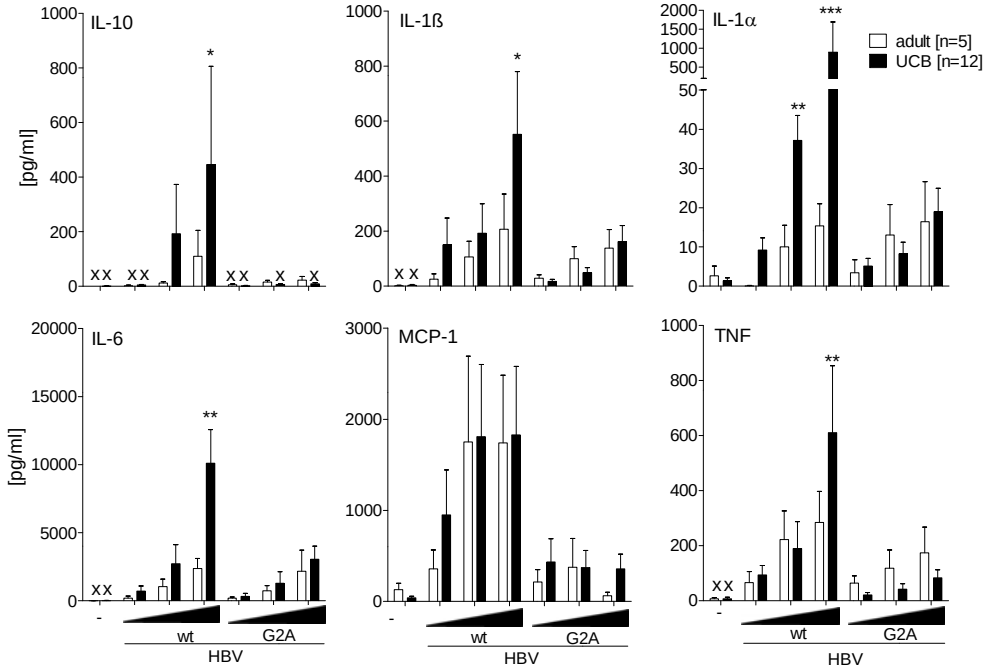

Figure 37. Sensitivity of healthy-mother's newborn and adult derived blood to HBV challenge. Adult peripheral blood or newborns UCB were challenged with purified wt and G2A HBV at final concentrations of 6/240/1000 x10^6 virion/ml (black triangle) or left unchallenged as negative control for 6 h. Cells were then centrifuged and plasma supernatant was assayed for cytokine analysis using luminex. Individual assays were performed in triplicates upon which the supernatant were pooled for cytokine measurement by luminex analysis. Statistical analysis was performed with One-Way-Anova, Turkey test and error bars represent SEM. (x: not detectable, (-): untreated).

Due to the nature of HBV as DNA virus, cGAMP ligand activating the cytosolic DNA sensor (cyclic GMP-AMP synthase) was tested. Here, adult-derived peripheral blood responded better to ligand challenge as compared to newborns, indicating that cGAS in newborns is possibly minimally operative unlike TLRs (Fig. 39).

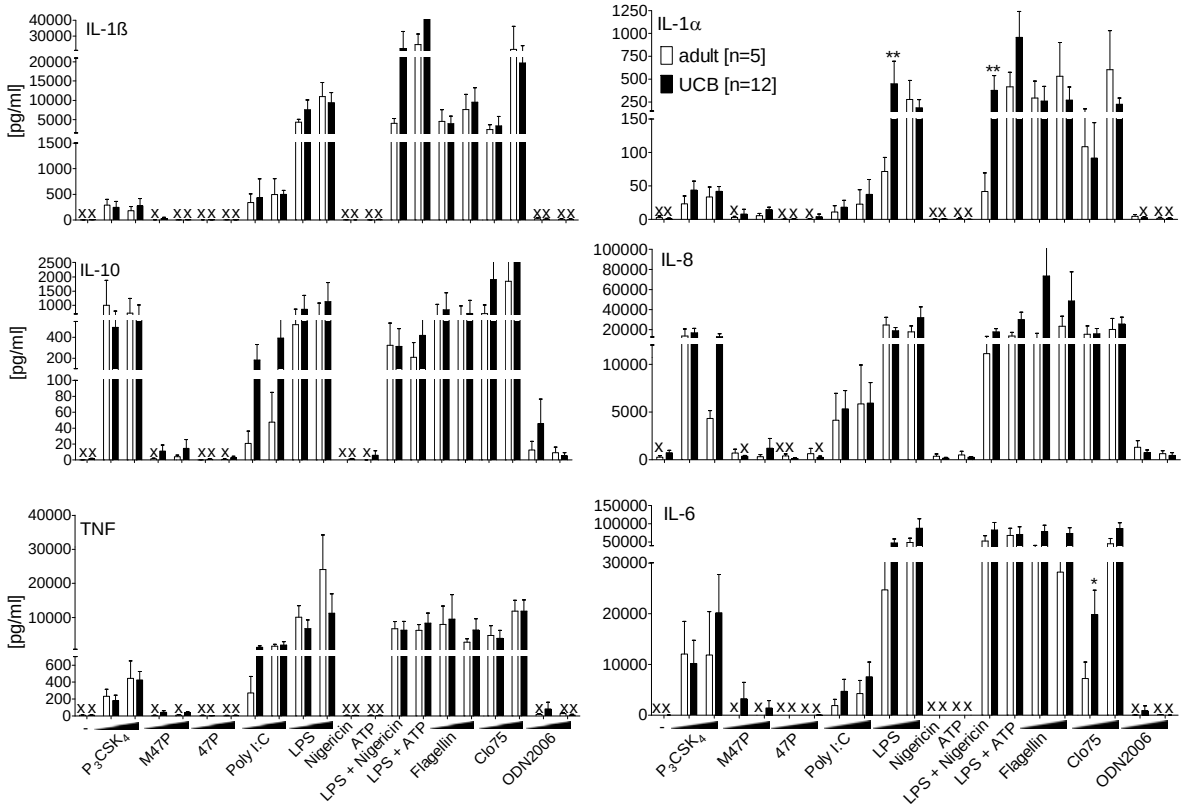

Figure 38. Comparable activation of adult and healthy mother's newborn full blood cells by TLR specific challenges. Total blood derived from adult probands and newborn UCB was challenged for 6 h with TLR ligands (P_3CSK_4 ,2 / 10 µg/ml; M47pep, 2 /10 µg/ml; polyI:C,10 / 20 µg/ml; LPS, 100/ 1000 ng/ml; nigericin, 30 min; 20 µM; ATP, 30 min 10 mM ; LPS, 100 ng/ml + nigericin, 30 min; 20 µM; LPS, 100 ng/ml + ATP, 30 min 10 mM; flagellin, 2/10 µg/ml; Clo75, 2/10 µg/ml; or ODN2006, 10/20 µM). Cells were then centrifuged and plasma supernatant was assayed for cytokine contents by luminex. Samples were performed in triplicates and the three supernatants pooled together for measurement. Statistical analysis was performed with One-Way-Anova, Turkey test and error bars represent SEM. (x: not detectable, (-): untreated).

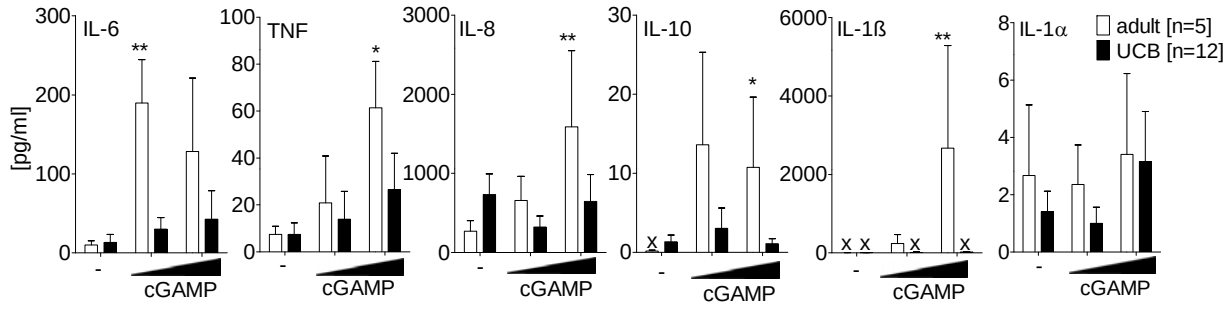

Figure 39. Largely reduced capability of healthy mother's newborn blood to respond to cGAS ligand challenge. Total blood from volunteers or newborns UCB were left untreated or challenged for 6 h with cGas ligand (cGAMP, 2/10 µg/ml). Cells were then centrifuged and plasma supernatant was saved for cytokine analysis. Samples were performed in triplicates and the three supernatants were pooled together for measurement by luminex. Statistical analysis was performed with One-Way-Anova, Turkey test and error bars represent SEM. (x, not detectable, (-): untreated).

Remarkably, low-dose Gram positive heat inactivated hi*Sa* bacterial challenge in newborns blood was non-responsive as compared to adult peripheral blood, while high-dose challenge of both Gram positive and negative (heat inactivated *E.coli*) renders them responsive (Fig. 40). This data comprehend that innate immune response in newborns seems to be sufficiently equipped to respond to stimuli confrontation.

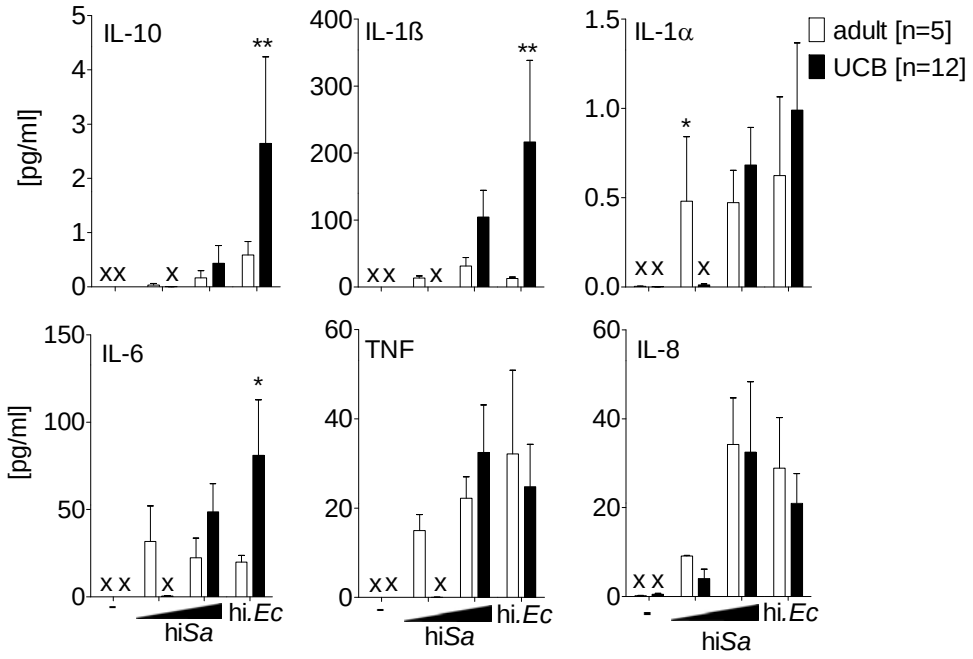

Figure 40. Specific parameters increased sensitivity of newborn-, as compared to adult, - full blood towards Gram positive and negative bacterial challenge. Total blood derived from adult volunteers and newborns UCB were challenged for 6 h with Gramm positive *S.aureus* (hi*Sa*, $2x10^7$ or $2x10^9$ CFU/ml) or Gram negative hi. *E.coli* (hi.*Ec*, $2x10^9$ CFU/ml). Cells were then centrifuged and supernatant was saved for cytokine analysis. Assays were performed in triplicates and three supernatants pooled together for cytokine measurement by luminex analysis. Statistical analysis was performed with One-Way-Anova, Turkey test and error bars represent SEM. (x, not detectable, (-): untreated).

4. Discussion

Hepatocellular carcinoma is the most common primary malignant liver cancer and the 10th leading cause of cancer-related death in the world [181]. Chronic HBV infection is the major risk factor for development of liver cirrhosis and consequent hepatocellular carcinoma. Despite an availability of an effective HBV vaccine, more than 350 million individuals are chronically infected worldwide. Chronic HBV infection precipitates severe morbidity and mortality prevalent specifically in developing countries. Whether the virus causes hepatocellular carcinoma or it is a consequence of repetitive liver inflammation and regeneration, is still a matter of investigation [182]. Lack of substantial anti HBV host immune activity against the background of effective immunity towards viral infection associated hepatitides might be due to three possible reasons: replication of HBV takes place in the nucleus of hepatocytes where immunity is generally weak. Second, reverse transcription of pregenomic RNA to DNA occurs simultaneously with virus encapsidation, thereby avoiding host cytoplasmic immune sensing. Third, the four RNA transcripts of HBV are poly adenylated at their 3' sequence ends and capped at their 5' ends, which assimilate them to host own RNA transcripts [183]. Possibly therefore the immune system fails to mount an efficient immune response and clear HBV from the liver upon which infection persistence is being channeled [184]. While the adaptive immunity arm employing mainly CD8$^+$ T cells is decisive in HBV clearance, the molecular interactions that lead to their activation must depend on HBV recognition and remain largely obscure [185]. Accordingly, a contribution of innate immunity in recognition and clearance of HBV is not yet broadly established. Principally, immune activation towards production of type I and III IFNs through signal transducer and activator of transcription (STAT) activation releases three major antiviral effector mechanisms. First is the activation of IFN-driven encoding antiviral effector molecules towards limitation of an infection spread. Second is amelioration of antigen presentation, natural killer (NK) cell activity, and limitation of proinflammatory cytokine production. Third is enhancement of adaptive immune activity through promotion of high affinity HBV antigen-specific T and B cell receptor evolvement [186][187]. Given that any adaptive immunity demands a prior innate immune impulse, a contribution to HBV immunity by innate immunity is compelling. Mandatory for this reason, the current thesis work based on high amount HBV virion production and macrophage activation. The results presented identify an acyl moiety, namely that of HBV L-HBsAg, as innate immune activating PAMP that activates TLR2 as its signal transducing PRR. Accordingly, endogenous eukaryotic- and

viral myristoylated proteins and synthetic peptides representing their N-termini did trigger TLR2 activation *in vitro* and *in vivo* unless they lacked N-terminal monomyristoylation. In contrast, hPBMCs TLR2 dependence of HBV recognition was less exclusive. Accordingly, purified HBV RNA activated TLR3, RIG-I, and MDA5 while purified HBV DNA activated murine TLR9 *in vitro*. Considering an impairment of innate HBV recognition in newborns because they are prone to chronification of vertical HBV infection, we analyzed umbilical full blood from healthy mothers upon cesarean birth of their current offspring. However, healthy mother's newborn blood appeared competent in respect to HBV and TLR ligand challenge recognition.

4.1 A role of TLR2 in HBV infection sensing

Previously, a correlation between levels of TLR2 expression on innate and adaptive immune cells with HBV infection and disease severity has been inferred [188]. Numerous TLR ligand applications were shown to support anti HBV immune activities. Like other TLR ligands, lipopeptides activating TLR2 suppressed hepadnaviral replication [189]. Therein, activation of TLR recruited the TAK1 adaptor molecule which inhibited the activity of the transcription factor hepatocytes nuclear factor 4 alpha (HNF4α) and HBV replication [190]. Furthermore, the large domain HBsAg (L-HBsAg) inhibited P_3CSK_4 driven TLR2 activation [191]. Also a HBxAg-TLR4 and L-HBsAg-TLR2 interactions were reported [192][105]. However, in respect to implications of recombinant proteins as TLR2/4 ligands, bacterial product contamination needs to be excluded experimentally, which has not been addressed by the respective authors explicitly. TLR2 expression levels in both hepatocytes and Kupffer cells of chronically infected HBV patient are significantly downregulated as compared to healthy controls [60]. Therapeutic activation of TLR2 on liver sinusoidal endothelial cells, which uniquely present antigen to liver T lymphocytes reverted hepatocyte immune suppressive properties towards immune activity one in order to induce HBV-specific T cell killing of infected hepatocytes [193]. Implicating TLR2 functionality, *Tlr2*$^{-/-}$mice injected with HBV replication mediating DNA plasmids to mimic infection carried elevated liver inflammatory markers such as alanine aminotransferase and displayed severe hepatic inflammation as compared to their littermate wt controls [194]. Furthermore, hydrodynamically *MyD88/Trif*$^{-/-}$, *Irak4*$^{-/-}$, and *Tlr2*$^{-/-}$ mice injected with HBV expression plasmid suffered higher virus carriage and reduced functionality of HBV-specific $CD8^+$ T cells as compared to wt [128]. Thus, IL1R and TLR signaling molecules MyD88/TRIF and IRAK4 as well as at least TLR2 are involved in HBV sensing. Collectively, these data qualify TLR2 as mediator of HBV immunity.

The three HBsAg protein variants present on HBV share a C-terminal small (S) domain S-HBsAg. Both, M- and L-HBsAg carry additionally N-terminally a preS2 domain. Exclusively L-HBsAg contains the N-terminally myristoylated preS1 domain. The L-HBsAg is critical for virus particle formation and virus infectivity operative specifically in the last extracellular phase of the life cycle (Fig. 41). L-HBsAg is N-terminally monomyristoylated co-translationally. Post translation, L-HBsAg remains in the ER upon interacting with the chaperone heat shock protein (HSP70) 70. There, the preS1 epitope is involved in assembly of the capsid, which then translocates across the ER membrane. preS1 is positioned below the particle surface and remains docked in the virus envelope till infection [195]. Camouflage of preS1 and its N-terminal myristoyl moiety under the virions membrane is a viral strategy to avoid immune surveillance. An exposure of virus to higher temperature resembling physiological hepatocytes temperature of up to 42 C°, but not to 4° C promoted a switch-out of the N terminus of preS1 from within toward outside of HBV virions to facilitate virus-uptake receptor interaction [196]. The former topology of L-HBsAg prevents non hepatic cell adhesion and possibly lets it evade host immune surveillance [197].

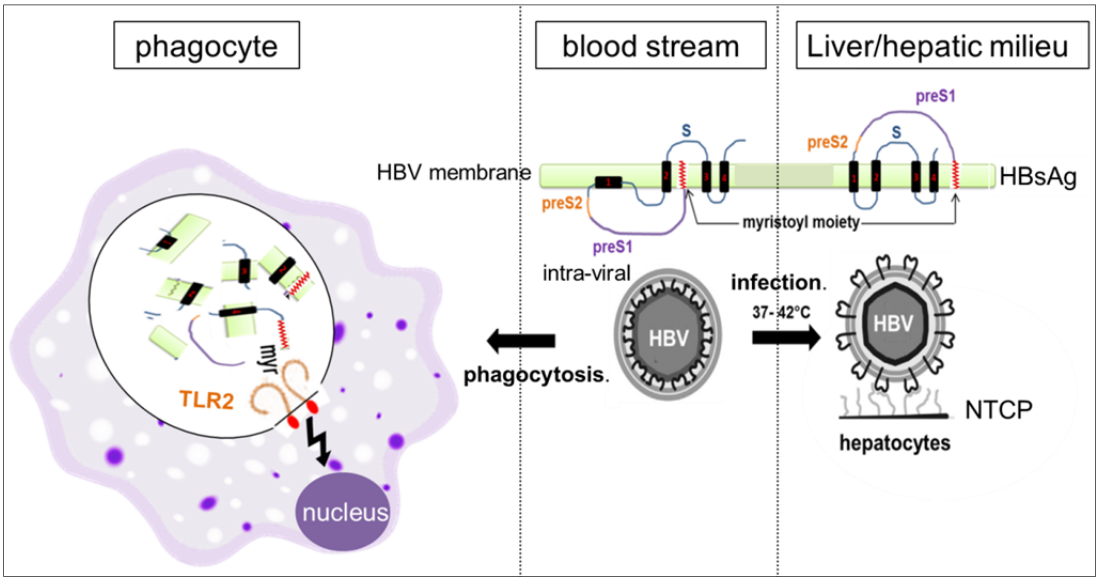

Figure 41. L-HBsAg topology phases: blood stream, hepatocyte contact, and upon phagocytosis. During particle assembly, L-HBsAg resides in the viral membrane towards the intra-viral space to stabilize the capsid. Upon maturation by crossing the ER, the PreS1 of L-HBsAg is positioned under the virus surface membrane. Temperature increase upon viral arrival to the sinusoidal space lets PreS1 switch to channel binding of HBV to the NTCP hepatocyte entry receptor membrane. Upon endocytosis by phagocytes, HBV undergoes lysosomal degradation in the phago-lysosome, which exposes nucleic acid and the N-terminus of L-HBsAg to endosomal TLRs. (Modified from Seitz et al. [196],).

In agreement with the evidences I observed 10 min 50°C pre-treatment of HBV virions to enhance TLR2- and NFκB- driven luciferase reporter gene activation, possibly by enhancing myristoyl moiety exposure. In contrary, analogous treatment at 100 °C abrogated luciferase gene activation, as if it caused virus disintegration and protein denaturation towards blockade of the TLR2 binding site.

Noninfectious HBV VLPs massively outnumber infectious HBV virions in blood plasma of HBV infected patients by factor of 10^3-10^6 [198]. While HBV VLPs carry M- and S –HBsAg variants, infectious virus particles carry the myristoylated L-HBsAg [199]. Possibly, VLPs ''dilute'' infectious HBV virions to minimize the likelihood of their immune recognition of.

Initially, we overexpressed the four proteins encoded by the HBV genome to evaluate their immune stimulatory capacity while nucleic acids, namely total RNA and total DNA were isolated from purified HBV virions. While both nucleic acid entities displayed substantial PRR stimulatory capacities *in vitro* (Fig. 34 / chapter 3.3), if at all exclusively overexpressed L-HBsAg elicited an immune activation in the experimental model system applied, namely mBMDM and hPBMCs culture challenge, while HBeAg, HBcAg, HBx were largely refractory. From within all HBV proteins, exclusively L-HBsAg is known to be co- or post-translationally modified by N-terminal monomyristoylation, reminding us of bacterial lipoprotein structure. Synthetic mono-, di, and tri-acylated hexapeptides are representing the N-termini of these bacterial lipoprotein. We previously applied lipopeptides such as tri-myristoylated hexapeptide to analyze TLR2 and TLR4 specificity [59]. Eukaryotic protein myristoylation such as of MARCKS is stress inducible such as by LPS challenge [142]. In this regard, endogenous MARCKS myristoylation might elicit a danger signal [200] and this qualifies it as good immune activating DAMP or in the case of viral provenance PAMP as candidate molecules. Consequently, surveying principal lipoprotein structure similarities on the background of cysteine in bacteria and glycine in eukaryotes N-termini acylated [57] (Fig. 10 /chapter 3.1.4), we ordered synthesis of a mono-myristoyl-hexapeptide. Our first ordered N-terminal-mono-myristoyl-G-pentapeptide displayed immune and therein TLR2 activating capacity (Fig.21, chapter 3.1.8) [Wurzenberger Master Thesis 2007], and inspired my analysis of L-HBsAg and MARCKS for a respective property. In the course of this thesis work, besides synthetic lipopeptides, also recombinant proteins and even biological entities such as HBV virions, MARCKS overexpressing cells co-overexpressing NMT and being experimentally supplied with myristoyl-CoA - the former of which is the N-myristoyl myristoylating enzyme and the latter is its substrate – were employed by me to rate their

immune stimulatory capacity in general and TLR2 activating property in particular (Fig. 26, chapter 3.1.12).

Previously, high amount HBV challenge of human monocytes already led to cell activation [201]. However, the bringing up of the HBV stealth virus concept upon absence of substantial immune activity in acutely HBV infected chimpanzee [112] and low to negligible IFN-driven gene activation in acutely HBV infected humans [113], overshadowed such initial finding including robust IL-6 and TNF production induction [201]. Accordingly, primary human monocyte-derived macrophages upregulated IL-6, TNF, IL-1β and IL-18 production upon encounter of up to 10^8 HBV particles/ml [162]. These evidences challenge the HBV stealth virus concept already and also activated both human and murine immune cells if 6-20 $x10^7$ virions/ml were applied at least. Also, FMuLV VLPs expressing wt Gag protein as well as synthetic HIV NEF and human/murine MARCKS N-terminal hexapeptides activated mouse and human immune cells as strong as wt HBV itself and L-HBsAg derived peptides in TLR2 dependent manner.

Point mutation of the residue 2 aa glycine towards alanine (G2A) rendered HBV virions and FMuLV VLPs TLR2activation refractory. Notably, G2A mutation of the L-HBsAg release into the supernatant of transfected hepatic cells was normal as compared to wt HBV controls (Fig. 14A). This observation might accord with increased replication of G1896A (mutant) HBeAg HBV [202]. HBV particles shedding from hepatic cells transiently transfected with wt or G2A constructs was indistinguishable as analyzed by HBV DNA quantification and electron microscopic analysis, indicating that the mutation did not affect virus replication. I also noticed that structural integrity of FMuLV VLPs was not myristoylation dependent (Fig. 27A). Myristoylation has been dispensable in respect to Arenavirus envelope protein also [203], yet indispensable in the case of gag of HIV [204]. Indicating a loss of function of G2A-L-HBsAg, mutant HBV particles failed to infect hepatic huh7-NTCP cells overexpressing virus surface receptor (huh7-NTCP). Notably, transfection compensated for this G2A HBV deficiency in that replication in G2A –HBV in transfected hepatocytes became evident.

Given the TLR2-dependent activation of immune cells by HBV challenge *in vitro*, synthetic short lipopeptide analogs representing the myristoylated N terminus of L-HBsAg and even L-HBsAg as a whole (M6pep or M47pep) were potent systemic immune stimulants in hyper sensitized mice. Cytokine and chemokine measurement released to the plasma was TLR2 dependent. Comparative analysis of wt and G2A HBV challenged hypersensitized mice remains an important experiment documenting an immune stimulatory potential of both HBV

species. Our previous experiments with hydrodynamically injected mice outlined that *Tlr2*$^{-/-}$ mice did clear infection and displayed merely moderately elevated serum circulating HBV antigens as compared to wt mice control [128]. In this regard, mice resemble the hPBMCs phenotype according to which HBV recognition was not exclusively TLR2 mediated compared to murine macrophages and splenocytes, which HBV recognition appeared as comprehensively TLR2 dependent. These evidences implicate PRRs beyond TLR2 in cellular HBV recognition.

In hPBMCs, which lack neutrophils, wt HBV recognition was prominently TLR2 dependent. Specifically, mAb TLR2 blockade significantly abrogated cell activation by wt HBV. However, ''still'' activated cells, yet endosomal TLR chloroquine treatment largely inhibited HBV driven immune activity. Therefore, TLR2 is a central but not exclusive HBV sensor as G2A HBV was a relatively weak, yet substantial activator of hPBMCs. We hypothesize that endosomal TLRs do contribute to recognition of HBV nucleic acid endosomally and in parallel to L-HBsAg-TLR2 pairing such as in immune surveilant phagocytes. Gain of function through experimental performance of NF-κB driven luciferase reporter gene activity assaying addressed this aspect by overexpressing specific PRRs and total DNA and RNA challenges. Cytosolic RNA helicase activation was analyzed by IFN-β promoter driven luciferase reporter gene activity assay upon challenge with RNA isolated from HBV particles. Results indicated HBV particles L-HBsAg driven TLR2, HBV RNA driven TLR3, RIG-I and MDA-5, as well as HBV DNA driven TLR9 activation.

Having identified the ''myr-G$(aa)_n$'' moiety of L-HBsAg as TLR2 specific immune stimulatory P/DAMP, I aimed at evaluation of the peptide's contribution to TLR2 activation. My observation of mild, yet substantial cell activation upon challenge with mere ''myr-G'' aa within a comparative analysis of successively elongated lipopeptides wherein all were applied in equimolar amounts rather excludes a substantial sequence specific contribution of the aa which follow the N-terminal G in L-HBsAg. The "myr-KSK_4" derivative as well as free myristic acid failed to induce detectable cell activity. Additionally, I observed a positive correlation between peptide length and strength of TLR2 activation, yet the peptide sequence was rather not relevant as far as has been analyzed here. Possibly representing a principle of broader pertinence, a tetradeca peptide length optimally stabilized a positioning of the myristoyl moiety towards TLR2 in my case (Fig. 22/ chapter 3.1.9).

Previously, diacylated lipopeptide Pam_2-C of different peptide lengths differentially activated DC-mediated NK cell activation [205]. Specifically, IFNγ production of NK challenged with

Pam_2-C$(aa)_6$ (homologous code to ''myr-G$(aa)_n$'') was slightly higher than Pam_2-C_1, and Pam_2-C$(aa)_{18}$ triggered NK cell activation stronger than Pam_2-Cys$(aa)_{11}$. Given that 0,5 - 0,8% of all eukaryotic proteins are myristoylated and even degradation products of them will exhibit immune activation such as in the course of trauma associated tissue damage upon which uncontrolled protease activity is operative certainly, therefore, the protein length and the acylation and aa length may be a factor in regulating the host immunity to limit host autoimmunity.

Aiming at quantification of L-HBsAg and cellular MARCKS myristoylation, as well as potential correlation of the myristoylation status with immune stimulatory capacity, I experimentally started by running PAA protein gel. However, N-terminal myristoylation failed to detectably alter band position of protein such as MARCKS. Therefore, I refrained from proteins to hexapeptides which I ran on high percentage gels. Not before adopting the ''Blue native PAGE'' method, I was able to visualize distinctness of myristoylated peptide and control peptides by PAGE. It was a peculiar application of 14% PAA gel electrophoresis under tricine and urea addition which enabled illustration of different characteristics of the two peptides. Due to urea's hydrophobic characteristics, it conferred accelerated migration of myristoylated peptides as compared to their ''pure peptide'' counterparts according with the different hydrophobicity scores of M47pep as compared to that of 47pep (43,75% and 26%, respectively, biosyn.com). Surprisingly, the non-myristoylated 6 peptide was never visible on silver stained gels by possibly due to unexplainable mobility characteristics. I also noticed that the peptide's theoretical molecular weights (6pep: 1,057 kDa, M6pep: 1,267 kDa, 47pep: 5,627 kDa, M47pep: 5,86 kDa) were not well presented on the urea gel; 47pep ran at ~ 10,5 kDa, M47pep ran at ~14 kDa, 6pep ran at ~ 4,6 kDa, while 6pep was undetectable. Notably, these peptides were biotinylated, rendering them ~ 0,244 kDa heavier.

The establishment of an experimental assay to demonstrate presence and absence of N-terminal mono-myristoylation enabled analysis of activities of acylase and lipases towards the myristoyl moiety. Specifically, I considered the polymyxin acylase as candidate although it deactivates a non-proteinaceous target molecule. According to functional analysis I performed, PA treatment specifically impaired M47pep and even HBV driven cell activation. Conflicting with this positive result, however, PA treatment failed to alter an M47pep gel electrophoretic property which puts the former result into relation (Fig. 24, chapter 3.1.10). Being unable to explain this discrepancy, I next evaluated N-terminus specific alpha aminopeptidase (α AP). By applying it for a timed period sufficient to cleave off the N-

terminal G, yet insufficient to cleave off the following aa, M47pep ran 47pep-like upon Blue native PAGE. This result paves the way towards enzymatic treatment of proteinaceous TLR2 ligands, whether it is for analytic or therapeutic purposes.

Quantitative measurement of protein myristoylation was optimized in this thesis using a novel click chemistry based method, which is, to the best of our knowledge, performed here for the first time to visualize changes of myristoylation of overexpressed proteins. Wt and G2A mutant MARCKS were overexpressed to visualize myristoylation of the former exclusively and thus prove the principle. According to common knowledge, wt L-HBsAg overexpression is virtually impossible. Accordingly, yeast-, but not mammalian cell derived S-HBsAg is the method for the standard HBV vaccine. Already MARCKS expression was upregulated in primary murine cells and RAW264.7 cells upon cell confrontation with LPS, IFNγ, PMA/ionomycin for 16 h. this results accords with observations of analogous properties of zymosan or PMA [142]. Accordingly, G2A MARCKS failed to become myristoylated upon overexpression, which proved click chemistry feasibility as alternative to tritium labeled myristic acid driven myristoylation analysis.

Activated myristic acid (N_3-myr) was exclusively connectable with wt MARCKS. Briefly, N_3-myr covalently bound to N-terminal G of MARCKS, rendering it reactive towards biotinylation that binds to streptavidin-HRP on the PAGE-gel immuno blot. Click chemistry also enabled visualization of protein myristoylation inhibition by application of the NMT inhibitor Tris-DBA to the transfected cells. Here, the protein myristoylation was attenuated but not the protein expression itself. Like Blue native gel, click chemistry analysis visualized demyristoylation through αAP or PA treatments. Subsequently, I optimized the enzyme concentration, pH (~pH 8), and the incubation time in respects to functional assays.

During the course of my analysis, recombinant HBsAg incubation with 2% β-D-octyl glucoside (OG) resulted in an abrogation of HBsAg-driven DC maturation, suggesting to the authors that the acylated fraction of HBsAg plays a major role in HBV driven DC activation [206]. Notably, inhibition of protein myristoylation is a current approach in cancer treatment [207]. Further analysis will visualize the myristoylation of L-HBsAg such as in cell culture bred HBV. However, visualizing endogenous L-HBsAg from lysed particles on western blot demands considerably high yield of lysed particles (1-2% of particle composition) to render the visible band, a characteristics that needs optimization of HBV productions.

In contrast to chemical and enzymatic attempts to abrogate protein myristoylation, I asked if enhancing protein myristoylation by promoting cellular myristoylation machinery promotes

TLR2 activation. Experimentally, I overexpressed MARCKS in HEK293 cells alone, coexpressed NMT (N-terminal myristoyl transferase) or supplied MARCKS$^+$ cells with synthetic myr-CoA (the NMT substrate), or applied myr-CoA to MARCKS/NMT doubly overexpressing cells while applying each compound also alone for control. Lysates were prepared synchronically and mBMDM confronted with them to analyze their activation by supernatant cytokine measurement. While controls were negative, mere MARCKS overexpression rendered lysates moderately yet substantially activating. Maximal stimulatory activity was contained in lysates of cells which co-overexpressed NMT and were fed myr-CoA, indicating that on the background of equal target protein expression, the grade of myristoylation is decisive for the consequent potential to elicit TLR2 activation. It will be interesting to analyze the HBV myristoylation grade in HBV patients to potentially correlate it with chronification of their infection. Also will a comparative analysis of cell culture borne and patient HBV myristoylation grade be interesting.

4.2 HBV derived nucleic acids DNA and dsRNA are possible PAMPs

Previous studies performed in analyzing the immunostimulatory potential of HBV nucleic acid are overall scarce. For instance, TLR9/HBV-DNA axis was described as the main mechanism in pDCs activation, leading to of NF-κB, MAPK and IRF7 activation and towards type I IFN production [208]. The downregulation of TLR9 expression on hepatocytes by HBV was also described [209]. In my experiments, DNA purified from HBV particles activated NFκB dependent luciferase reporter gene activation in a TLR9 dependent fashion. Unlike wt mBMDM, *Tlr379*$^{-/-}$ BMDM responded weekly to HBV DNA or RNA challenge (data not shown). However, DNaseI-specifically degraded my DNA preparation while RNaseA digested its RNA counterparts but not DNA, validating the method applied. Notably, DNA based HBV vaccines to combat HBV infection via activation of MHC-I/II expression towards induction of both CD8$^+$ and CD4$^+$ cells activities is an ongoing effort [210].

The nature and origin of serum HBV RNA were unclear until a study confirmed that circulating serum HBV RNA in HBV patients is indeed pgRNA [211]. Today, the disappearance of viral RNA in serum of chronic HBV patients during nucleo-side/-tide analogue therapy is instrumentalized marker of resolving infection resolution [212]. Collateral encapsidation of viral RNAs during the virus capsid formation may explain why HBV drives RNA sensors activation [211]. Demonstration of content DNA-RNA hybrid of HBV from a patient support an assumption [213]. According to which HBV carries RNA, I did not notice

TLR9 activation by HBV-RNA challenge or activation of RNA sensors by HBV-DNA, which rather excludes the DNA-RNA hybrid implication (data not shown).

Several studies pointed out a role of TLR3 in HBV infection clearance. Accordingly, HBV infected hepatocytes underwent apoptosis and upregulated IFN type I in a TLR3 dependent manner [63]. Furthermore, TLR3, but not TLR7, was upregulated in woodchucks upon resolving infection with woodchuck HBV [214]. Moreover, application of supernatant from TLR3 treated human non parenchymal hepatic stellate cells to HBV expressing hepatic HepG2 cells suppressed HBV replication [215]. Contrast to my observation with HBV-DNA, I observed that purified HBV-RNA was more stimulatory in respect to both mouse and human immune cells. Moreover, HBV-derived RNA triggered type III IFN-λ release in murine and human immune cells as well as TNF cytokine production (data not shown). IFN-λ secretion upon RIG-I activation during HBV derived RNA challenge had been shown already [126]. Moreover, induction of luciferase activity in HEK293 overexpressing murine TLR3, RIG-I or MDA5 upon HBV RNA challenge were evident but not in those overexpressing human TLR8 or murine TLR13. Thus, dsRNA rather than ssRNA might be immunostimulatory HBV nucleic acid PAMP.

4.3 Largely full competence of healthy mother's newborn blood borne innate immunity.

Although vaccination of newborns significantly reduces the likelihood of perinatal transmission of HBV from infected mothers by 79–90 % and likely further reduction by concurrent administration of anti HBV immunoglobulin [216], maternofetal transmission is still the major route of HBV-transmission and cause of subsequent chronic infectiousness of 90% of infected newborns [111], and accounts for up to 30 % of all HBV cases worldwide [217]. HBV infected mothers might transmit HBV to their newborns by one of three routes: first intrauterinally by passing little amounts of the virus through the placenta, second prenatally by viral transmission during delivery, and third postnatally upon failure of immune prophylaxis by newborn vaccination [218]. Fortunately, 90% of vertically infected newborn ($HBsAg^+$) cases receiving HBV vaccine within the first six month of life clear infection [91]. In order to clarify whether newborns, from HBV^+ mothers carry a lifelong HBV infection either due to a tolerogenic immune response toward the virus or due to an inefficient innate immunity, I analyzed comparatively umbilical cord blood (UCB) from newborns from healthy mothers and adult isolated peripheral blood. Full blood cultures were challenged with HBV, TLR ligands, cGAS ligand, and bacterial suspensions.

Specific newborn blood carried less innate immune cells such as basophils and neutrophils yet more lymphocytes as compared to adult blood. This finding accords of a normal proliferative capacity of UCB isolated T cells and presence of less reactive monocyte to respond to allogeneic cell challenge [219]. The slight discrepancy in the composition of the immune cell populations might also contribute in differential outcomes of immune stimulations observed. Overall, a stronger immune response of newborn isolated UCB confronted with HBV and TLR ligands was observed as compared to adult peripheral blood controls. Newborn derived UCB responded exclusively to wt HBV and not its G2A counterpart which was ''still'' well recognized by adult peripheral blood as if the HBV nucleic acid sensing was impaired or immature in UCB (see above). Analysis of the age : TLR relationship positively correlated TLR1 and TLR3 expression in the intestinal epithelial cells to the ageing of mice (measured from day 3 till day 27), while TLR5 expression correlated inversely with the respective age [220]. In my hand, TLR-2, -3, -4, -5, -7, -9 ligands as well as L-HBsAg representing M47pep did all trigger potent immune responses in UCB as compared to adult controls. These results infer that the intrinsic sensing machinery is fully operative in newborn to let them respond to a variety of D/PAMP challenges. Inflammasome activity, measured by IL-1β release, was stronger in newborn as compared to adult blood. In contrary, the cytosolic DNA sensor cGAS was barely in newborns as compared to adult peripheral blood control. Young children and newborns are known for their decreased expression of cGAS [221]. Therefore, given that STING driven HBV recognition is dominantly important - due to the DNA nature of HBV- here I identified an important leak in the newborn line of defense towards HBV infection. It is thus mandatory to analyze cGAS and STING protein expression and whether their activation with HBV RNA drives type I and III IFN expression in adult and newborns blood because these cytokines failed to be in my focus yet. Newborns UCB failed also to respond to low dose of Gram-positive bacterial challenge. Notably, Gram-positive bacterial *S.aureus* and Gram-negative *E.coli* bacteria are the most common cause of sepsis in newborns [222]. Therefore, although newborn UCB efficiently mounted a generally efficient immune response towards TLR ligands, low dose confrontation with bacterial challenge was rather not sufficient to activate their blood immune cells to a degree displayed by adult peripheral blood. Notably, human monocytes from newborns that had been exposed to HBV were at enhanced activation status compared to those from unexposed neonates [223] suggesting that a ''tolerogenicity'' towards HBV in HBV^{+} mother-born-neonates is operative rather than defective innate immune response.

Comparative analysis of healthy and HBV infected mothers wherein those infected were sub classified if they transmitted HBV to their newborns or not, revealed that the mother's innate and adaptive immune system shape the infection outcome in their offspring [91]. Accordingly, the immune system of HBV infected mothers who transmit HBV to their newborns displayed from low frequencies of innate immune cells such as DC as well as low TLR7/9 expression on these cells as compared to healthy mothers or HBV mothers that did not transmit HBV to their newborns. Less $CD4/8^+$ T cell secreted cytokines as well as a lower frequency of B cells characterized these mothers. Also, IL-10 and TGF-β secretions in this group of mothers and their newborns were markedly stronger and IL-12 and IL-21 productions were lower as compared to the other two groups. Moreover, soluble CD14 (sCD14), a coreceptors of TLR4 and known to shape HBV immunity in neonates, mediated HBsAg-driven DC maturation and IL-6 and IL-12 productions but was absent in neonate UCB yet present in adult blood [206].

Collectively, these data demonstrate that healthy newborns are well protected from HBV challenge upon HBV exposure given that their TLR2 is functional. Unfortunately, analysis of newborn derived UCB from HBV^+ mothers was not performed in this course of this thesis due to sample unavailability throughout the experimentation time at the Clinic for Obstetrics and Gynecology at the University Hospital Essen. It remains therefore very mandatory to characterize the TLR2 ligand responsiveness of UCB from HBV^+ mothers upon *in vitro* re-challenge with HBV as well as TLR ligands. My analysis brought up arguments towards as well as against the hypothesis which triggered it. In relation to adult control diminished responses of newborn blood towards G2A HBV, low dose bacterial challenge, and cGAS the hypothesis is supported. In respect to our mainly targeted aspects, namely HBV and lipopeptide driven TLR2 activation, newborns were unremarkable by being fully sensing competent. Due to an availability of HBV^+ delivering mothers -which in ''our'' optimal case would be untreated – we intend now to induce a tolerogenic state of blood cells *in vitro* by triggering LPS tolerance to ask whether in regard to HBV responsiveness newborn blood might be remarkable. The free findings which support our hypothesis deserve continuation of respective analysis.

4.4 Two-facedness of L-HBsAg N-terminus lipopeptides: adjuvanticity besides competitive entry inhibition and T cell epitope provision

The development of HBV vaccines went through three generations. The recent one is the most effective towards combating HBV infection worldwide. The first generation plasma derived

HBV vaccine was brought up in 1970 in France and the USA. In 1980, a second generation recombinant HBV was produced in yeast a targeted S-HBsAg domain. The second generation vaccine is now the standard vaccine for HBV in more than 170 countries. The modern third generation of HBV vaccine had been developed in Germany, France, Korea, and Israel by L-HBsAg production in CHO [224]. It induced more HBV surface antigen-specific antibodies than traditional HBV vaccines in HBV infected mice [225]. Used currently to treat HBV patient, the current third HBV vaccine is identical with M47pep and named Myrcludex B. Its mode of action is competitive entry receptor binding and T cell epitope provision according to common view. My work, however, brings up an adjuvant property. It is tempting to speculate that TLR2 activation is the foremost clinical effector mechanism. Besides Myrcludex B, TLR7/8 ligand Cl097 is a promising adjuvant candidate molecule [226].

Finally, to test myristoylated lipopeptide as adjuvant to enhance immune response in mouse- and human- derived cells, in collaboration with the Institute of Chemistry at the University Duisburg Essen, calcium phosphate nanoparticles were decorated with myristoylated peptides was synthesized. Here we observed up to 7 fold elevated immune response in mouse macrophage challenged with nanoparticles as compared to unbound myristoylated lipopeptides. However, hPBMCs were strongly background activated possibly due to a composition of the nanoparticle itself since non-myristoylated peptide enriched nanoparticles were at least 30% immune stimulatory as compared to myristoylated lipopeptide enriched nanoparticles (data not shown).

The results collected in the course of preparation of this thesis may help to comprehend the steps involved in HBV innate immune response development, which is critical towards adequate adaptive HBV-specific immune responses upon HBV exposure. Hopefully, these will result in a development of more effective immunotherapies for this disease and reduce its global burdens.

5. Summary

Chronic HBV infection is the 10th leading global cause of death and the infection accounts for the vast majority of chronic liver diseases in endemic areas to levels up to 75%–80%. The assumption that HBV is a stealth virus due to a lack of host immune stimulatory potential conflicts with an ability of immunocompetent adults in 95% of cases to clear the virus upon exposure, which implicates innate immunity involvement. However, in 90% of newborns infected by their HBV positive mothers the infection becomes chronic. This discrepancy infers distinctness of adult and newborn immunity towards HBV exposure. While the central role of adaptive immunity, mediated mainly through CD8$^+$ T cells, is well established, innate immunity towards HBV remains largely incompletely understood. The main aim of this study was identification of the pattern recognition receptor/s (PRR/s) that mediate/s HBV recognition and its ligand/s. In this regard, the N-terminally monomyristoylated surface antigen of HBV (L-HBsAg), that is essential in positioning of L-HBsAg towards the hepatocytes entry receptor NTCP, is being identified as TLR2 ligand. Results of *in vivo* and *in vitro* analyses showed myristoylation-dependent immune recognition of HBV through TLR2 in mouse and human. G2A-L-HBsAg lacking the myristoylation largely failed to activate murine cells, yet triggered moderate endosomal TLR dependent human PBMC activation as deduced from effective endosome inhibition. However, healthy mother newborn's full blood sensed HBV as efficient as adult volunteer controls. G2A-HBV mutant particles were morphologically intact, as replicative as wt HBV, yet non-infectious. Short synthetic lipopeptides mimicking the myristoylated N-termini of HBV L-HBsAg, HIV NEF, FMuLV GAG, and eukaryote endogenous myristoylated alanine-rich C-kinase substrate (MARCKS) activated TLR2 to similar degrees. N-myristoyl transferase (NMT) coexpression and myristoyl-CoA administration promoted myristoylation of overexpressed MARCKS and TLR2 stimulatory capacity of the latter. ''Myristoyl-G'' carries a substantial TLR2 activation capacity and is the minimal moiety of the immune stimulatory pathogen and endogenous danger associated molecular pattern (P/DAMP) analog "MyrGSK$_4$".

6. Zusammenfassung

Die chronische Hepatitis-B-Infektion ist die zehnthäufigste Todesursache weltweit und verantwortet die große Mehrheit chronischer Lebererkrankungen, in endemischen Gebieten mit einem Anteil von bis zu 80%. Die Annahme dass HBV wegen des Fehlens einer instant immunaktivierenden Aktivität ein Stealth-Virus sei kollidiert mit der Fähigkeit immunokompetenter Erwachsener in 95% der Fälle das Virus auf Exposition hin zu klären weil letzteres eine Involvierung von angeborener Immunität impliziert. Allerdings chronifiziert sich in von HBV positiven Müttern infizierten Neugeborenen die Infektion in 90% der Fälle. Diese Diskrepanz deutet auf Unterscheide der HBV Immunität von Erwachsenen und Neugeborenen hin. Obwohl der Beitrag der adaptiven Immunantwort, hauptsächlich durch $CD8^+$ T-Zellen, umfassend etabliert ist, ist die angeborene Immunität gegen HBV Infektion noch weitgehend unverstanden. Das Hauptziel dieser Studie war die Identifizierung von Mustererknnungsrezeptoren (PRR) die eine immunologische Erkennung von HBV vermitteln sowie ihrer Liganden. Das N-Terminal mono-myristoylierte Oberflächenantigen von HBV (L-HBsAg), das HBsAg zur wirksamen Wechselwirkung mit dem Hepatozyteneintrittsrezeptor NTCP positioniert, wurde als TLR2 Ligand identifiziert. Ergebnisee von *in-vivo* und *in-vitro* durchgeführten Untersuchungen zeigen eine myristolierungsabhängige Immunerkennung von HBV über TLR2 in Maus und Mensch. G2A-HBsAg welches keine Myristoylierungen trägt aktivierte Mauszellen nicht, jedoch humane PBMC auf moderatem Niveau über endosomale TLR was aus einer wirksamen Endosminhibition schließbar war. Allerdings erkannte das Vollblut von Neugeborenen gesünder Mütter HBV so effektiv wie jenes gesunder Erwachsener. G2A-HBsAg HBV Partikel waren morphologisch intakt, so replikativ wie wt HBV jedoch nicht infektiös. Kurze synthetische Lipopeptide die myristoylierte N-termini von HBV L-HBsAg, HIV NEF, FmuLV GAG und eukaryotisch endogenes myristoyliertes alaninreiches C-Kinase Substrat (MARCKS) aktivierten TLR2 gleichermaßen. N-Myristoyltransferase (NMT) Koexpression und myristoyl-CoA Verabreichung verstärkte die Myristoylierung von überexprimiertem MARCKS und seine TLR2 aktivierende Aktivität. „Myristoyl-G“ hat ein substantielles TLR2 aktivierendes Potential inne und ist die Minimalstruktur des immunstimulativen Pathogen und endogene Gefahr assoziierten molekularen Musters (P/DAMP) Analogons ‘‘$MyrGSK_4$“.

7. Bibliography

[1] S. Bustin, “Molecular Biology of the Cell, Sixth Edition; ISBN: 9780815344643; and Molecular Biology of the Cell, Sixth Edition, The Problems Book; ISBN 9780815344537,” *Int. J. Mol. Sci.*, vol. 16, no. 12, pp. 28123–28125, Nov. 2015.

[2] C. A. J. Janeway, “Pillars article: approaching the asymptote? Evolution and revolution in immunology. Cold spring harb symp quant biol. 1989. 54: 1-13.,” *J. Immunol.*, vol. 191, no. 9, pp. 4475–4487, Nov. 2013.

[3] B. R. Herrin and M. D. Cooper, “Alternative Adaptive Immunity in Jawless Vertebrates,” *J. Immunol.*, vol. 185, no. 3, p. 1367 LP-1374, Aug. 2010.

[4] F. Sallusto, D. Lenig, R. Förster, M. Lipp, and A. Lanzavecchia, “Two subsets of memory T lymphocytes with distinct homing potentials and effector functions,” *Nature*, vol. 401, p. 708, Oct. 1999.

[5] I. Gutcher and B. Becher, “APC-derived cytokines and T cell polarization in autoimmune inflammation.,” *J. Clin. Invest.*, vol. 117, no. 5, pp. 1119–1127, May 2007.

[6] M. P. Murphy, “How mitochondria produce reactive oxygen species,” *Biochem. J.*, vol. 417, no. 1, p. 1 LP-13, Jan. 2009.

[7] “Life of Elie Metchnikoff, 1845–1916,” *Nature*, vol. 109, p. 163, Feb. 1922.

[8] R. J. Boyton and D. M. Altmann, “Is selection for TCR affinity a factor in cytokine polarization?,” *Trends Immunol.*, vol. 23, no. 11, pp. 526–529, Nov. 2002.

[9] V. Brinkmann *et al.*, “Neutrophil Extracellular Traps Kill Bacteria,” *Science (80-.).*, vol. 303, no. 5663, p. 1532 LP-1535, Mar. 2004.

[10] P. Italiani and D. Boraschi, “From Monocytes to M1/M2 Macrophages: Phenotypical vs. Functional Differentiation,” *Front. Immunol.*, vol. 5, p. 514, Oct. 2014.

[11] P. N. Nesargikar, B. Spiller, and R. Chavez, “The complement system: history, pathways, cascade and inhibitors,” *Eur. J. Microbiol. Immunol. (Bp).*, vol. 2, no. 2, pp. 103–111, Jun. 2012.

[12] H. F. Rosenberg, S. Phipps, and P. S. Foster, “Eosinophil trafficking in allergy and asthma,” *J. Allergy Clin. Immunol.*, vol. 119, no. 6, pp. 1303–1310, 2007.

[13] E. Z. M. da Silva, M. C. Jamur, and C. Oliver, *Mast Cell Function: A New Vision of an Old Cell*, vol. 62, no. 10. 2014.

[14] T. Groot Kormelink *et al.*, “Mast Cell Degranulation Is Accompanied by the Release of a Selective Subset of Extracellular Vesicles That Contain Mast Cell–Specific Proteases,” *J. Immunol.*, vol. 197, no. 8, pp. 3382–3392, 2016.

[15] A. G. Freud, B. L. Mundy-Bosse, J. Yu, and M. A. Caligiuri, “The Broad Spectrum of Human Natural Killer Cell Diversity,” *Immunity*, vol. 47, no. 5, pp. 820–833, 2017.

[16] E. Vivier, E. Tomasello, M. Baratin, T. Walzer, and S. Ugolini, “Functions of natural killer cells,” *Nat. Immunol.*, vol. 9, no. 5, pp. 503–510, 2008.

[17] L. J. Sigal, H. Reiser, and K. L. Rock, “The Role of B7-1 and B7-2 Costimulation for the Generation of CTL Responses In Vivo,” *J. Immunol.*, vol. 161, no. 6, p. 2740 LP-2745, Sep. 1998.

[18] J. P.-Y. Ting *et al.*, “The NLR gene family: a standard nomenclature,” *Immunity*, vol. 28, no. 3, pp. 285–287, Mar. 2008.

[19] T.-D. Kanneganti, M. Lamkanfi, and G. Núñez, “Intracellular NOD-like Receptors in Host Defense and Disease,” *Immunity*, vol. 27, no. 4, pp. 549–559, 2007.

[20] L. Franchi *et al.*, “Intracellular NOD-like receptors in innate immunity, infection and disease,” *Cell. Microbiol.*, vol. 10, no. 1, pp. 1–8, Jan. 2008.

[21] C. Dostert, V. Pétrilli, R. Van Bruggen, C. Steele, B. T. Mossman, and J. Tschopp, “Innate Immune Activation Through Nalp3 Inflammasome Sensing of Asbestos and Silica,” *Science (80-.).*, vol. 320, no. 5876, p. 674 LP-677, May 2008.

[22] T. Fernandes-Alnemri, J.-W. Yu, P. Datta, J. Wu, and E. S. Alnemri, “AIM2 activates the inflammasome and cell death in response to cytoplasmic DNA,” *Nature*, vol. 458, p. 509, Jan. 2009.

[23] N. B. Bryan, A. Dorfleutner, S. J. Kramer, C. Yun, Y. Rojanasakul, and C. Stehlik, “Differential splicing of the apoptosis-associated speck like protein containing a caspase recruitment domain (ASC) regulates inflammasomes.,” *J. Inflamm. (Lond).*, vol. 7, p. 23, May 2010.

[24] K. Schroder and J. Tschopp, “The inflammasomes.,” *Cell*, vol. 140, no. 6, pp. 821–832, Mar. 2010.

[25] T.-D. Kanneganti *et al.*, “Bacterial RNA and small antiviral compounds activate caspase-1 through cryopyrin/Nalp3,” *Nature*, vol. 440, p. 233, Jan. 2006.

[26] I. C. Allen *et al.*, “The NLRP3 Inflammasome Mediates In Vivo Innate Immunity to Influenza A Virus through Recognition of Viral RNA,” *Immunity*, vol. 30, no. 4, pp. 556–565, 2009.

[27] W. Sha *et al.*, “Human NLRP3 inflammasome senses multiple types of bacterial RNAs,” *Proc. Natl. Acad. Sci.*, vol. 111, no. 45, p. 16059 LP-16064, Nov. 2014.

[28] S. Liu *et al.*, “MAVS recruits multiple ubiquitin E3 ligases to activate antiviral signaling cascades.,” *Elife*, vol. 2, p. e00785, Aug. 2013.

[29] J. Freaney, R. Kim, R. Mandhana, and C. Horvath, “Extensive cooperation of immune master regulators IRF3 and NFκB in RNA Pol II recruitment and pause release in human innate antiviral transcription,” *Cell Rep.*, vol. 4, no. 5, pp. 959–973, 2013.

[30] T. Kawai *et al.*, “IPS-1, an adaptor triggering RIG-I- and Mda5-mediated type I interferon induction,” *Nat. Immunol.*, vol. 6, p. 981, Aug. 2005.

[31] P. J. Kranzusch, A. S.-Y. Lee, J. M. Berger, and J. A. Doudna, “Structure of human cGAS reveals a conserved family of second-messenger enzymes in innate immunity.,” *Cell Rep.*, vol. 3, no. 5, pp. 1362–1368, May 2013.

[32] N. Bhat and K. A. Fitzgerald, “Recognition of cytosolic DNA by cGAS and other STING-dependent sensors,” *Eur. J. Immunol.*, vol. 44, no. 3, pp. 634–640, 2014.

[33] S. Stavrou, A. N. Aguilera, K. Blouch, and S. R. Ross, “DDX41 Recognizes RNA/DNA Retroviral Reverse Transcripts and Is Critical for In Vivo Control of Murine Leukemia Virus Infection,” *MBio*, vol. 9, no. 3, pp. e00923-18, Jul. 2018.

[34] Z. Zhang, B. Yuan, M. Bao, N. Lu, T. Kim, and Y.-J. Liu, “The helicase DDX41 senses intracellular DNA mediated by the adaptor STING in dendritic cells,” *Nat. Immunol.*, vol. 12, p. 959, Sep. 2011.

[35] L. Unterholzner *et al.*, “IFI16 is an innate immune sensor for intracellular DNA,” *Nat. Immunol.*, vol. 11, p. 997, Oct. 2010.

[36] A. Matsumoto *et al.*, “Human macrophage scavenger receptors: primary structure, expression, and localization in atherosclerotic lesions.,” *Proc. Natl. Acad. Sci.*, vol. 87, no. 23, pp. 9133–9137, 1990.

[37] K. J. Moore and M. W. Freeman, “Scavenger receptors in atherosclerosis: Beyond lipid uptake,” *Arterioscler. Thromb. Vasc. Biol.*, vol. 26, no. 8, pp. 1702–1711, 2006.

[38] K. Wilkinson and J. El Khoury, “Microglial scavenger receptors and their roles in the pathogenesis of Alzheimer’s disease,” *Int. J. Alzheimers. Dis.*, vol. 2012, 2012.

[39] J. Tang, G. Lin, W. Y. Langdon, L. Tao, and J. Zhang, “Regulation of C-Type Lectin Receptor-Mediated Antifungal Immunity,” *Front. Immunol.*, vol. 9, p. 123, 2018.

[40] J. A. Hoffmann, B. Lemaitre, E. Nicolas, L. Michaut, and J.-M. Reichhart, “The Dorsoventral Regulatory Gene Cassette spätzle/Toll/cactus Controls the Potent Antifungal Response in Drosophila Adults,” *Cell*, vol. 86, no. 6, pp. 973–983, 1996.

[41] S. Valanne, J.-H. Wang, and M. Ramet, “The Drosophila Toll Signaling Pathway,” *J. Immunol.*, vol. 186, no. 2, pp. 649–656, 2011.

[42] C. J. Kirschning, H. Wesche, T. Merrill Ayres, and M. Rothe, “Human Toll-like Receptor 2 Confers Responsiveness to Bacterial Lipopolysaccharide,” *J. Exp. Med.*, vol. 188, no. 11, p. 2091 LP-2097, Dec. 1998.

[43] R.-B. Yang *et al.*, “Toll-like receptor-2 mediates lipopolysaccharide-induced cellular signalling,” *Nature*, vol. 395, p. 284, Sep. 1998.

[44] J. K. Bell, G. E. D. Mullen, C. A. Leifer, A. Mazzoni, D. R. Davies, and D. M. Segal, “Leucine-rich repeats and pathogen recognition in Toll-like receptors,” *Trends Immunol.*, vol. 24, no. 10, pp. 528–533, 2003.

[45] A. Ozinsky *et al.*, “The repertoire for pattern recognition of pathogens by the innate immune system is defined by cooperation between Toll-like receptors,” *Proc. Natl. Acad. Sci.*, vol. 97, no. 25, p. 13766 LP-13771, Dec. 2000.

[46] S. E. Ewald *et al.*, “The ectodomain of Toll-like receptor 9 is cleaved to generate a functional receptor,” *Nature*, vol. 456, p. 658, Sep. 2008.

[47] S. Akira, S. Uematsu, and O. Takeuchi, “Pathogen Recognition and Innate Immunity,” *Cell*, vol. 124, no. 4, pp. 783–801, 2006.

[48] M. S. Jin *et al.*, “Crystal Structure of the TLR1-TLR2 Heterodimer Induced by Binding of a Tri-Acylated Lipopeptide,” *Cell*, vol. 130, no. 6, pp. 1071–1082, 2007.

[49] H. D. Brightbill *et al.*, "Host defense mechanisms triggered by microbial lipoproteins through toll-like receptors.," *Science*, vol. 285, no. 5428, pp. 732–6, Jul. 1999.

[50] A. O. Aliprantis *et al.*, "Cell Activation and Apoptosis by Bacterial Lipoproteins Through Toll-like Receptor-2," *Science (80-.).*, vol. 285, no. 5428, p. 736 LP-739, Jul. 1999.

[51] S. D. C. Müller *et al.*, "Triacyl-lipopentapeptide adjuvants: TLR2-dependent activation of macrophages and modulation of receptor-mediated cell activation by altering acyl-moieties," *Int. Immunopharmacol.*, vol. 4, no. 10, pp. 1287–1300, 2004.

[52] P. Massari *et al.*, "Meningococcal Porin PorB Binds to TLR2 and Requires TLR1 for Signaling," *J. Immunol.*, vol. 176, no. 4, p. 2373 LP-2380, Feb. 2006.

[53] R. Schwandner, R. Dziarski, H. Wesche, M. Rothe, and C. J. Kirschning, "Peptidoglycan- and lipoteichoic acid-induced cell activation is mediated by Toll-like receptor 2," *J. Biol. Chem.*, vol. 274, no. 25, pp. 17406–17409, 1999.

[54] K. Hoebe *et al.*, "CD36 is a sensor of diacylglycerides," *Nature*, vol. 433, p. 523, Feb. 2005.

[55] J. Y. Kang *et al.*, "Recognition of Lipopeptide Patterns by Toll-like Receptor 2-Toll-like Receptor 6 Heterodimer," *Immunity*, vol. 31, no. 6, pp. 873–884, 2009.

[56] K. Hantke and V. Braun, "Covalent binding of lipid to protein. Diglyceride and amide-linked fatty acid at the N-terminal end of the murein-lipoprotein of the Escherichia coli outer membrane.," *Eur. J. Biochem.*, vol. 34, no. 2, pp. 284–296, Apr. 1973.

[57] W. G. Bessler *et al.*, "Bacterial lipopeptides constitute efficient novel immunogens and adjuvants in parenteral and oral immunization.," *Behring Inst. Mitt.*, no. 98, pp. 390–399, Feb. 1997.

[58] A. Grabiec, G. Meng, S. Fichte, W. Bessler, H. Wagner, and C. J. Kirschning, "Human but not murine toll-like receptor 2 discriminates between tri-palmitoylated and tri-lauroylated peptides.," *J. Biol. Chem.*, vol. 279, no. 46, pp. 48004–48012, Nov. 2004.

[59] S. Spiller *et al.*, "cellular recognition of trimyristoylated peptide or enterobacterial lipopolysaccharide via both TLR2 and TLR4," *J. Biol. Chem.*, vol. 282, no. 18, pp. 13190–13198, 2007.

[60] K. Visvanathan *et al.*, "Regulation of Toll-like receptor-2 expression in chronic hepatitis B by the precore protein," *Hepatology*, vol. 45, no. 1, pp. 102–110, Jan. 2007.

[61] Y. Wang, L. Liu, D. R. Davies, and D. M. Segal, "Dimerization of Toll-like receptor 3 (TLR3) is required for ligand binding," *J. Biol. Chem.*, vol. 285, no. 47, pp. 36836–36841, 2010.

[62] L. Zhou *et al.*, "Activation of Toll-like receptor-3 induces interferon-λ expression in human neuronal cells," *Neuroscience*, vol. 159, no. 2, pp. 629–637, 2009.

[63] X.-L. Chen, Y.-Y. Xu, L. Chen, G.-L. Wang, and Y. Shen, "TLR3 Plays Significant Roles against HBV-Associated HCC," *Gastroenterol. Res. Pract.*, vol. 2015, p. 572171, 2015.

[64] J. M. Lund *et al.*, "Recognition of single-stranded RNA viruses by Toll-like receptor 7," *Proc. Natl. Acad. Sci. U. S. A.*, vol. 101, no. 15, p. 5598 LP-5603, Apr. 2004.

[65] P. Yu *et al.*, "Nucleic Acid-Sensing Toll-like Receptors Are Essential for the Control of Endogenous Retrovirus Viremia and ERV-Induced Tumors," *Immunity*, vol. 37, no. 5, pp. 867–879, 2012.

[66] K. B. Gorden *et al.*, "Synthetic TLR Agonists Reveal Functional Differences between Human TLR7 and TLR8," *J. Immunol.*, vol. 174, no. 3, p. 1259 LP-1268, Feb. 2005.

[67] H. Hemmi *et al.*, "A Toll-like receptor recognizes bacterial DNA," *Nature*, vol. 408, p. 740, Dec. 2000.

[68] F. Heil *et al.*, "The Toll-like receptor 7 (TLR7)-specific stimulus loxoribine uncovers a strong relationship within the TLR7, 8 and 9 subfamily," *Eur. J. Immunol.*, vol. 33, no. 11, pp. 2987–2997, Nov. 2003.

[69] R. E. Lanford *et al.*, "GS-9620, an Oral Agonist of Toll-Like Receptor-7, Induces Prolonged Suppression of Hepatitis B Virus in Chronically Infected Chimpanzees," *Gastroenterology*, vol. 144, no. 7, p. 1508–1517.e10, 2013.

[70] F. Heil *et al.*, "Species-Specific Recognition of Single-Stranded RNA via Toll-like Receptor 7 and 8," *Science (80-.).*, vol. 303, no. 5663, p. 1526 LP-1529, Mar. 2004.

[71] V. Lombardi, L. Van Overtvelt, S. Horiot, and P. Moingeon, "Human Dendritic Cells Stimulated via TLR7 and/or TLR8 Induce the Sequential Production of Il-10, IFN-γ, and IL-17A by Naive CD4⁺ T Cells," *J. Immunol.*, vol. 182, no. 6, p. 3372 LP-3379, Mar. 2009.

[72] L. K. M. Shoda *et al.*, "DNA from Protozoan Parasites Babesia bovis, Trypanosoma cruzi, and T. brucei Is Mitogenic for B Lymphocytes and Stimulates Macrophage Expression of Interleukin-12, Tumor Necrosis Factor Alpha, and Nitric Oxide," *Infect. Immun.*, vol. 69, no. 4, p. 2162 LP-2171, Apr. 2001.

[73] B. Kobe and A. V Kajava, "The leucine-rich repeat as a protein recognition motif," *Curr. Opin. Struct. Biol.*, vol. 11, no. 6, pp. 725–732, 2001.

[74] T. M. Burch-Smith and S. P. Dinesh-Kumar, "The Functions of Plant TIR Domains," *Sci. STKE*, vol. 2007, no. 401, p. pe46 LP-pe46, Aug. 2007.

[75] C. Brikos and L. A. J. O'Neill, "Signalling of Toll-Like Receptors BT - Toll-Like Receptors (TLRs) and Innate Immunity," S. Bauer and G. Hartmann, Eds. Berlin, Heidelberg: Springer Berlin Heidelberg, 2008, pp. 21–50.

[76] M. Colonna, "TLR pathways and IFN-regulatory factors: To each its own," *Eur. J. Immunol.*, vol. 37, no. 2, pp. 306–309, 2007.

[77] T. D. Troutman *et al.*, "Role for B-cell adapter for PI3K (BCAP) as a signaling adapter linking Toll-like receptors (TLRs) to serine/threonine kinases PI3K/Akt," *Proc. Natl. Acad. Sci.*, vol. 109, no. 1, p. 273 LP-278, Jan. 2012.

[78] S. Akira and K. Takeda, "Toll-like receptor signalling," *Nat. Rev. Immunol.*, vol. 4, no. 7, pp. 499–511, 2004.

[79] V. Baud, Z. G. Liu, B. Bennett, N. Suzuki, Y. Xia, and M. Karin, "Signaling by proinflammatory cytokines: Oligomerization of TRAF2 and TRAF6 is sufficient for JNK and IKK activation and target gene induction via an amino-terminal effector domain," *Genes Dev.*,

vol. 13, no. 10, pp. 1297–1308, 1999.

[80] H. Häcker, P.-H. Tseng, and M. Karin, "Expanding TRAF function: TRAF3 as a tri-faced immune regulator," *Nat. Rev. Immunol.*, vol. 11, p. 457, Jun. 2011.

[81] O. Adachi *et al.*, "Targeted Disruption of the MyD88 Gene Results in Loss of IL-1- and IL-18-Mediated Function," *Immunity*, vol. 9, no. 1, pp. 143–150, 1998.

[82] N. Tanimura, S. Saitoh, F. Matsumoto, S. Akashi-Takamura, and K. Miyake, "Roles for LPS-dependent interaction and relocation of TLR4 and TRAM in TRIF-signaling," *Biochem. Biophys. Res. Commun.*, vol. 368, no. 1, pp. 94–99, 2008.

[83] B. L. Lee *et al.*, "UNC93B1 mediates differential trafficking of endosomal TLRs," *Elife*, vol. 2, p. e00291, 2013.

[84] P. J. Zamor, A. S. deLemos, and M. W. Russo, "Viral hepatitis and hepatocellular carcinoma: etiology and management," *J. Gastrointest. Oncol.*, vol. 8, no. 2, pp. 229–242, Apr. 2017.

[85] B. Mühlemann *et al.*, "Ancient hepatitis B viruses from the Bronze Age to the Medieval period," *Nature*, vol. 557, no. 7705, pp. 418–423, 2018.

[86] M.-F. Yuen *et al.*, "Role of Hepatitis B Virus Genotypes in Chronic Hepatitis B Exacerbation," *Clin. Infect. Dis.*, vol. 37, no. 4, pp. 593–597, Aug. 2003.

[87] R. Zampino *et al.*, "Hepatitis B virus burden in developing countries," *World J. Gastroenterol.*, vol. 21, no. 42, pp. 11941–11953, Nov. 2015.

[88] C. Seeger and W. S. Mason, "Molecular biology of hepatitis B virus infection.," *Virology*, vol. 479–480, pp. 672–86, May 2015.

[89] W. Li, "The Hepatitis B Virus Receptor," *Annu. Rev. Cell Dev. Biol.*, vol. 31, no. 1, pp. 125–147, 2015.

[90] I. Gentile and G. Borgia, "Vertical transmission of hepatitis B virus: challenges and solutions.," *Int. J. Womens. Health*, vol. 6, pp. 605–11, 2014.

[91] A. Vyas *et al.*, *Maternal Immunity Influences Vertical Transmission of Hepatitis B to Newborns*. 2019.

[92] A. Alberti, S. Diana, G. H. Scullard, W. F. Eddleston, and R. Williams, "Full and empty Dane particles in chronic hepatitis B virus infection: relation to hepatitis B e antigen and presence of liver damage.," *Gastroenterology*, vol. 75, no. 5, pp. 869–874, Nov. 1978.

[93] J. Hu and K. Liu, "Complete and Incomplete Hepatitis B Virus Particles: Formation, Function, and Application," *Viruses*, vol. 9, no. 3, p. 56, Mar. 2017.

[94] T. Tu, M. Budzinska, N. Shackel, and S. Urban, *HBV DNA Integration: Molecular Mechanisms and Clinical Implications*, vol. 9. 2017.

[95] S. Fazle Akbar, "HBeAg negative chronic Hepatitis B: An overview," *Hepat. B Annu.*, vol. 6, no. 1, pp. 131–140, Jan. 2009.

[96] F. Bonino, T. Piratvisuth, M. R. Brunetto, and Y.-F. Liaw, "Diagnostic markers of chronic hepatitis B infection and disease.," *Antivir. Ther.*, vol. 15 Suppl 3, pp. 35–44, 2010.

[97] M. Feitelson, “The DNA Polymerase Activity of HBV BT - Molecular Components of Hepatitis B Virus,” M. Feitelson, Ed. Boston, MA: Springer US, 1985, pp. 123–132.

[98] N. P. Klein and R. J. Schneider, “Activation of Src family kinases by hepatitis B virus HBx protein and coupled signaling to Ras,” *Mol. Cell. Biol.*, vol. 17, no. 11, pp. 6427–6436, Nov. 1997.

[99] A. Decorsiere *et al.*, “Hepatitis B virus X protein identifies the Smc5/6 complex as a host restriction factor.,” *Nature*, vol. 531, no. 7594, pp. 386–389, Mar. 2016.

[100] T. J. Liang, “Hepatitis B: the virus and disease,” *Hepatology*, vol. 49, no. 5 Suppl, pp. S13–S21, May 2009.

[101] A. Meier, S. Mehrle, T. S. Weiss, W. Mier, and S. Urban, “Myristoylated PreS1-domain of the hepatitis B virus L-protein mediates specific binding to differentiated hepatocytes.,” *Hepatology*, vol. 58, no. 1, pp. 31–42, Jul. 2013.

[102] “viral Hepatitis, Moelcular Biology, Diagnosis and control Isa K.” .

[103] A. Barrera, B. Guerra, L. Notvall, and R. E. Lanford, “Mapping of the hepatitis B virus pre-S1 domain involved in receptor recognition,” *J. Virol.*, vol. 79, no. 15, pp. 9786–9798, Aug. 2005.

[104] D. L. Peterson, D. A. Paul, J. Lam, I. I. Tribby, and D. T. Achord, “Antigenic structure of hepatitis B surface antigen: identification of the ‘d’ subtype determinant by chemical modification and use of monoclonal antibodies.,” *J. Immunol.*, vol. 132, no. 2, pp. 920–927, Feb. 1984.

[105] S. Wang *et al.*, “Hepatitis B Virus Surface Antigen Selectively Inhibits TLR2 Ligand-Induced IL-12 Production in Monocytes/Macrophages by Interfering with JNK Activation,” *J. Immunol.*, vol. 190, no. 10, pp. 5142–5151, 2013.

[106] R. Salpini *et al.*, “Hepatitis B surface antigen genetic elements critical for immune escape correlate with hepatitis B virus reactivation upon immunosuppression.,” *Hepatology*, vol. 61, no. 3, pp. 823–833, Mar. 2015.

[107] W. Li, “The Hepatitis B Virus Receptor,” *Annu. Rev. Cell Dev. Biol.*, vol. 31, no. 1, pp. 125–147, Nov. 2015.

[108] W. Gao and J. Hu, “Formation of Hepatitis B Virus Covalently Closed Circular DNA: Removal of Genome-Linked Protein,” *J. Virol.*, vol. 81, no. 12, p. 6164 LP-6174, Jun. 2007.

[109] J. Habig and D. D Loeb, *The Conformation of the 3’ End of the Minus-Strand DNA Makes Multiple Contributions to Template Switches during Plus-Strand DNA Synthesis of Duck Hepatitis B Virus*, vol. 77. 2004.

[110] S. Urban, A. Schulze, M. Dandri, and J. Petersen, “The replication cycle of hepatitis B virus.,” *J. Hepatol.*, vol. 52, no. 2, pp. 282–284, Feb. 2010.

[111] S. K. Sarin, M. Kumar, S. Shrivastava, S. Sinha, and N. T. Pati, “Influence of chronic HBV infection on pregnancy: a human model of maternofetal virus host interactions.,” *Gastroenterology*, vol. 141, no. 4, pp. 1522–1525, Oct. 2011.

[112] S. F. Wieland and F. V Chisari, “Stealth and cunning: hepatitis B and hepatitis C viruses,” *J. Virol.*, vol. 79, no. 15, pp. 9369–9380, Aug. 2005.

[113] A. Suslov, T. Boldanova, X. Wang, S. Wieland, and M. H. Heim, "Hepatitis B Virus Does Not Interfere With Innate Immune Responses in the Human Liver.," *Gastroenterology*, vol. 154, no. 6, pp. 1778–1790, May 2018.

[114] L. G. Guidotti, R. Rochford, J. Chung, M. Shapiro, R. Purcell, and F. V Chisari, "Viral clearance without destruction of infected cells during acute HBV infection.," *Science*, vol. 284, no. 5415, pp. 825–829, Apr. 1999.

[115] S. Wieland, R. Thimme, R. H. Purcell, and F. V Chisari, "Genomic analysis of the host response to hepatitis B virus infection," *Proc. Natl. Acad. Sci. U. S. A.*, vol. 101, no. 17, p. 6669 LP-6674, Apr. 2004.

[116] R. Thimme *et al.*, "CD8(+) T cells mediate viral clearance and disease pathogenesis during acute hepatitis B virus infection.," *J. Virol.*, vol. 77, no. 1, pp. 68–76, Jan. 2003.

[117] P. L. Yang *et al.*, "Immune effectors required for hepatitis B virus clearance," *Proc. Natl. Acad. Sci.*, vol. 107, no. 2, p. 798 LP-802, Jan. 2010.

[118] R. Thimme *et al.*, "CD8+ T Cells Mediate Viral Clearance and Disease Pathogenesis during Acute Hepatitis B Virus Infection," *J. Virol.*, vol. 77, no. 1, pp. 68–76, 2003.

[119] G. K. K. Lau *et al.*, "Resolution of chronic hepatitis B and anti-HBs seroconversion in humans by adoptive transfer of immunity to hepatitis B core antigen.," *Gastroenterology*, vol. 122, no. 3, pp. 614–624, Mar. 2002.

[120] G. F. Grady *et al.*, "Hepatitis B immune globulin for accidental exposures among medical personnel: final report of a multicenter controlled trial.," *J. Infect. Dis.*, vol. 138, no. 5, pp. 625–638, Nov. 1978.

[121] Y. Bian *et al.*, "Vaccines targeting preS1 domain overcome immune tolerance in hepatitis B virus carrier mice.," *Hepatology*, vol. 66, no. 4, pp. 1067–1082, Oct. 2017.

[122] A. Bertoletti and C. Ferrari, "Innate and adaptive immune responses in chronic hepatitis B virus infections: towards restoration of immune control of viral infection.," *Gut*, vol. 61, no. 12, pp. 1754–1764, Dec. 2012.

[123] H. Guo *et al.*, "Activation of pattern recognition receptor-mediated innate immunity inhibits the replication of hepatitis B virus in human hepatocyte-derived cells.," *J. Virol.*, vol. 83, no. 2, pp. 847–858, Jan. 2009.

[124] M. Isogawa, M. D. Robek, Y. Furuichi, and F. V Chisari, "Toll-Like Receptor Signaling Inhibits Hepatitis B Virus Replication In Vivo," *J. Virol.*, vol. 79, no. 11, p. 7269 LP-7272, Jun. 2005.

[125] H.-L. Lu and F. Liao, "Melanoma differentiation-associated gene 5 senses hepatitis B virus and activates innate immune signaling to suppress virus replication.," *J. Immunol.*, vol. 191, no. 6, pp. 3264–3276, Sep. 2013.

[126] S. Sato *et al.*, "The RNA Sensor RIG-I Dually Functions as an Innate Sensor and Direct Antiviral Factor for Hepatitis B Virus," *Immunity*, vol. 42, no. 1, pp. 123–132, 2015.

[127] Y.-Q. Lu, H. Ma, X.-B. Pan, and L. Wei, "Nuclear DNA sensor protein IFI16 recognizes hepatitis B virus covalently closed circular DNA and regluates the antiviral innate immunity," *J. Hepatol.*, vol. 68, pp. S796–S797, Apr. 2018.

[128] Z. Ma *et al.*, "The IL-1R/TLR signaling pathway is essential for efficient CD8 + T-cell responses against hepatitis B virus in the hydrodynamic injection mouse model," *Cell. Mol. Immunol.*, vol. 14, no. 12, pp. 997–1008, 2017.

[129] Y.-C. Wang, S. E. Peterson, and J. F. Loring, "Protein post-translational modifications and regulation of pluripotency in human stem cells," *Cell Res.*, vol. 24, p. 143, Nov. 2013.

[130] K. K. Han and A. Martinage, "Post-translational chemical modification(s) of proteins.," *Int. J. Biochem.*, vol. 24, no. 1, pp. 19–28, 1992.

[131] A. Drazic, L. M. Myklebust, R. Ree, and T. Arnesen, "The world of protein acetylation," *Biochim. Biophys. Acta - Proteins Proteomics*, vol. 1864, no. 10, pp. 1372–1401, 2016.

[132] R. K. Mann and P. A. Beachy, "Cholesterol modification of proteins.," *Biochim. Biophys. Acta*, vol. 1529, no. 1–3, pp. 188–202, Dec. 2000.

[133] C. L. Lamphear, E. A. Zverina, J. L. Hougland, and C. A. Fierke, "12 - Global Identification of Protein Prenyltransferase Substrates: Defining the Prenylated Proteome," in *Protein Prenylation PART A*, vol. 29, F. Tamanoi, C. A. Hrycyna, and M. O. B. T.-T. E. Bergo, Eds. Academic Press, 2011, pp. 207–234.

[134] T. Kinoshita and M. Fujita, "Biosynthesis of GPI-anchored proteins: special emphasis on GPI lipid remodeling.," *J. Lipid Res.*, vol. 57, no. 1, pp. 6–24, Jan. 2016.

[135] J. B. de Souza *et al.*, "Neutralization of malaria glycosylphosphatidylinositol in vitro by serum IgG from malaria-exposed individuals.," *Infect. Immun.*, vol. 78, no. 9, pp. 3920–3929, Sep. 2010.

[136] M. Matsubara *et al.*, "Myristoyl moiety of HIV Nef is involved in regulation of the interaction with calmodulin in vivo," *Protein Sci.*, vol. 14, no. 2, pp. 494–503, Feb. 2005.

[137] A. Rein, M. R. McClure, N. R. Rice, R. B. Luftig, and A. M. Schultz, "Myristylation site in Pr65gag is essential for virus particle formation by Moloney murine leukemia virus," *Proc. Natl. Acad. Sci. U. S. A.*, vol. 83, no. 19, pp. 7246–7250, Oct. 1986.

[138] M. Veit, E. Ponimaskin, and M. F. G. Schmidt, "Analysis of S-acylation of proteins.," *Methods Mol. Biol.*, vol. 446, pp. 163–182, 2008.

[139] J. Zha, S. Weiler, K. J. Oh, M. C. Wei, and S. J. Korsmeyer, "Posttranslational N-myristoylation of BID as a molecular switch for targeting mitochondria and apoptosis.," *Science*, vol. 290, no. 5497, pp. 1761–1765, Dec. 2000.

[140] S. J. Wakil, J. K. Stoops, and V. C. Joshi, "Fatty Acid Synthesis and its Regulation," *Annu. Rev. Biochem.*, vol. 52, no. 1, pp. 537–579, 1983.

[141] W. Benetka *et al.*, "Experimental testing of predicted myristoylation targets involved in asymmetric cell division and calcium-dependent signalling.," *Cell Cycle*, vol. 7, no. 23, pp. 3709–3719, Dec. 2008.

[142] A. A. Aderem, M. M. Keum, E. Pure, and Z. A. Cohn, "Bacterial lipopolysaccharides, phorbol myristate acetate, and zymosan induce the myristoylation of specific macrophage proteins," *Proc Natl Acad Sci U S A*, vol. 83, no. 16, pp. 5817–5821, 1986.

[143] A. Arbuzova, A. A. P. Schmitz, and G. Vergères, "Cross-talk unfolded: MARCKS

proteins," *Biochem. J.*, vol. 362, no. Pt 1, pp. 1–12, Feb. 2002.

[144] D. I. Udenwobele, R.-C. Su, S. V Good, T. B. Ball, S. Varma Shrivastav, and A. Shrivastav, "Myristoylation: An Important Protein Modification in the Immune Response ," *Frontiers in Immunology* , vol. 8. p. 751, 2017.

[145] B. Bjorkblom *et al.*, "c-Jun N-terminal kinase phosphorylation of MARCKSL1 determines actin stability and migration in neurons and in cancer cells.," *Mol. Cell. Biol.*, vol. 32, no. 17, pp. 3513–3526, Sep. 2012.

[146] K. Fujita *et al.*, "HMGB1, a pathogenic molecule that induces neurite degeneration via TLR4-MARCKS, is a potential therapeutic target for Alzheimer's disease," *Sci. Rep.*, vol. 6, p. 31895, Aug. 2016.

[147] A. Kovacs-Simon, R. W. Titball, and S. L. Michell, "Lipoproteins of bacterial pathogens," *Infect. Immun.*, vol. 79, no. 2, pp. 548–561, Feb. 2011.

[148] M. Schenk, J. T. Belisle, and R. L. Modlin, "TLR2 looks at lipoproteins.," *Immunity*, vol. 31, no. 6, pp. 847–849, Dec. 2009.

[149] M. Moradzadeh *et al.*, "The Possible Role of TLR2 in Chronic Hepatitis B Patients with Precore Mutation," *Adv. Virol.*, vol. 2013, p. 780319, 2013.

[150] M. A. Sells, M. L. Chen, and G. Acs, "Production of hepatitis B virus particles in Hep G2 cells transfected with cloned hepatitis B virus DNA.," *Proc. Natl. Acad. Sci. U. S. A.*, vol. 84, no. 4, pp. 1005–1009, Feb. 1987.

[151] F. Galibert, E. Mandart, F. Fitoussi, P. Tiollais, and P. Charnay, "Nucleotide sequence of the hepatitis B virus genome (subtype ayw) cloned in E. coli," *Nature*, vol. 281, no. 5733, pp. 646–650, 1979.

[152] P. Chomczynski and N. Sacchi, "Single-step method of RNA isolation by acid guanidinium thiocyanate-phenol-chloroform extraction.," *Anal. Biochem.*, vol. 162, no. 1, pp. 156–159, Apr. 1987.

[153] K. Ito, X. Ma, N. Azmi, H.-S. Huang, M. Fujii, and T. Yoshimoto, "Novel aminopeptidase specific for glycine from Actinomucor elegans.," *Biosci. Biotechnol. Biochem.*, vol. 67, no. 1, pp. 83–88, Jan. 2003.

[154] L. C. Green, D. A. Wagner, J. Glogowski, P. L. Skipper, J. S. Wishnok, and S. R. Tannenbaum, "Analysis of nitrate, nitrite, and [15N]nitrate in biological fluids.," *Anal. Biochem.*, vol. 126, no. 1, pp. 131–138, Oct. 1982.

[155] S. Voss, A. J. Ulmer, G. Jung, K.-H. Wiesmuller, and R. Brock, "The activity of lipopeptide TLR2 agonists critically depends on the presence of solubilizers.," *Eur. J. Immunol.*, vol. 37, no. 12, pp. 3489–3498, Dec. 2007.

[156] H. Schägger, "Tricine–SDS-PAGE," *Nat. Protoc.*, vol. 1, p. 16, May 2006.

[157] C. Hacker *et al.*, "Nanoparticle suspensions enclosed in methylcellulose: a new approach for quantifying nanoparticles in transmission electron microscopy," *Sci. Rep.*, vol. 6, p. 25275, May 2016.

[158] B. J. McMahon *et al.*, "Acute hepatitis B virus infection: relation of age to the clinical expression of disease and subsequent development of the carrier state.," *J. Infect. Dis.*, vol.

151, no. 4, pp. 599–603, Apr. 1985.

[159] P. T. F. Kennedy, S. Litwin, G. E. Dolman, A. Bertoletti, and W. S. Mason, “Immune tolerant chronic hepatitis B: The unrecognized risks,” *Viruses*, vol. 9, no. 5, pp. 1–19, 2017.

[160] A. Untergasser *et al.*, “Dendritic cells take up viral antigens but do not support the early steps of hepatitis B virus infection,” *Hepatology*, vol. 43, no. 3, pp. 539–547, Mar. 2006.

[161] G. M. GREEN and E. H. KASS, “THE ROLE OF THE ALVEOLAR MACROPHAGE IN THE CLEARANCE OF BACTERIA FROM THE LUNG,” *J. Exp. Med.*, vol. 119, no. 1, pp. 167–176, Jan. 1964.

[162] X. Cheng *et al.*, “Hepatitis B virus evades innate immunity of hepatocytes but activates cytokine production by macrophages.,” *Hepatology*, vol. 66, no. 6, pp. 1779–1793, Dec. 2017.

[163] C. J. Kirschning and R. R. Schumann, “TLR2: cellular sensor for microbial and endogenous molecular patterns.,” *Curr. Top. Microbiol. Immunol.*, vol. 270, pp. 121–144, 2002.

[164] T. Shikata, T. Karasawa, K. Abe, T. Takahashi, M. Mayumi, and T. Oda, “Incomplete inactivation of hepatitis B virus after heat treatment at 60 C for 10 hours.,” *J. Infect. Dis.*, vol. 138, no. 2, pp. 242–244, Aug. 1978.

[165] K. Watashi, S. Urban, W. Li, and T. Wakita, “NTCP and beyond: opening the door to unveil hepatitis B virus entry,” *Int. J. Mol. Sci.*, vol. 15, no. 2, pp. 2892–2905, Feb. 2014.

[166] M. Mansour, *Characterization of Subviral Particles of Hepatitis B Virus Produced by HepG2.2.15 Cell Line - In vitro Study*. 2018.

[167] P. Gripon, J. Le Seyec, S. Rumin, and C. Guguen-Guillouzo, “Myristylation of the hepatitis B virus large surface protein is essential for viral infectivity.,” *Virology*, vol. 213, no. 2, pp. 292–299, Nov. 1995.

[168] E. J. Patzer *et al.*, “Cell Culture Derived Recombinant HBsAg is Highly Immunogenic and Protects Chimpanzees from Infection with Hepatitis B Virus,” *Bio/Technology*, vol. 4, no. 7, pp. 630–636, 1986.

[169] M. Mancek-Keber *et al.*, *MARCKS as a Negative Regulator of Lipopolysaccharide Signaling*, vol. 188. 2012.

[170] R. J. Fair and Y. Tor, “Antibiotics and bacterial resistance in the 21st century,” *Perspect. Medicin. Chem.*, vol. 6, pp. 25–64, Aug. 2014.

[171] D. L. Bienvenue, R. S. Mathew, D. Ringe, and R. C. Holz, “The aminopeptidase from Aeromonas proteolytica can function as an esterase.,” *J. Biol. Inorg. Chem.*, vol. 7, no. 1–2, pp. 129–135, Jan. 2002.

[172] S. M. Riordan *et al.*, “Peripheral blood mononuclear cell expression of toll-like receptors and relation to cytokine levels in cirrhosis.,” *Hepatology*, vol. 37, no. 5, pp. 1154–1164, May 2003.

[173] I. Sabroe, E. C. Jones, L. R. Usher, M. K. B. Whyte, and S. K. Dower, “Toll-Like Receptor (TLR)2 and TLR4 in Human Peripheral Blood Granulocytes: A Critical Role for Monocytes in Leukocyte Lipopolysaccharide Responses,” *J. Immunol.*, vol. 168, no. 9, p. 4701 LP-4710, May 2002.

[174] A. Kuznik, M. Bencina, U. Svajger, M. Jeras, B. Rozman, and R. Jerala, "Mechanism of endosomal TLR inhibition by antimalarial drugs and imidazoquinolines.," *J. Immunol.*, vol. 186, no. 8, pp. 4794–4804, Apr. 2011.

[175] A. Rein, "Murine leukemia viruses: objects and organisms," *Adv. Virol.*, vol. 2011, p. 403419, 2011.

[176] A. Kolokithas *et al.*, "The Glycosylated Gag Protein of a Murine Leukemia Virus Inhibits the Antiretroviral Function of APOBEC3," *J. Virol.*, vol. 84, no. 20, p. 10933 LP-10936, Oct. 2010.

[177] J. Martin-Serrano, S. W. Eastman, W. Chung, and P. D. Bieniasz, "HECT ubiquitin ligases link viral and cellular PPXY motifs to the vacuolar protein-sorting pathway," *J. Cell Biol.*, vol. 168, no. 1, pp. 89–101, Jan. 2005.

[178] H. C. Kolb, M. G. Finn, and K. B. Sharpless, "Click Chemistry: Diverse Chemical Function from a Few Good Reactions," *Angew. Chemie Int. Ed.*, vol. 40, no. 11, pp. 2004–2021, Jun. 2001.

[179] U. K. LAEMMLI, "Cleavage of Structural Proteins during the Assembly of the Head of Bacteriophage T4," *Nature*, vol. 227, no. 5259, pp. 680–685, 1970.

[180] H. Schagger and G. von Jagow, "Tricine-sodium dodecyl sulfate-polyacrylamide gel electrophoresis for the separation of proteins in the range from 1 to 100 kDa.," *Anal. Biochem.*, vol. 166, no. 2, pp. 368–379, Nov. 1987.

[181] P. Golabi, S. Fazel, M. Otgonsuren, M. Sayiner, C. T. Locklear, and Z. M. Younossi, "Mortality assessment of patients with hepatocellular carcinoma according to underlying disease and treatment modalities," *Medicine (Baltimore).*, vol. 96, no. 9, pp. e5904–e5904, Mar. 2017.

[182] S. P. Hussain, J. Schwank, F. Staib, X. W. Wang, and C. C. Harris, "TP53 mutations and hepatocellular carcinoma: insights into the etiology and pathogenesis of liver cancer.," *Oncogene*, vol. 26, no. 15, pp. 2166–2176, Apr. 2007.

[183] H.-J. Lee, J. Lee, M.-K. Shin, and W.-S. Ryu, "Polyadenylation is dispensable for encapsidation and reverse transcription of hepatitis B viral pregenomic RNA.," *Mol. Cells*, vol. 25, no. 4, pp. 545–552, Jun. 2008.

[184] L. G. Guidotti and F. V Chisari, "Immunobiology and pathogenesis of viral hepatitis.," *Annu. Rev. Pathol.*, vol. 1, pp. 23–61, 2006.

[185] F. V Chisari and C. Ferrari, "Hepatitis B virus immunopathogenesis.," *Annu. Rev. Immunol.*, vol. 13, pp. 29–60, 1995.

[186] L. B. Ivashkiv and L. T. Donlin, "Regulation of type I interferon responses," *Nat. Rev. Immunol.*, vol. 14, no. 1, pp. 36–49, Jan. 2014.

[187] F. Souza-Fonseca-Guimaraes, M. Adib-Conquy, and J.-M. Cavaillon, "Natural killer (NK) cells in antibacterial innate immunity: angels or devils?," *Mol. Med.*, vol. 18, no. 1, pp. 270–285, Nov. 2011.

[188] Z. Ma, E. Zhang, D. Yang, and M. Lu, "Contribution of Toll-like receptors to the control of hepatitis B virus infection by initiating antiviral innate responses and promoting

specific adaptive immune responses," *Cell. Mol. Immunol.*, vol. 12, no. 3, pp. 273–282, May 2015.

[189] X. Zhang *et al.*, "Role of Toll-like receptor 2 in the immune response against hepadnaviral infection.," *J. Hepatol.*, vol. 57, no. 3, pp. 522–528, Sep. 2012.

[190] J. Pang *et al.*, "Transforming growth factor β-activated kinase 1 transcriptionally suppresses hepatitis B virus replication," *Sci. Rep.*, vol. 7, p. 39901, Jan. 2017.

[191] S. Cheng, B. Zhang, J.-Y. Du, Y.-H. Jin, H.-Y. Lang, and L.-H. Zeng, "Hepatitis B Surface Antigen Promotes the Invasion of Hepatitis B Virus-Related Hepatocellular Carcinoma Cells by Upregulation of Toll-Like Receptor 2," *Viral Immunol.*, vol. 30, no. 3, pp. 232–239, Jan. 2017.

[192] Y. Wang *et al.*, "Downregulation of toll-like receptor 4 induces suppressive effects on hepatitis B virus-related hepatocellular carcinoma via ERK1/2 signaling," *BMC Cancer*, vol. 15, p. 821, Oct. 2015.

[193] B. Liu *et al.*, "Liver Sinusoidal Endothelial Cell Lectin Inhibits CTL-Dependent Virus Clearance in Mouse Models of Viral Hepatitis," *J. Immunol.*, p. 1203091, Mar. 2013.

[194] Y. Han *et al.*, "Association of Mutations in Toll-like Receptor 2 Signaling Genes With Fulminant Form of Hepatitis B-Related Acute Liver Failure.," *J. Infect. Dis.*, vol. 215, no. 8, pp. 1221–1230, Apr. 2017.

[195] S. Urban, R. Bartenschlager, R. Kubitz, and F. Zoulim, "Strategies to inhibit entry of HBV and HDV into hepatocytes.," *Gastroenterology*, vol. 147, no. 1, pp. 48–64, Jul. 2014.

[196] S. Seitz *et al.*, "A Slow Maturation Process Renders Hepatitis B Virus Infectious," *Cell Host Microbe*, vol. 20, no. 1, pp. 25–35, 2016.

[197] I. N. Crispe, "Immune tolerance in liver disease.," *Hepatology*, vol. 60, no. 6, pp. 2109–2117, Dec. 2014.

[198] V. Bruss, "Hepatitis B virus morphogenesis.," *World J. Gastroenterol.*, vol. 13, no. 1, pp. 65–73, Jan. 2007.

[199] K. H. Heermann, U. Goldmann, W. Schwartz, T. Seyffarth, H. Baumgarten, and W. H. Gerlich, "Large surface proteins of hepatitis B virus containing the pre-s sequence.," *J. Virol.*, vol. 52, no. 2, pp. 396–402, Nov. 1984.

[200] P. Matzinger, "Tolerance, danger, and the extended family.," *Annu. Rev. Immunol.*, vol. 12, pp. 991–1045, 1994.

[201] A. Boltjes, Z. M. Groothuismink, G. W. van Oord, H. L. A. Janssen, A. M. Woltman, and A. Boonstra, "Monocytes from chronic HBV patients react in vitro to HBsAg and TLR by producing cytokines irrespective of stage of disease.," *PLoS One*, vol. 9, no. 5, p. e97006, 2014.

[202] P. Revill and Z. Yuan, "New insights into how HBV manipulates the innate immune response to establish acute and persistent infection," *Antivir. Ther.*, vol. 18, no. 1, pp. 1–15, 2013.

[203] J. York and J. H. Nunberg, "Myristoylation of the Arenavirus Envelope Glycoprotein Stable Signal Peptide Is Critical for Membrane Fusion but Dispensable for Virion

Morphogenesis," *J. Virol.*, vol. 90, no. 18, p. 8341 LP-8350, Sep. 2016.

[204] S. Datta *et al.*, *On the Role of the SP1 Domain in HIV-1 Particle Assembly: a Molecular Switch?*, vol. 85. 2011.

[205] M. Azuma *et al.*, "The peptide sequence of diacyl lipopeptides determines dendritic cell TLR2-mediated NK activation," *PLoS One*, vol. 5, no. 9, p. e12550, Sep. 2010.

[206] N. van Montfoort *et al.*, "Hepatitis B Virus Surface Antigen Activates Myeloid Dendritic Cells via a Soluble CD14-Dependent Mechanism.," *J. Virol.*, vol. 90, no. 14, pp. 6187–6199, Jul. 2016.

[207] L. Paige, G. Qiang Zheng, S. A. DeFrees, J. M. Cassady, and R. Geahlen, *Metabolic activation of 2-substituted derivatives of myristic acid to form potent inhibitors of myristoyl CoA:protein N-myristoyltransferase*, vol. 29. 1990.

[208] G.-Y. Cui and H.-Y. Diao, "Recognition of HBV antigens and HBV DNA by dendritic cells.," *Hepatobiliary Pancreat. Dis. Int*, vol. 9, no. 6, pp. 584–592, Dec. 2010.

[209] I. E. Vincent *et al.*, "Hepatitis B virus impairs TLR9 expression and function in plasmacytoid dendritic cells.," *PLoS One*, vol. 6, no. 10, p. e26315, 2011.

[210] L. Cova, "DNA vaccine: a promising new approach for chronic hepatitis B therapy," *Future Virol.*, vol. 2, no. 5, pp. 421–424, Sep. 2007.

[211] J. Wang *et al.*, "Serum hepatitis B virus RNA is encapsidated pregenome RNA that may be associated with persistence of viral infection and rebound.," *J. Hepatol.*, vol. 65, no. 4, pp. 700–710, Oct. 2016.

[212] J. Kock, L. Theilmann, P. Galle, and H. J. Schlicht, "Hepatitis B virus nucleic acids associated with human peripheral blood mononuclear cells do not originate from replicating virus.," *Hepatology*, vol. 23, no. 3, pp. 405–413, Mar. 1996.

[213] R. H. Miller, C. T. Tran, and W. S. Robinson, "Hepatitis B virus particles of plasma and liver contain viral DNA-RNA hybrid molecules.," *Virology*, vol. 139, no. 1, pp. 53–63, Nov. 1984.

[214] J. B. Williams, A. Hüppner, P. M. Mulrooney-Cousins, and T. I. Michalak, "Differential Expression of Woodchuck Toll-Like Receptors 1-10 in Distinct Forms of Infection and Stages of Hepatitis in Experimental Hepatitis B Virus Infection," *Front. Microbiol.*, vol. 9, p. 3007, Dec. 2018.

[215] B. Zhang *et al.*, "TLR3 Activation of Hepatic Stellate Cell Line Suppresses HBV Replication in HepG2 Cells ," *Frontiers in Immunology* , vol. 9. p. 2921, 2018.

[216] A. K. Lee, H. M. Ip, and V. C. Wong, "Mechanisms of maternal-fetal transmission of hepatitis B virus.," *J. Infect. Dis.*, vol. 138, no. 5, pp. 668–671, Nov. 1978.

[217] C. E. Stevens, R. P. Beasley, J. Tsui, and W. C. Lee, "Vertical transmission of hepatitis B antigen in Taiwan.," *N. Engl. J. Med.*, vol. 292, no. 15, pp. 771–774, Apr. 1975.

[218] N. Trehanpati, S. Hissar, S. Shrivastav, and S. K. Sarin, "Immunological mechanisms of hepatitis B virus persistence in newborns.," *Indian J. Med. Res.*, vol. 138, no. 5, pp. 700–710, Nov. 2013.

[219] M. G. Roncarolo, M. Bigler, E. Ciuti, S. Martino, and P. A. Tovo, "Immune responses by cord blood cells.," *Blood Cells*, vol. 20, no. 2–3, pp. 573–576, 1994.

[220] J. Pott *et al.*, "Age-dependent TLR3 expression of the intestinal epithelium contributes to rotavirus susceptibility," *PLoS Pathog.*, vol. 8, no. 5, 2012.

[221] Z. Wang, Y. Liu, N. Mi, and D. Duan, *Intracellular DNA sensing pathway of cGAS-cGAMP is decreased in human newborns and young children*, vol. 87. 2017.

[222] Z. Muhammad, A. Ahmed, U. Hayat, M. S. Wazir, Rafiyatullah, and H. Waqas, "Neonatal sepsis: causative bacteria and their resistance to antibiotics.," *J. Ayub Med. Coll. Abbottabad*, vol. 22, no. 4, pp. 33–36, 2010.

[223] M. Hong *et al.*, "Trained immunity in newborn infants of HBV-infected mothers.," *Nat. Commun.*, vol. 6, p. 6588, Mar. 2015.

[224] Y. Itoh *et al.*, "A synthetic peptide vaccine involving the product of the pre-S(2) region of hepatitis B virus DNA: protective efficacy in chimpanzees.," *Proc. Natl. Acad. Sci. U. S. A.*, vol. 83, no. 23, pp. 9174–9178, Dec. 1986.

[225] D. Shouval *et al.*, "Improved immunogenicity in mice of a mammalian cell-derived recombinant hepatitis B vaccine containing pre-S1 and pre-S2 antigens as compared with conventional yeast-derived vaccines.," *Vaccine*, vol. 12, no. 15, pp. 1453–1459, Nov. 1994.

[226] Y. Wang *et al.*, "Immunizations with hepatitis B viral antigens and a TLR7/8 agonist adjuvant induce antigen-specific immune responses in HBV-transgenic mice," *Int. J. Infect. Dis.*, vol. 29, pp. 31–36, Dec. 2014.

8. List of figures

9. Acknowledgements

I treasure the unconditional support, guidance, effort and encouragement from my supervisor *Professor Carsten Kirschning*. Thank you for providing me with this interesting project, and continuous discussions and patience with me. I am deeply grateful for giving me the chance to accomplish my promotion in your group. I am fortunate to have you as my supervisor and I learned a lot from you.

I would like to thank all the colleges working at the institute of Medical Microbiology and especially the Pathogen Regulated Immunity group (AG Kirschning); *Sabine Schimanski, Thomas Scholtysik, Veena Marathe, Yetunde Adegboye, Rabea Madel, Wilhelm Buys*. Thanks for your assistance and fruitful discussion in every step of the way during this project. Thanks for having a good friendly atmosphere all over the journey.

I acknowledge the director of the institute of Medical Microbiology at the University Clinic Essen *Professor Jan Buer* and *Dr. med. Evelyn Heintschel von Heinegg* for offering me the condition to precede my PhD thesis at optimal working condition.

I want to thank all members of the Institute of Virology at the University Clinic Essen especially *Professor Ulf Ditmar*, the director of the institute and my graduate school TRR60 for funding my project. Special thank for *Professor Mengji Lu* for providing me with HBV samples. Without your support nothing would be realized. I also acknowledge the help from *Mrs. Thekla Kemper* at AG Lu. I appreciate the collaborative work with *Dr. Wibke Bayer* and *Mrs. Sonja Windmann* at the Institute of Virology for production of FMuLV VLPs. I would like to thank all the workers of the Clinic for Obstetrics and Gynecology at the University Clinic Essen for supporting me with getting the umbilical cord blood. I am grateful for support of PD *Dr. Angela Köninger*, *Professor Kimmig*, and the nurses *Mrs. Cleven*. My gratitude further extends to the members of the core facility department Image Center Essen (IMCES) for their technical support in transmission electron microscopy analysis. Thank you *Dr. Mark Hasenberg*, *Mr.s Sylvia Voortmann*, *Dr.Holger Jastrow*.

Finally, I deeply thank my parents for their infinite encouragement, trust in my decisions. I realized today one of my best life achievement that came true only by your support, thank you Dad *Dr. Adel Eldesouki* and my beautiful Mom *Seham ElMahdy*. This work is dedicated to my lovely daughter *Leyan Sofia*.

10. Erklärung:

Hiermit erkläre ich, gem. § 6 Abs. 2, g der Promotionsordnung der Fakultät für Biologie zur Erlangung der Dr. rer. nat., dass ich das Arbeitsgebiet, dem das Thema *„Host recognition of Hepatitis B virus (HBV) and related pathogen- / danger associated molecular pattern (P/DAMPs) through pattern recognition receptors (PRRs)“* zuzuordnen ist, in Forschung und Lehre vertrete und den Antrag von **Mazen Atia** befürworte.

Essen, den _____ _____

Erklärung:

Hiermit erkläre ich, gem. § 7 Abs. 2, d und f der Promotionsordnung der Fakultät für Biologie zur Erlangung des Dr. rer. nat., dass ich die vorliegende Dissertation selbständig verfasst und mich keiner anderen als der angegebenen Hilfsmittel bedient habe und alle wörtlich oder inhaltlich übernommenen Stellen als solche gekennzeichnet habe.

Essen, den _____ _____

Erklärung:

Hiermit erkläre ich, gem. § 7 Abs. 2, e und g der Promotionsordnung der Fakultät für Biologie zur Erlangung des Dr. rer. nat., dass ich keine anderen Promotionen bzw. Promotionsversuche in der Vergangenheit durchgeführt habe, dass diese Arbeit von keiner anderen Fakultät abgelehnt worden ist, und dass ich die Dissertation nur in diesem Verfahren einreiche.

Essen, den _____ _____

Der Lebenslauf ist aus datenschutzrechtlichen Gründen in der Online-Version nicht enthalten